National Library
of Canada

Acquisitions and
Bibliographic Services Branch

395 Wellington Street
Ottawa, Ontario
K1A 0N4

Bibliothèque nationale
du Canada

Direction des acquisitions et
des services bibliographiques

395, rue Wellington
Ottawa (Ontario)
K1A 0N4

Your file   Votre référence

Our file   Notre référence

NOTICE

The quality of this microform is heavily dependent upon the quality of the original thesis submitted for microfilming. Every effort has been made to ensure the highest quality of reproduction possible.

If pages are missing, contact the university which granted the degree.

Some pages may have indistinct print especially if the original pages were typed with a poor typewriter ribbon or if the university sent us an inferior photocopy.

Reproduction in full or in part of this microform is governed by the Canadian Copyright Act, R.S.C. 1970, c. C-30, and subsequent amendments.

AVIS

La qualité de cette microforme dépend grandement de la qualité de la thèse soumise au microfilmage. Nous avons tout fait pour assurer une qualité supérieure de reproduction.

S'il manque des pages, veuillez communiquer avec l'université qui a conféré le grade.

La qualité d'impression de certaines pages peut laisser à désirer, surtout si les pages originales ont été dactylographiées à l'aide d'un ruban usé ou si l'université nous a fait parvenir une photocopie de qualité inférieure.

La reproduction, même partielle, de cette microforme est soumise à la Loi canadienne sur le droit d'auteur, SRC 1970, c. C-30, et ses amendements subséquents.

Canada

UNIVERSITY OF ALBERTA

Growth and Behaviour of Short Cracks in a Ferritic/Pearlitic Steel

by

©

David F. Craig

A thesis

Submitted to the Faculty of Graduate Studies and Research in partial
fulfilment of the requirements for the degree of
Master of Science

Department of Mechanical Engineering

Edmonton, Alberta

Spring 1994

National Library
of Canada

Acquisitions and
Bibliographic Services Branch

395 Wellington Street
Ottawa, Ontario
K1A 0N4

Bibliothèque nationale
du Canada

Direction des acquisitions et
des services bibliographiques

395, rue Wellington
Ottawa (Ontario)
K1A 0N4

Your file Votre référence

Our file Notre référence

The author has granted an irrevocable non-exclusive licence allowing the National Library of Canada to reproduce, loan, distribute or sell copies of his/her thesis by any means and in any form or format, making this thesis available to interested persons.

L'auteur a accordé une licence irrévocable et non exclusive permettant à la Bibliothèque nationale du Canada de reproduire, prêter, distribuer ou vendre des copies de sa thèse de quelque manière et sous quelque forme que ce soit pour mettre des exemplaires de cette thèse à la disposition des personnes intéressées.

The author retains ownership of the copyright in his/her thesis. Neither the thesis nor substantial extracts from it may be printed or otherwise reproduced without his/her permission.

L'auteur conserve la propriété du droit d'auteur qui protège sa thèse. Ni la thèse ni des extraits substantiels de celle-ci ne doivent être imprimés ou autrement reproduits sans son autorisation.

ISBN 0-612-11182-2

Canada

UNIVERSITY OF ALBERTA

RELEASE FORM

Name of Author: **David F. Craig**

Title of Thesis: **The Growth and Behaviour of Short Cracks in a Ferritic/Pearlitic Steel**

Degree: Master of Science

Year this degree granted: Spring 1994

Permission is hereby granted to The University of Alberta Library to reproduce single copies of this thesis and to lend or sell such copies for private, scholarly or scientific research purposed only.

The author reserves all other publication and other rights in association with the copyright in the thesis, and except as hereinbefore provided neither the thesis nor any substantial portion thereof may be printed or otherwise reproduced in any material form whatever without the author's prior written permission.

David Craig

David Craig
32 Sunset Drive North
Whitehorse, Yukon
Canada
Y1A 4M8

Date: 7 March 1994

UNIVERSITY OF ALBERTA

FACULTY OF GRADUATE STUDIES AND RESEARCH

The undersigned certify that they have read, and recommend to the Faculty of Graduate Studies and Research for acceptance, a thesis entitled **Growth and Behaviour of Short Cracks in a Ferritic/Pearlitic Steel** submitted by **David F. Craig** in partial fulfilment of the requirements for the degree of **Master of Science**.

Dr. F. Ellyin (Supervisor)

Dr. A.C. Pierre

David Steigmann

Dr. D. Steigmann

Date: 2 March 1994

DEDICATION

My heart is steadfast, O God;
I will sing and make music with all my soul.
Awake, harp and lyre!
I will awaken the dawn.
I will praise you, O Lord, among the nations;
I will sing of you among the peoples.
For great is your love, higher than the heavens;
your faithfulness reaches to the skies.
Be exalted, O God, above the heavens,
and let your glory be over all the earth.

Psalm 108:1-5, NIV

ABSTRACT

The growth and closure behaviour of short cracks has been investigated. This was an experimental investigation applied to a widely used, low carbon, ferritic/pearlitic steel. This provides a practical look at the threshold fatigue crack growth in this material. There are two main aspects to the investigation: initiating small cracks and monitoring their behaviour during subsequent fatigue loading.

Innovative procedures were developed specifically to look at the early growth behaviour of these very small cracks:

- specimen preparation. Employing a pre-crack specimen where in a crack is grown in cyclic compression, to produce a final specimen with two shallow corner cracks.
- compliance measurement. Placing an active gauge on the mouth of the crack and subtracting the response of a dedicated far field gauge to obtain a signal dependent on the crack.
- opening load determination. Fitting a Ramberg-Osgood relation to the differential compliance curve to determine the opening load.

The results are divided into two stages, the first pertaining to the stationary crack, and subsequently to the crack as it is growing. The cracks were shown to exhibit an irregular growth rate, based on crack replica measurements. These irregularities were, in part, identified with microstructural features. Attempts to associate the growth rate to the applied stress intensity factor range, ΔK, were shown to work well for longer cracks and to agree with the work of other investigators. In the short crack regime, the ΔK was shown to break down and the use of a ΔK_{eff} based on the effective applied load provided little improvement.

ACKNOWLEDGEMENTS

The author would like to thank the many individuals who provided assistance, encouragement and support that made the completion of this effort possible. Special thanks and appreciation to Professor F. Ellyin and Dr. D. Kujawski for their supervision and guidance throughout this research.

I would also like to thank the technicians and machinists for their efforts and technical advice. In particular, Mr. Ian Buttar, Mr. Bernie Faulkner, Mr. Albert Yuen and Mr. Allan Muir, deserve acknowledgement for their considerable contribution to this project.

Appreciation is due my friends and family for their unfailing encouragement and prayer support. To mention but a few of many: Douglas, Joan, Marion and Pauline Craig, Scott, Laurel and baby Tyson, Jill, Shahin, Trish, Paul, Eugene, Shahani and Gaya, Sam and Ann, Sarah and Baoshan.

Finally, I would like to thank the Natural Sciences and Engineering Research Council for, providing me with financial support and, funding for parts of this research.

Table of Contents

1.0 Introduction . . . . Page 1

2.0 Background . . . . Page 3
  2.1 What is a "Short Crack?" . . . . Page 9
  2.2 Literature on Short Cracks . . . . Page 10
    2.2.1 Crack Measurement . . . . Page 10
      2.2.1.1 Potential Drop . . . . . . Page 10
      2.2.1.2 Travelling Microscope . . . Page 11
      2.2.1.3 Scanning Electron Microscope Page 11
      2.2.1.4 Plastic Replica . . . . . . Page 12
      2.2.1.5 Ultrasonic Methods . . . . Page 12
      2.2.1.6 Acoustic Microscopy . . . . Page 13
      2.2.1.7 Summary of Crack Length Measurement Techniques . Page 13
    2.2.2 Crack Initiation . . . . Page 14
      2.2.2.1 Smooth Specimen . . . . . . Page 14
      2.2.2.2 Small Notch Specimen . . . Page 15
      2.2.2.3 Large Notch Specimen with Tensile Loading . . . . . Page 15
      2.2.2.4 Large Notch Specimen with Compressive Loading . . . Page 15
      2.2.2.5 Summary of Crack Initiation Methods . . . . Page 16
    2.2.3 Growth Rate Analysis . . . . Page 16
    2.2.4 Crack Opening Load Measurement . . Page 17
      2.2.4.1 Strain Gauge Method . . . . Page 18
      2.2.4.2 Plastic Replicas Method . . Page 20
      2.2.4.3 Scanning Electron Microscope Method . . . . Page 20
      2.2.4.4 Crack Mouth Displacement Gauge Method . . . . Page 20

2.2.4.5 Laser Displacement System Method . . . . Page 21

2.2.4.6 Summary of Opening Load Measurement Techniques . Page 21

2.3 Crack Closure . . . . Page 22

2.4 Microstructural Influence . . . . Page 24

3.0 Experimental Procedure . . . . Page 26

3.1 Introduction to the Experimental Investigation . . . . Page 26

3.2 Experimental Details . . . . Page 31

3.2.1 Preparation of the Pre-crack Specimen . . . . Page 31

3.2.2 Preparation of the Final Specimen Page 35

3.2.3 Aspect Ratio . . . . Page 37

3.2.4 Fatigue Loading . . . . Page 38

3.2.5 Growth Rate Measurement . . . . . Page 40

3.2.6 Compliance Measurement . . . . . . Page 41

3.2.7 Opening Load Determination . . . . Page 44

3.2.8 Summary of Experimental Details . Page 48

4.0 Experimental Results . . . . Page 49

4.1 Development of Crack Length and Depth . . Page 49

4.2 Strain Gauge Responsiveness . . . . Page 56

4.2.1 Differential Compliance . . . . . Page 56

4.2.2 Far Field Compliance . . . . Page 62

4.3 Opening Load Development . . . . Page 64

4.3.1 Opening Load Development, c-face Gauges . . . . Page 64

4.3.2 Opening Load Development, a-face Gauges . . . . Page 71

4.4 Growth Rate Through the Test . . . . . . Page 76

4.5 Growth Rate versus Crack Depth . . . . . Page 85

4.6 Opening Load versus Crack Extension . . . Page 90

4.7 Growth Rate versus Aspect Ratio . . . . . Page 92
4.7 Microstructural Observations . . . . . . Page 96

5.0 Data Interpretation . . . . Page 103
5.1 Stationary Crack . . . . Page 103
5.2 Growing Crack . . . . Page 108
5.3 Discussion . . . . Page 112
5.4 Conclusion . . . . Page 114

6.0 References . . . . Page 118

Appendix A: Data for specimens B4, B6, B7 and B8 . Page 125
Appendix B: Computer code for collection and analysis of strain gauge data . . . . Page 136
Appendix C: Opening load data for specimens B7 and B8 . . . . Page 169

List of Tables

1: Composition of A516 Grade 70 . . . . Page 27

2: Material properties of A516 Grade 70 . . . . . Page 28

3: Microstructural parameters . . . . Page 28

4: Initial crack size (mm) and loading condition . Page 37

5: Fracture measurements of initial and final crack size . . . . Page 49

6: Range of valid opening load data from the adjacent side gauges . . . . Page 72

7: ΔK corresponding to initial growth of the c-face crack . . . . Page 92

List of Figures

1: Wöhler curve . . . . Page 3

2: Four stages of crack development . . . . Page 4

3: Schematic illustration of short and long crack growth . . . . Page 5

4: Compliance curve . . . . Page 19

5: Plasticity induced closure . . . . Page 22

6: Oxidation induced closure . . . . Page 23

7: Roughness induced closure . . . . Page 23

8: Kitagawa-Takahashi curve showing the short crack regime . . . . Page 27

9: Photographs of the microstructure . . . . Page 29

10: Surface crack, corner cracks . . . . Page 30

11: Pre-crack (CT) specimen . . . . Page 32

12: Estimated radius of the plastic zone, and resulting pre-crack size emanating from the notch . . . . Page 33

13: Crack front shape generated in the CT specimen Page 34

14: FT specimen cut from the CT specimen . . . . . Page 35

15: FT specimen cross section . . . . Page 36

16: Calculated stress intensity factor range along the front of the crack . . . . Page 38

17: Location of the strain gauges . . . . Page 42

18: Differential compliance response; Linear fit method . . . . Page 45

19: Differential Compliance Response; Curvilinear fit method . . . . Page 45

20: Crack fronts based on after fracture measurements . . . . Page 50

21: Crack depth and Length vs. number of cycles, Specimen B4 . . . . Page 52

22: Crack depth and Length vs. number of cycles, Specimen B6 . . . . Page 52

23: Crack depth and Length vs. number of cycles, Specimen B7 . . . . Page 53

24: Crack depth and Length vs. number of cycles, Specimen B8 . . . . Page 53

25: Evolution of the aspect ratio, Specimen B4 and B6 . . . . Page 55

26: Evolution of the aspect ratio, Specimen B7 and B8 . . . . Page 55

27: Measured differential compliance through the test, Specimen B7, left side . . . . Page 58

28: Measured differential compliance through the test, Specimen B7, right side . . . . Page 58

29: Measured differential compliance through the test, Specimen B8, left side . . . . Page 59

30: Measured differential compliance through the test, Specimen B8, right side . . . . Page 59

31: Comparison of adjacent side gauge response through the test, Specimen B7 . . . . Page 61

32: Comparison of adjacent side gauge response through the test, Specimen B8 . . . . Page 61

33: Far field gauge response, Specimen B7 . . . . Page 63

34: Far field gauge response, Specimen B8 . . . . Page 63

35: Relative opening load through the test, Active gauge on top of the c-face crack, Specimen B7, left side . . . . Page 67

36: Relative opening load through the test, Active gauge on top of the c-face crack, Specimen B7, right side . . . . Page 68

37: Relative opening load through the test, Active gauge on top of the c-face crack, Specimen B8, left side . . . . Page 69

38: Relative opening load through the test, Active gauge on top of the c-face crack, Specimen B8, right side . . . . Page 70

39: Relative opening load through the test, Active gauge adjacent the a-face crack, Specimen B7 . . . . Page 73

40: Relative opening load through the test, Active gauge adjacent the a-face crack, Specimen B8 . . . . Page 73

41: Crack opening load during the test, Active gauge adjacent to the crack, Specimen B8, right side . . . . Page 75

42: Growth rate versus number of cycles, Specimen B4, left side . . . . Page 78

43: Growth rate versus number of cycles, Specimen B4, right side . . . . Page 79

44: Growth rate versus number of cycles, Specimen B6, right side . . . . Page 80

45: Growth rate versus number of cycles, Specimen B7, left side . . . . Page 81

46: Growth rate versus number of cycles, Specimen B7, right side . . . . Page 82

47: Growth rate versus number of cycles, Specimen B8, left side . . . . Page 83

48: Growth rate versus number of cycles, Specimen B8, right side . . . . Page 84

49: Growth rate, da/dN, dc/dN versus crack depth, Specimen B4 . . . . Page 86

50: Growth rate, da/dN, dc/dN versus crack depth, Specimen B7 . . . . Page 87

51: Growth rate, da/dN, dc/dN versus crack depth, Specimen B8 . . . . Page 88

52: Growth rate versus crack depth for six cracks, Specimen B4, B7 and B8 . . . . Page 89

53: Relative opening loads versus crack extension Page 91

54: Crack growth rate, da/dN and dc/dN versus aspect ratio, Specimen B4 . . . . Page 93

55: Crack growth rate, da/dN and dc/dN versus aspect ratio, Specimen B7 . . . . Page 94

56: Crack growth rate, da/dN and dc/dN versus aspect ratio, Specimen B8 . . . . Page 95

57: Microstructure of the a and c faces . . . . . Page 96

58: Comparison of growth rate to microstructural features, Specimen B7, a_R crack . . . . . . Page 98

59: Comparison of growth rate to microstructural features, Specimen B8, a_L crack . . . . . . Page 99

60: Comparison of growth rate to microstructural features, Specimen B8, a_R crack . . . . . . Page 100

61: Comparison of opening load to microstructural features, Specimen B7, a_R crack . . . . . . Page 101

62: Comparison of opening load to microstructural features, Specimen B8, a_R crack . . . . . . Page 102

63: Opening load prior to crack extension, Specimen B7 . . . . Page 105

64: Opening load prior to crack extension, Specimen B8 . . . . Page 105

65: Applied stress intensity factors for the stationary crack . . . . Page 107

66: Growth rate for six cracks versus crack depth . . . . Page 109

67: Growth rate for six cracks versus ΔK . . . . . Page 109

68: Growth rate versus ΔK_{eff} for three cracks . . . Page 111

THE GROWTH AND BEHAVIOUR OF SHORT CRACKS IN A FERRITIC/PEARLITIC STEEL

1.0 Introduction

Approximately two-thirds of all mechanical component failures observed are fatigue failures. These fatigue failures commonly result from the propagation of a defect, which was for some part of its history, a short crack. Often such cracks reside in the "short crack" regime for a considerable portion of the component life. Further, this study is being conducted on a material commonly used in industry, and hence will provide some insight into this material's behaviour. This will provide an improved understanding of short crack behaviour to assist in determination of component life.

The objective of this study is to examine the behaviour of short cracks in a low-alloy carbon steel. There are two aspects to the investigation: initiating small corner cracks and monitoring their subsequent behaviour during fatigue loading on a sub-specimen. A far-field cyclic compression pre-cracking technique is adopted to minimize damage and residual stresses at the tip of the crack on the subsequent fatigue tension specimen. The closure and growth behaviour of the cracks in the fatigue tension specimen is observed in terms of shape and size. Consideration is also given to the contribution of microstructural influences and the inherent difficulties of experimental work.

Following the introductory chapter, the second chapter looks at fatigue failure in general and specifically where the short crack problem fits in. Large cracks have received considerable attention and efforts have been made to extend the methodology of these larger cracks into the short crack regime. The extension of this methodology is shown to break down for the short cracks. This investigation, which focuses on early growth rate and closure behaviour as well as the microstructural influence, is a continuation of work conducted by Professor F. Ellyin and Dr. D. Kujawski. Their efforts are reviewed and some of the techniques they present are applied. The second chapter concludes with a brief look at and evaluation of numerous techniques used in the study of short cracks.

The third chapter concentrates on the experimental procedures employed in this investigation. This includes details of the material used, the loading strategy and how the growth rate, specimen compliance and opening load are measured.

The experimental results of growth rate, compliance and opening load are graphically presented in the fourth chapter with the numerical data given in Appendix A. Photomicrographs of the microstructure are also included to permit comparison of growth rate events with microstructural features.

In the final chapter an assessment of the results is provided based on a separation of the data according to whether the crack is stationary or growing. An assessment of the influence the material microstructure has on the behaviour of the crack is also included. The conclusion of this study concentrates on two areas: observation and interpretation of the behaviour of the cracks investigated, and an assessment of some of the investigative methods applied.

2.0 Background

The investigation of fatigue and fracture of engineering materials has been a focus of study for many years. The first formal investigation was conducted by Wöhler in the 1860's [1]*. His classical method of describing the fatigue life of a given material is by plotting the stress amplitude (σ_a) versus the number of cycles to failure (N_f). For certain materials, eg. steels, a curve such as Figure 1, identifies the fatigue limit, σ_{FL}, as that state of stress below which there will be no fatigue failure. A fairly high applied stress cycle will result in a short life and is referred to as low cycle fatigue (LCF). Conversely, reducing the applied stress brings about a longer life and is described as high cycle fatigue (HCF).

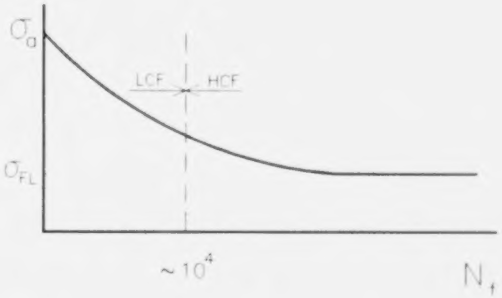

Figure 1: Wöhler curve

The development of a fatigue crack can be divided into four stages, as shown in Figure 2:

- initiation
- early propagation, when the crack is small
- late propagation, when the crack has grown relatively large
- final fracture.

---

[*] Refers to numbered references at the end of the text.

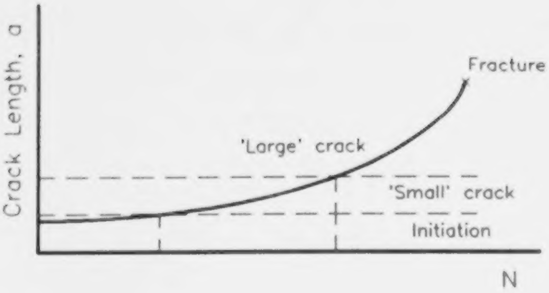

Figure 2: Four stages of crack development

For an applied stress slightly above σ_{FL}, an HCF situation, the component may undergo a considerable number of cycles during the initiation stage. Once the crack is initiated there may still be significant life left in the part, as the crack may exhibit a stage of slow growth, or even self arrest for a time. Upon reaching the large crack region, the crack will grow at a steadily increasing rate. This later stage is referred to as the Paris region [2] and is identified in Figure 3, which shows a linear relationship between log da/dN versus log ΔK[*]. When the crack has grown

---

[*] The stress intensity factor range, ΔK, is a measure of stress and strain around the tip of a crack and is assumed to be the driving force for crack propagation. It is derived in terms of Linear Elastic Fracture Mechanics (LEFM) and does not include such local crack tip effects as closure, residual stresses, crack blunting or crack branching [16].

$$\Delta K = f(g)\,\Delta\sigma\sqrt{\pi a}$$

Where:

f(g) - geometry factor accounting for the finite dimensions of the specimen. In the case of an infinite plate with a centre crack it is equal 1.0.

$\Delta\sigma$ - nominal applied stress range.

a - crack length.

to such size that the remaining ligament can no longer carry the applied load, the component fails.

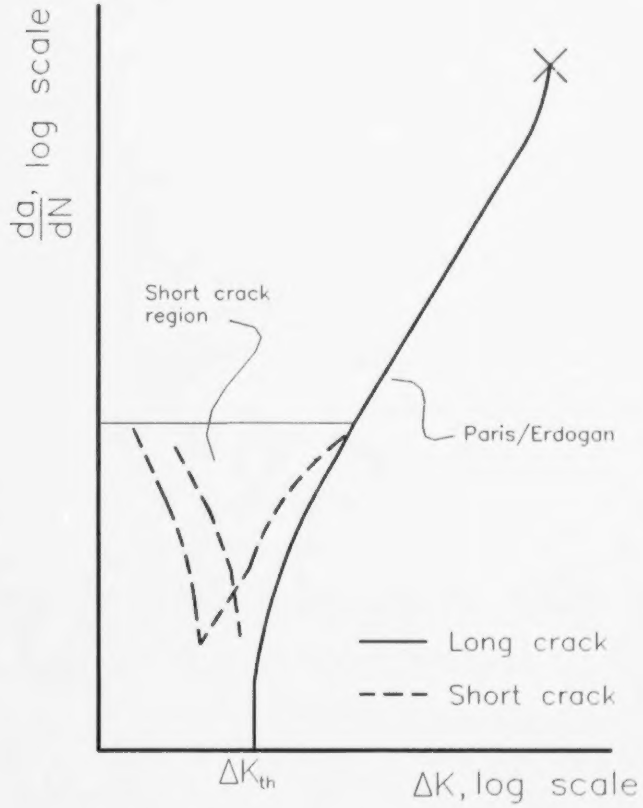

Figure 3: Schematic illustration of short and long crack growth

Propagation of the crack through the Paris region, the linear section of the curve in Figure 3, has been studied extensively and is well described using LEFM. This analysis is effective because the crack is large compared to the size of the plastic zone at the tip. Such cracks are much larger than the grain size of the material and are able to propagate at a rate that is not strongly influenced by the microstructure.

This work by Paris and Erdogan permits one to calculate the component life. The Paris line can be modelled by:

$$\frac{da}{dN}=A(\Delta K)^{m}$$ [*]

This equation can be rearranged and integrated to obtain component life:

$$N=\int_{a_{initial}}^{a_{final}}\frac{da}{A(\Delta K)^{m}}$$

The initial crack length, $a_{initial}$, is extremely important for this calculation to be accurate. If it is assumed to be 1mm, then this technique can be used to calculate an estimate of the number of cycles which will elapse, starting when the crack is 1mm long to near failure. The question that may well be asked is, how many cycles are necessary to develop a crack 1mm in size?

In LCF it may be that only 10% of the number of cycles to failure, N_f, are necessary to obtain a crack 1mm long. Hence, the calculation should give a reasonable value for N_f. However, in the case of LCF there will be significant plastic deformation hence the application of elastic plastic fracture mechanics would be more appropriate. If one were to consider a situation of HCF, 50 - ≈100% of N_f may be required to obtain a crack of 1mm. For example, if 95% of the component's life is taken up in the development of a 1mm crack, then one can only calculate 5% of the life by the above equation. Therefore, to improve ones estimate of total component life, it is important that a better understanding of the early growth stages be pursued.

---

[*] Where A and m are fitted constants.

The significant role the short cracks play in determining component life is now receiving considerable attention. Numerous studies have been conducted which in turn have been summarized by Suresh and Ritchie [3]. These short cracks exhibit "anomalous" behaviour when compared to long cracks, behaviour such as:

- growth at a higher rate than would be predicted by extending the long-crack growth curve.
- growth rate perturbations.
- growth at a stress intensity factor range, ΔK, below the long-crack growth threshold.
- growth for a given crack decreasing to a minimum rate even with an increasing ΔK.

These phenomena have been identified by numerous investigators, for example Tokaji et al. [4], and summarized in related texts, such as Taylor [5].

This particular study is a continuation of work by Kujawski and Ellyin [6][7]. Their work concentrated on small corner cracks, in ASTM A516 Grade 70, low carbon steel, undergoing tension-tension fatigue loading. In their investigations short corner cracks were studies, however closure loads were not taken into consideration.

It was observed that the cracks in these specimens initially grew more quickly than larger cracks, though in an irregular fashion, before approaching the long crack growth values. Also, it was seen that the corner cracks initially grew in the depth direction until a certain aspect ratio (depth/length) was reached whereupon they grew in both length and depth. The shape of the crack front was found to tend towards a quarter circle in shape as the test progressed. The variation of crack opening load with crack extension was presented for one specimen.

In a continuation of their study, Kujawski and Ellyin [7] investigated the growth of small inclined, corner and through thickness cracks. Once again the growth rate was found to be discontinuous in the depth direction. When a certain aspect ratio was reached the cracks were noted to grow steadily in both length and depth.

The present investigation focuses on the early stage of crack propagation. During this stage the crack is short enough to be influenced by the microstructure. The behaviour of the crack in this region reveals characteristics that are different from larger cracks. For example, the growth rate may be erratic, from high (10^{-5} mm/cycle), to arrested. As pointed out by Hussey et al. [8] this crack arrest is primarily due to microstructural barriers . The microstructural influence has received considerable attention in the literature [3][9][10].

The significance of the region below the long crack threshold, ΔK_{th}, is that cracks of this size, which correspond to cracks of less than ≈1mm, are difficult to detect. Inspection programs commonly implemented during manufacturing and maintenance, using techniques such as radiographic, magnetic particle, ultrasonic, dye penetrant, etc. are unable to detect such small cracks. As pointed out by Ellyin and Li [11], most commonly utilized engineering materials contain defects and during fabrication additional flaws are often introduced. The design engineer should take into consideration that there may be small defects in the completed component or structure before it goes into service. For example, the aerospace industry defines safety requirements for assumed initial damage in various structures [12]. This approach to design, of assuming there are flaws present in the material, is referred to as damage, or defect-tolerant, design.

2.1 What is a "Short Crack?"

The term **short crack** will mean something different to individuals from different disciplines [3]. To a metallurgist 5μm is seen as short in that it is the next size up from a small flaw. To a non-destructive testing specialist, a short crack may be considered to be 2mm or less because that is the lower resolution of the detection equipment being used.

In very simple terms a short crack is one which shows the anomalous behaviour described in section 2.0. For the purpose of this investigation a **short crack** is defined as one which is of a similar order to the dominant microstructural dimension of the material. In the case of the A516 Grade 70 steel the dominant feature is the ferrite/pearlite boundary. These boundaries are irregularly spaced 0.1 - 0.3mm apart. A crack of this size, will experience an influence on the growth rate from the microstructure until three times greater than the boundary spacing.

2.2 Literature on Short Cracks

The early stages of the growth of fatigue cracks have been receiving considerable attention for several years. A number of experimental techniques have been developed to aid in this effort. These techniques include:

a) crack length measurement
b) crack initiation
c) growth rate analysis
d) crack opening load measurement.

2.2.1 Crack Measurement

There are numerous approaches available to an investigator for the measurement of crack length and calculation of growth rate. No single method is ideal and different problems arise with each technique. In the field of non-destructive testing several methods are used for the detection of cracks. In studying small cracks these techniques are typically not sufficiently sensitive to be useful. For the purpose of investigating small cracks the main techniques employed are described in the following sections.

2.2.1.1 Potential Drop

This involves passing a current through the specimen and monitoring the voltage drop. The main application of this approach has been in the investigation of long cracks. It may utilize either direct [13][14] or alternating current arrangements [15][16]. This technique provides an indication of the size of the remaining ligament. There are numerous articles addressing this topic. These articles have been assembled by C. J. Beevers [17].

2.2.1.2 Travelling Microscope

A microscope, having relatively high magnification capability, is mounted on a travelling, micrometer base. It is widely used for surface observations of crack length [18]. Resolution down to 1μm is attainable [19], though 10μm is more commonly the case. In studying short cracks one may require at least 1μm resolution to observe irregularities in the growth behaviour. Although the equipment cost is low; consisting of a microscope, travelling base and illumination system; the technique is expensive because of the labour involved. The very shallow depth of field inherent in this technique encourages the design of flat specimens. Video recording capabilities have been added to enhance the performance of this method [20][21], or to automate the method [8][22].

2.2.1.3 Scanning Electron Microscope

Utilizing a Scanning Electron Microscope, (SEM), permits one to observe the surface of the specimen. This is usually done by periodically removing the specimen from the loading arrangement. However, systems have been built to conduct the SEM observations in-situ. This has the advantage that it does not disturb the loading or set up of the specimen. Typically these involve small loading machines [23], but larger machines, to 25 kN, have been built [24]. Such methods entail considerable equipment expense, and perhaps time as well.

2.2.1.4 Plastic Replica

The plastic replica technique allows one to make a detailed copy of the surface, including the crack. The replica is made of the crack by first applying a static load of 60 - 80% of P_{max} to the specimen. Then, wetting either the specimen or the replica tape with acetone, the plastic replica material is touched to the surface of the specimen, covering the crack. Once the acetate has dried the replica can be removed and mounted on a microscope slide or otherwise stored.

The cellulose acetate can be a film as thin as 25μm or a sheet up to 5mm thick [25][26][27]. The replicas may then be viewed using either an optical microscope or an SEM. Using the SEM for direct observation provides a resolution of $\approx$0.1μm and involves first coating the replica, generally with gold. Alternatively a heavy copper or solder backing can be applied to support the shape and the actual replica dissolved away.

This method provides a permanent record and does not necessitate removal of the specimen. Though elegant in its simplicity, this method is labour intensive.

2.2.1.5 Ultrasonic Methods

The ultrasonic method, reviewed by Silk [28], involves subjecting the specimen to high frequency compressional waves and monitoring the transmittance or reflection of these waves. The use of ultrasonic approaches generally found favour in the investigation of short cracks because the resolution is not typically adequate. However, recent efforts have improved the applicability of this approach. These include use of a surface acoustic wave technique [29][30], and a focused ultrasonic system [31].

2.2.1.6 Acoustic Microscopy

This technique, though still under development, entails focusing acoustic radiation at a point on the specimen surface and recording the response. A region is thus scanned on a regular pattern and an image generated. This method is able to provide some information to just below the surface [32], which is useful in distinguishing between a crack and a scratch. Reliable systems are expensive.

2.2.1.7 Summary of Crack Length Measurement Techniques

None of the crack length measurement techniques described here are ideal. They are either not sufficiently precise for an investigation such as this or they are expensive in terms of specialized equipment or manual effort. The plastic replica approach is often favoured in preliminary work, because it gives good results and does not involve expensive, specialized, equipment. A high quality light microscope or conventional SEM is often locally available to observe the replicas. A further benefit of the replica approach is that it provides a permanent record. Even if more sophisticated methods are introduced, it still provides a means to cross check their validity.

2.2.2 Crack Initiation

To investigate the early growth behaviour of cracks, as separate from crack initiation phenomena, a number of methods have been explored to facilitate the initiation process. Most of the commonly used approaches are given in the following sections.

2.2.2.1 Smooth Specimen

A crack is allowed to initiate naturally, perhaps from a naturally occurring flaw. To accomplish this, a smooth specimen is loaded to slightly above the fatigue limit. The surface is scanned at regular intervals to search for small cracks. The scanning can be conducted with either a light microscope or an electron microscope, hence it may be necessary to remove the specimen. Once a crack is detected the load may be reduced which will effectively lower the ΔK and perhaps the growth rate. The application of a light microscope or an SEM, for early crack detection on smooth specimens, have both been automated by a team of investigators at Rolls Royce [8][33].

Alternately, replicas can be made at regular intervals of the region where the crack is likely to initiate. Once a crack develops to the point where it is evident, one can examine the earlier replicas to evaluate the crack development [34].

By allowing the crack to initiate naturally one eliminates any stress concentration associated with a notch. However, it is time consuming to do this since it is difficult to anticipate where or when the crack may start. This is particularly true if the search technique involves examining replicas.

2.2.2.2 Small Notch Specimen

Introducing a small notch, or stress concentration, to the test region results in a local increase in stress. This has the effect of promoting the initiation of a crack at that point. Several techniques for starting cracks from small notches have been explored; a number of these are reviewed or referenced by Gangloff et al. [35]. The two principal methods are, very small abrupt notches or larger notches contributing a small stress concentration. Examples of the small notches might be a hole 0.25mm ϕ × 0.25mm deep or a diamond scratch such as that used by Järvine [36]. A gradual notch, similar to that utilized by Larsen et al. [19], Sharpe and Su [37] or Pearson [38], will also reduce the region in which the crack will initiate.

2.2.2.3 Large Notch Specimen with Tensile Loading

Employing a larger notch and tensile loading results in fairly rapid initiation of a crack. The notch and part of the crack can then be machined away, leaving a small crack [39]. This method is fast, but has the disadvantage of introducing a plastically effected zone ahead of, and in the wake of, the crack. This technique also involves two stages of machining, which may in turn introduce residual stresses. This plastically deformed region may not be desirable when studying the development of crack growth and closure.

2.2.2.4 Large Notch Specimen with Compressive Loading

Using a large notch and compressive loading drives a crack, which will initiate at the notch root. This approach has been employed by several investigators, Kujawski and Ellyin [6][7], and the references therein. This occurs even though the far field loading is entirely compressive. At the notch root the effective stress will be tensile-compressive due to the plastic outward flow during the greatest applied compressive load. Further from the notch the stresses will be entirely compressive, hence the crack tip driving force will be less than that required to sustain crack propagation and so the crack will self arrest. The notch and part of the crack can be machined away leaving just the tip of the crack. This results in a small pre-crack with minimal damage ahead of the tip or in the wake. However, this procedure does have the drawback of involving a second stage of machining.

2.2.2.5 Summary of Crack Initiation Methods

Of the techniques reviewed here, no single approach satisfies all the desirable aspects of initiating a very small crack. Ideally the specimen should be free of any damage associated with growing the crack or manufacturing the specimen, and be quick and cheap to make. The approach of beginning with a specimen having a large notch, applying compressive loading and subsequently machining the notch and most of the crack away is among the most labour intensive. However, other than the time involved, it comes the closest to resulting in a specimen having the desired attributes.

2.2.3 Growth Rate Analysis

There are numerous means that can be applied to the calculation of the growth rate. Larsen et al. [19] and Kendall and King [40] have separately looked at short crack data. For example, Kendall and King [40] have conducted a comparative investigation of several of the more common approaches using the same data set to reveal that real crack growth events can be disguised (smoothed out), exaggerated or displaced. The ASTM Standard Test Method for Measurement of Fatigue Crack Growth Rates [16] and The Metals Handbook [41], provide very good suggestions for the interpretation of long crack growth data, using either an incremental polynomial or secant method. However these tend to fail in the short crack regime due to the perturbations of the growth event.

Inevitably there will be some error in the measurements. One would hope to minimize the effect of these errors, while revealing actual growth events, including, for example, temporary self arrest. For short cracks the secant method is generally preferred over an incremental polynomial as the incremental polynomial tends to smooth out events of interest. Two of the more common secant approaches used are:

$$\left.\frac{da}{dN}\right|_{N=i}=\frac{a_{i+1}-a_{i-1}}{N_{i+1}-N_{i-1}} \qquad\qquad \left.\frac{da}{dN}\right|_{a=\bar{a}}=\frac{a_{i+1}-a_{i}}{N_{i+1}-N_{i}}$$

Where the subscript i denotes successive discrete length measurements and $\bar{a} = (a_{i+1}+a_i)/2$.

2.2.4 Crack Opening Load Measurement

The opening load is usually defined as the load required to open the entire crack. Measuring the load at which the crack is fully open is complicated by the fact that the crack does not open all at once. Typically the crack begins to open at the mouth, and gradually opens with increase in load right to the tip. Crack opening load measurements are also sensitive to surface residual stresses.

There are a number of approaches employed to determine the opening load. Several of those most applicable to short cracks are described in the following sections.

2.2.4.1 Strain Gauge Method

One conventional method is to place a small strain gauge adjacent to the tip of the growing crack. When the crack opens, in response to increasing load, the plastic zone associated with the tip of the crack will impinge on the strain gauge. The gauge will then indicate a strain greater than the nominal background value.

In the case of a short crack, the plastic zone which develops ahead of the crack tip in response to cyclic loading is very small, ≈0.02 mm. To place a strain gauge small enough to average the strain over an area which is comparable in size to the plastic zone and still not interfere with crack length measurements is difficult. Even with a small gauge, carefully placed, and with the use of an extremely high gain on the amplifier, the opening load is still difficult to measure. A further means of increasing the sensitivity of a gauge, say ε_1, adjacent to the crack is to mount a second strain gauge (ε_2) far from the crack so as to record the nominal applied strain. The output from this second gauge can then be subtracted from the output of the active gauge, (ε_1-ε_2), leaving in a sense, just the crack effect. This difference technique may still not be sufficiently sensitive to reveal the opening load. A modification used by various groups; Ogura et al. [39], Chen et al. [42], DuQuesnay [43]; is to place the active gauge (ε_1) on top of the crack. A far field gauge, employed as above, in conjunction with the active gauge on top of the crack, results in excellent sensitivity. A drawback to this approach is that the gauge life may be short, as the majority of the strain occurs over a very small region.

The compliance curves, which these strain gauge techniques yield, are examined to determine the opening load. The opening load is identified by the point on the loading curve, above the main change in slope, where the slope becomes nearly linear.

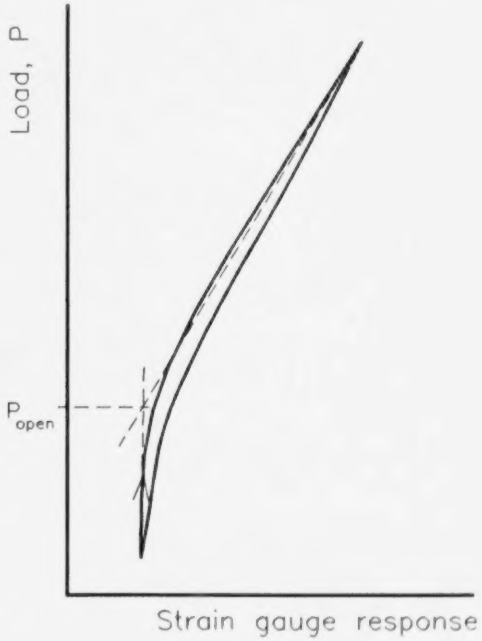

Figure 4: Compliance curve

One common technique is to fit a straight line to the upper part of the curve and a straight line to the lower part of the curve. The point where the two lines intersect is taken as the opening load, P_{open}.

2.2.4.2 Plastic Replica Method

Another means of investigating the crack opening load is to make several replicas at successive increases in applied load. These replicas are examined in detail, with an SEM, to ascertain when the crack at the surface is open all the way to the tip [36]. Clearly this approach is only applicable to the crack at the surface.

2.2.4.3 Scanning Electron Microscope Method

In a similar fashion to the above described replica technique, a crack can be observed with the SEM while the load is increased. Of necessity, the loading mechanism must be part of the microscope system, such that the observations will be made in-situ. Once again this is only applicable to surface observations and involves expensive equipment.

2.2.4.4 Crack Mouth Displacement Gauge Method

A crack mouth opening displacement (CMOD) gauge is sometimes used. The CMOD gauge is a device made up of two arms that are fixed to the specimen on either side of the crack. These two arms are connected via a small frame which in turn deflects in response crack opening. An arrangement of strain gauges is subsequently used to measure this deflection and hence the movement of the arms. This method generally finds application in studying long cracks [44] as it is not sensitive enough to detect short crack phenomena. The method is reviewed in detail by Fleck [45], with comparisons to other techniques.

2.2.4.5 Laser Displacement System Method

A laser displacement monitoring system, focused on two points very near the crack tip, can be used. Sharpe and Su [37], have implemented a laser based interferometric technique; and the method is reviewed in depth by Jenkins et al. [46]. Though the laser displacement system is reported to be very effective, such a system is expensive and specialized.

2.2.4.6 Summary of Opening Load Measurement Techniques

Of the opening load measurement techniques reviewed here, none is ideal. Due to the small scale of the event associated with the opening of a very small crack, any technique must be very sensitive. CMOD gauges and conventional strain gauge systems are not sensitive enough. An in-situ SEM, or a laser displacement system are often unattractive because they involve expensive specialized equipment. Placing an active gauge on top of the crack results in a short gauge life, hence; either limiting the amount of data collected or necessitating disruption of the experiment to replace the gauge. However, placing the active gauge on top of the crack does not require expensive, specialized equipment, and does provide sensitivity adequate for preliminary investigations. For a small number of specimens the effort associated with repeated gauge changes is acceptable.

2.3 Crack Closure

In the field of fracture mechanics it is now widely recognized that fatigue cracks remain closed near the tip, even under the application of considerable tensile load. P_{open}, see Figure 4, is the minimum tensile load required to fully open the crack. This phenomenon was first experimentally observed by Wolf Elber in the late 1960's [25]. Since then, numerous investigators have confirmed his findings. An international symposium was dedicated to this topic in 1986 [47] and several other conferences have given serious attention to the phenomenon [48][49][50].

There are a number of mechanisms that may contribute to the closure event. These depend on such factors as the environment and the type of material. Taylor [5], provides a review of some of the likely closure mechanisms, in a chapter dedicated to the topic. In this study, the main aspects relevant to closure are described below.

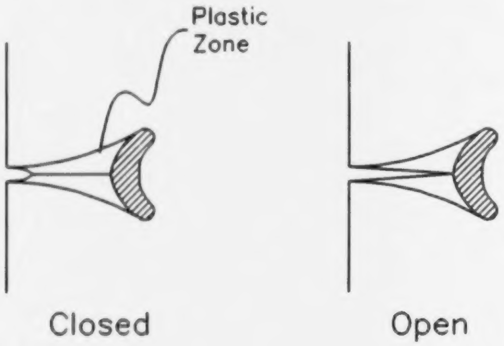

Figure 5: Plasticity induced closure

The plastic deformation ahead of the crack tip results in residual strain. As the crack grows through the plastically deformed region ahead of the crack tip, the resulting permanent deformation in the wake results in premature contact of the fracture surfaces.

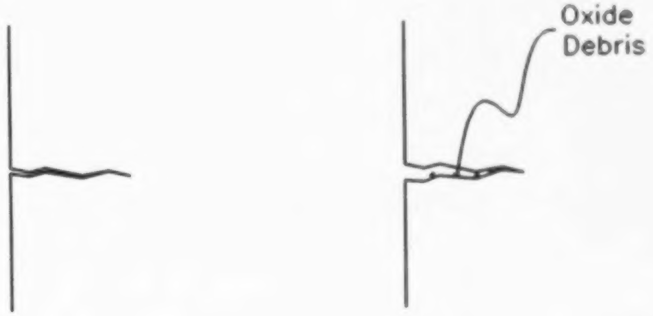

Figure 6: Oxidation or debris induced closure

Oxide products on the faces of the crack bring about premature contact of the faces of the crack. Effectively this means the crack closes while considerable load is still present. Any phenomenon that serve to introduce debris into the crack will contribute to this effect. What this does, is to increase the load required to open the crack and hence increase the closure.

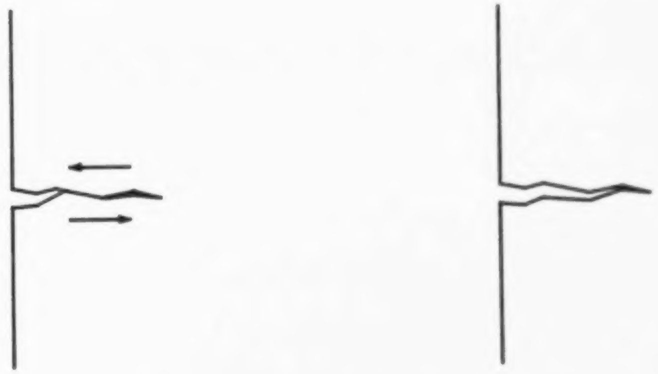

Figure 7: Roughness induced closure

When the crack is open relative motion can occur between the two surfaces if the plane of the crack, at that location, is not transverse to the loading direction. The result is that when the two faces come back together during unloading they no longer line up perfectly. Consequently the surfaces impinge at the high points. Effectively, this props the crack open in a fashion similar to the oxidation induced closure.

The conventional understanding is that a crack will not grow until it is fully open. This means that part of the applied load does not contribute to crack growth; thus, is non-damaging. In this way the crack's driving force is reduced.

One of the observations which Elber made as part of his early investigations into crack closure [25] was that due to the plastic deformation that is part of the fracture process, the actual contact area of the resulting crack faces was commonly 30 to 50% of the fracture surface. Particularly in the near tip region, the extent to which the fracture surfaces contact may be very sensitive to the compressive stresses between the crack faces.

2.4 Microstructural Influence

The microstructural influence on a crack is that as the crack passes through a domain, the growth rate will change. This occurs even though the loading cycle remains constant. For example, in a single phase material the rate of crack propagation will decrease or even self arrest at grain boundaries. In a dual phase material, such as a ferritic/pearlitic steel, the crack growth will slow down on passing through a pearlite region.

3.0 Experimental Procedure

3.1 Introduction to the Experimental Investigation

An experimental investigation has been conducted into the early stages of fatigue crack growth. It focuses on a low carbon (0.25% C) ferritic/pearlitic steel undergoing uniaxial loading. The material used in this study is ASTM A516 Grade 70. This steel is commonly used in the construction of pressure vessels. As well as being of interest to those industries that utilize this material, the findings should reveal a general understanding of short crack behaviour.

The objectives of this study are to investigate:

- Rate of crack growth, how it changes during the life of the specimen and with increasing crack depth, length, and changes in shape.
- Load required to open the crack and how the opening load changes during the test as the crack increases in size.
- Microstructural influence, particularly the effect on the growth rate and possibly on P_{open}.
- Experimental procedures relevant to investigating short cracks.

The region of crack growth being investigated is shown on the Kitagawa diagram, Figure 8, as those cracks which are physically small. In this case, the initial depth of the cracks is 0.08 - 0.35 mm. This is of similar order to the dominant microstructural feature, the ferrite/pearlite regions. The role of the dominant microstructural dimension is presented as d_1, d_2 and d_3 in Figure 8. When the crack length is less than d_3 the crack will exhibit a more pronounced microstructural influence than larger cracks.

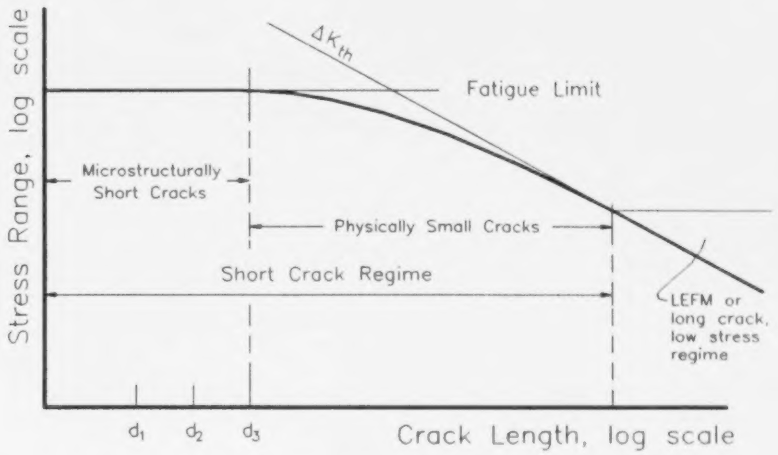
Stress Range, log scale
ΔK_{th}
Fatigue Limit
Microstructurally Short Cracks
Physically Small Cracks
Short Crack Regime
LEFM or long crack, low stress regime
d_1
d_2
d_3
Crack Length, log scale

Figure 8: The Kitagawa-Takahashi curve showing the short crack regime

The composition and material properties are given in Tables 1 and 2. The microstructural parameters are given in Table 3 with photographs of the microstructure following in Figure 9.

Table 1: Composition of A516 Grade 70

Chemical Composition, (weight %)	
Carbon	0.25
Manganese	1.1
Phosphorous	0.015
Sulphur	0.02
Silicon	0.25
Iron	Balance (≈98.4)

Table 2: Material Properties of A516 Gr. 70, [51].

Mechanical Properties	
Young's modulus	204 GPa
Ultimate Tensile Strength	540 MPa
0.2% proof stress	325 MPa
fracture stress	993 MPa
strain to failure	38.6%
cyclic strength coef.	1067 MPa
cyclic hardening exponent	0.193

Table 3: Microstructural Parameters.

	Grain Size [*]	Pearlite % [$]
Rolling face, a-face (side view)	13μm	42
In the rolling direction, c-face	13μm	44
Perpendicular to the rolling direction.	12μm	31

---

[*] ASTM E112: Standard Test Methods for Determining Average Grain Size

[$] Based on the ratio of dark and light coloured areas of photomicrographs similar to Figure 9 interpreted with an image analysis system.

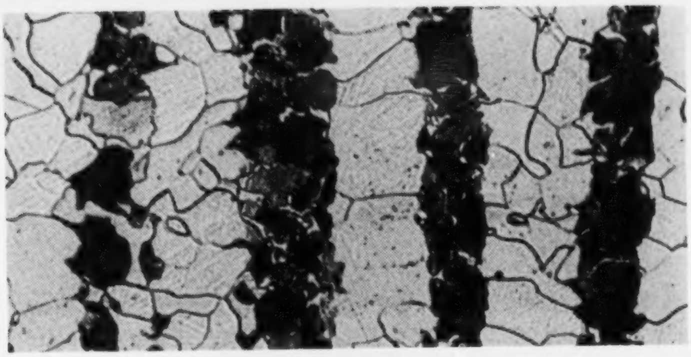

a) c-face

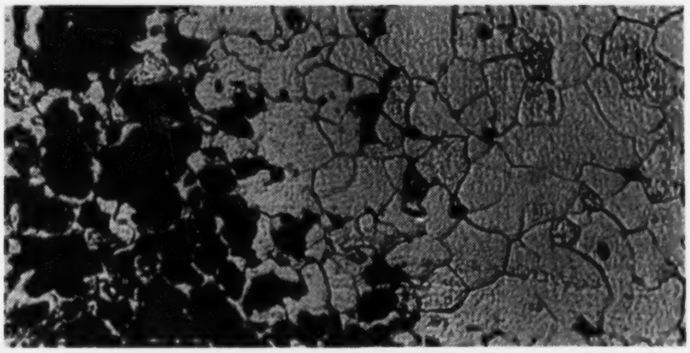

b) a-face

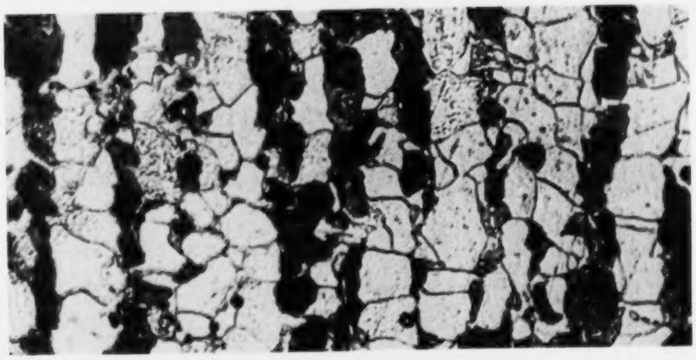

c) Perpendicular to the rolling direction

Figure 9: Photographs of the microstructure (Mag. 425×)

In conducting an investigation into the behaviour of surface cracks there are two main crack geometries used:

a) Penny shaped crack, which though a very practical problem has two disadvantages. First only surface length measurements are possible, thus the aspect ratio cannot be measured. Second, there will always be some residual damage in front of the crack due to plastic deformation ahead of the tip.

b) Corner crack, which has the advantage of permitting measurement of both length and depth directions and is almost free of residual stresses when the crack is grown in compression [6]. As it is part of a penny shaped crack, it has the disadvantage of only approximating the behaviour of such surface cracks, see Figure 10.

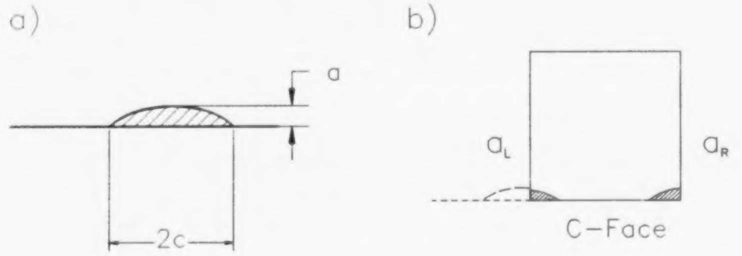

Figure 10: a) Surface crack, b) Corner cracks

If the crack front is assumed to be elliptical, knowledge of the length and depth provides an estimate of the shape, and allows one to monitor the shape changes during the test. Since the primary purpose of this investigation is to determine the behaviour of short cracks, test specimens were prepared with pre-existing short cracks.

3.2 Experimental Details

The specimens are prepared in two stages, similar to the procedure employed by Kujawski and Ellyin [6][7]:

Pre-crack Specimen[*] (CT) - preparation
- loading

Fatigue Tension Specimen (FT) - preparation
- loading
- post loading.

3.2.1 Preparation of the Pre-crack Specimen

To prepare the pre-crack specimen, a steel blank is normalized at 900°C for 6 hours, and oven cooled for 16 hours, resulting in equidimensional grains in a banded structure, see Figure 9. A pre-crack specimen of the shape and size of a compact type (CT) specimen, with the sides reduced, having a sharp notch with 60° included angle, is manufactured as shown in Figure 11.

The purpose of reducing the thickness of the sides is so that no further machining is required on these surfaces, during subsequent specimen preparation. Any machining may introduce some surface residual stresses which could influence the crack development, such influence is thus minimized. The orientation of the specimen is such that the initial direction of crack growth is along the a-face. The crack will not propagate across the ferrite/pearlite bands shown in Figure 9a until well into the test.

---

[*] The pre-crack specimen is dimensionally very similar to the standard, Compact-Type Specimen [16]. Hence, this will be abbreviated as the CT specimen.

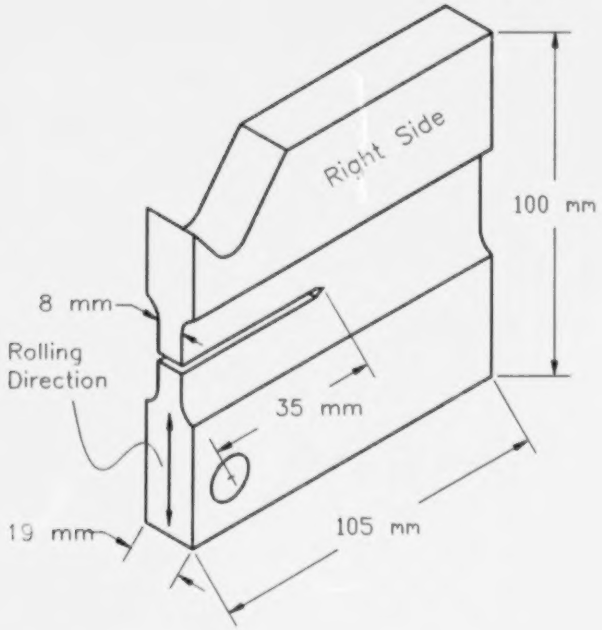

Figure 11: Pre-crack (CT) specimen

An Amsler Vibrophore loading machine operating at ≈90 Hz was used to load the CT specimen. The loading was in a sinusoidal, cyclic compression - compression manner with $R=P_{min}/P_{max}=10$, ($P_{min}=-8.0$ kN, $P_{max}=-0.8$ kN). Although the applied loading is entirely compressive, at the root of the notch the stress will be tensile-compressive. This is due to the plastic outward flow of the material in the notch region at P_{min}, which results in local residual tensile stresses, upon unloading to $P=P_{max}$.

The radius of the monotonic plastic zone (r_p) emanating from the notch can be estimated using any of a number of available models. None of the equations are exactly applicable as the loading is entirely compressive. However, since the geometry of the pre-crack specimen is such that the faces of the initial notch do not touch during loading they provide a reasonable estimate of the monotonic plastic zone size. The cyclic plastic zone can then be estimated at one quarter of the monotonic plastic zone size. Figure 12 presents the estimated size of both the monotonic and cyclic plastic zone sizes using the Dugdale, Irwin and elastic-plastic models for r_p, and the resulting size of the final cracks in the pre-crack specimens.

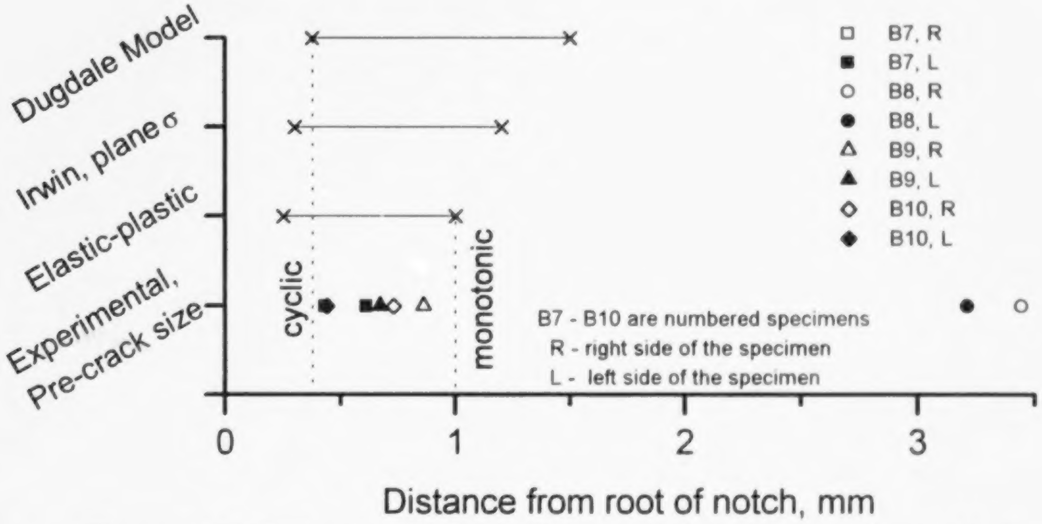

Figure 12: Estimated radius of the plastic zone, and resulting pre-crack size emanating from the notch

With the exception of specimen B8, the resulting pre-cracks fell between the estimated monotonic and cyclic plastic zones in size. One can anticipate that there may be some residual stresses at the tip of the crack due to the strain within the monotonic plastic zone. However, this residual stress will be compressive, which will leave the crack open. Therefore, these residual stresses will not contribute to increasing the initial closure level.

The pre-cracking of specimen B8 resulted in cracks four times the length of the pre-cracks in the other specimens. No explanation is given as to why this specimen had much longer cracks than the other specimens.

It was found that, in the CT specimens, the crack would self arrest after about 2×10^6 cycles. One would expect this to be the case as the tensile stresses at the notch root are local, hence the driving force of the crack naturally drops off as the crack propagates. The Vibrophore was permitted to run for 15×10^6 cycles to ensure complete self arrest.

The shape of the crack front is also important, particularly in generating a final specimen having corner cracks. This shape can be influenced by the loading condition and the notch radius, as described by Pippan [52] and shown in Figure 13. For small shallow corner cracks an arrangement such as shown by Figure 13c will give the best results.

For example:

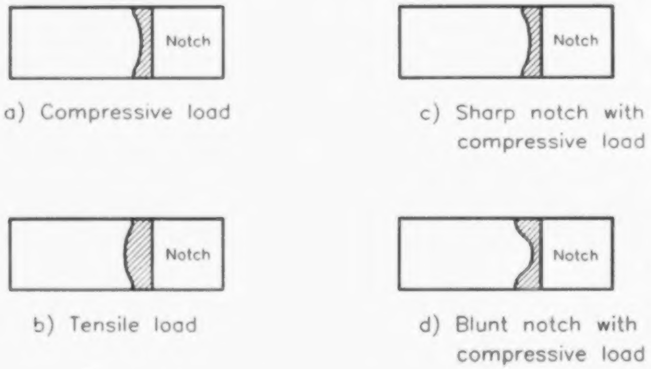

a) Compressive load

c) Sharp notch with compressive load

b) Tensile load

d) Blunt notch with compressive load

Figure 13: Crack front shape generated in the CT specimen

Cutting the FT specimen out of the CT specimen, Figure 14, allows for precise control of the depth of the crack along the a-face of the final specimen.

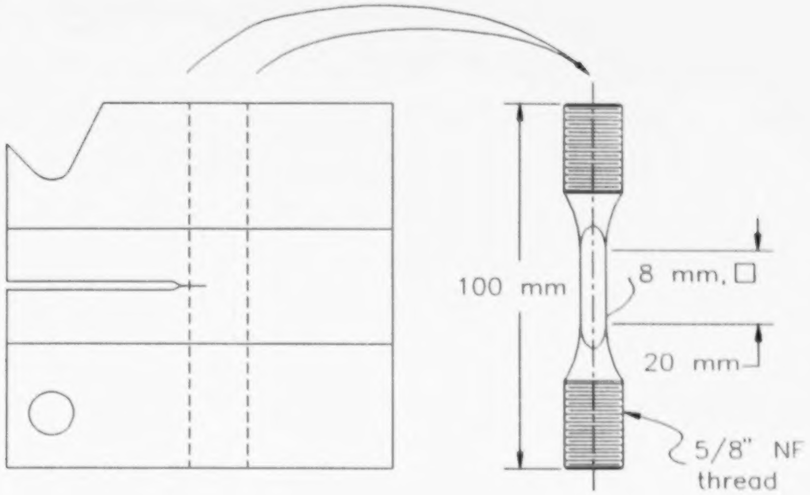

Figure 14: FT specimen cut from the CT specimen

This technique produces a specimen having a crack of favourable geometry with minimal damage ahead of the crack tip. Further advantages are that, since the initial crack has been grown in compression the wake of the crack does not exhibit closure. Additionally the damage ahead of the crack tip, and the subsequent closure which may be associated with such a damaged zone, is small.

3.2.2 Preparation of the Final Specimen

Upon being cut from the CT specimen, the FT specimen, is polished in successive stages. The last stage involves the use of $\frac{1}{4}\mu$m diamond paste. The crack can then be measured, using the thin replica technique.

The specimen is then heated to 325°C in a small closed container, and allowed to soak at this temperature for 45 minutes. This treatment serves two purposes. First it effects a stress relief, with no microstructural change, of stresses introduced during manufacture of the specimen. Second, the treatment oxidizes the crack surfaces so that upon final fracture the shape of the initial crack front can be identified. A final polish with the ¼ μm diamond paste follows this heating step. The FT specimen cross section is shown in Figure 15, together with the corresponding nomenclature used. The corner cracks shown are exaggerated in size to assist the visibility. In the actual specimens they represent about 1% of the total cross sectional area.

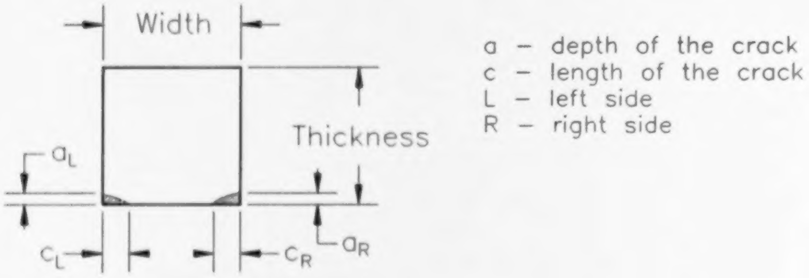

Figure 15: FT specimen cross section

The specimen is then cleaned in an ultrasonic bath for half an hour in distilled water with a small amount of detergent. The next step is to subject the specimen to a 10 μm Hg vacuum, for the purpose of clearing polishing debris from the crack. This cleaning was followed with the specimen being immersed in paraffin wax, at 140°C, such that the crack will be filled with wax and not draw in adhesive during mounting of the strain gauges.

The dimensions of the pre-cracks in the final specimens prior to fatigue loading are presented in Table 4. On this table, when both the replica method, and direct SEM observations have been used, then both results have been included; first the replica result, then the SEM result. Although the SEM observations may be more accurate, they could only be made with the specimen removed from the testing machine. Therefore it is the replica measurements that will be used for all comparative assessments.

Table 4: Initial crack size (mm) and loading condition.

	B4	B6	B7	B8
a_L	0.574	0.014	0.266/0.275	0.050/0.089
c_L	1.61	0.150	1.280/1.280	2.003/2.003
$a/c\|_{replica}$	0.36	0.09	0.21	0.02
a_R	0.520	0.08	0.088/0.092	0.377/0.383
c_R	1.93	0.83	0.820/0.825	2.404/2.404
$a/c\|_{replica}$	0.27	0.10	0.11	0.16
$R=P_m/P_M$	0.05	0.05	-0.1	-0.1

3.2.3 Aspect Ratio

In considering corner cracks having fairly low aspect ratios ($a/c < 0.3$), one can be reasonably certain that the crack will first grow in the depth direction. Newman and Raju [53] have provided a formulation for calculating the crack tip stress intensities, ΔK, along the entire front of a corner crack. A separate means of calculating ΔK has been provided by Pickard [54], which gives results within 3% of those obtained using Newman and Raju's formulation. Although ΔK is a parameter derived using LEFM and hence is more directly applicable to large cracks, it does provide an indication of the relative crack driving force. Using the data presented in Table 4, the applied stress intensity along the front of the initial crack is graphed in Figure 16, for each of the specimens. This clearly indicates that the corner cracks ought to begin growing in the depth direction first (ϕ=90°).

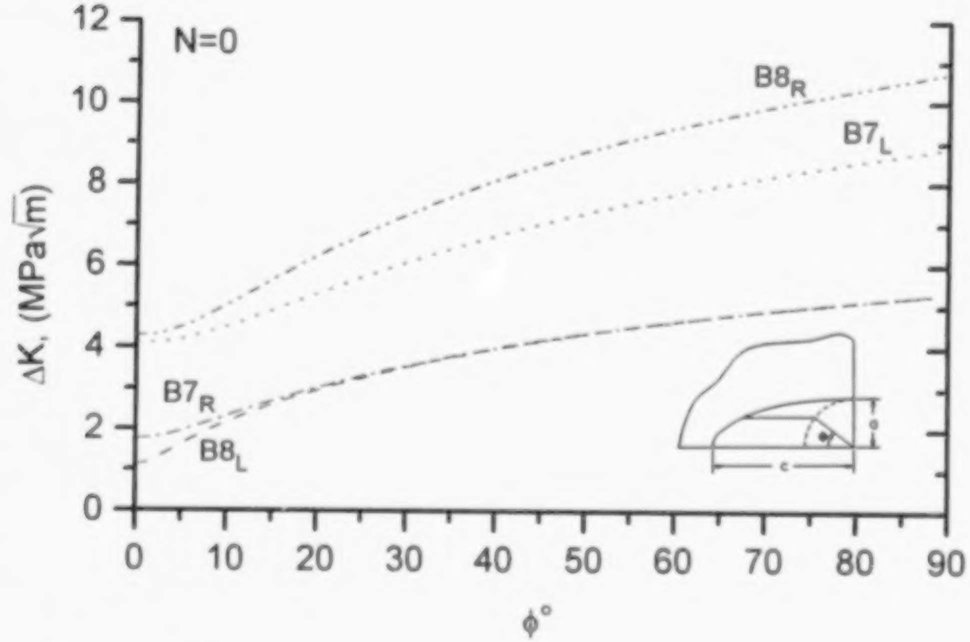

Figure 16: Calculated stress intensity factor range along the front of the crack

3.2.4 Fatigue Loading

Initially a stress ratio, $R=\sigma_{min}/\sigma_{max}=0.05$ (with $\sigma_{max}=250$ MPa, or 77% of σ_y) was chosen to be compatible with earlier experiments by Kujawski and Ellyin [6][7]. With the specimen preparation technique being employed, this results in an initial opening load below P_{min}. In the experiments it proved difficult to detect the changes in the opening load occurring close to the bottom of the differential strain loop.

Therefore, in further tests, a load ratio of R=-0.10 was adopted, wherein the lower part of the curve the crack is more likely to be closed. This was adopted for the following reasons:

- to include a mean stress effect.
- the loading to include P=0 so as not to introduce a load which was not part of the load cycle in the event of temporary specimen removal.
- to promote a region of the compliance trace where the crack will almost certainly be closed.
- the small crack effect will be more pronounced at R<0 for plane stress conditions [55].

The actual loading of the FT specimens was conducted on a 250 kN Gilmore servo hydraulic testing machine, at room temperature in air. The load cell was replaced with one having a maximum range of 45 kN to more closely reflect the anticipated loading requirements. This change of the load cell also permitted modifications to be made to the upper grip system, which was more compact and amenable to alignment adjustments. The lower grip system was changed to a Wood's metal grip, similar to that used by DuQuesnay [43]. On fatigue tests this was permitted to air cool with a slight compressive load to eliminate misalignment due to the lower threaded connections.

Two unflawed specimens were fabricated with 4 strain gauges equally spaced around the circumference specifically for the purpose of assessing alignment quality. Through careful attention to setup details, the strain indicated on the 4 gauges could be reduced to within 4% of each other. The tolerance of the gauges being used was ±1%. In the actual test specimens, bending is unavoidable due to the asymmetry of the of the flaws.

3.2.5 Growth Rate Measurement

A number of techniques were investigated for monitoring crack length. The most suitable technique examined, was found to be the thin 25μm replica method, wherein one wets the metal surface with acetone and applies the replica tape to the specimen surface. All replicas were made at an applied load of 8000N or one half of P_{max}. Then the replica was allowed to dry for three minutes, removed with adhesive tape and stored on a microscope slide. To make a full set of replicas, in duplicate, resulted in a hold time on average of 30 minutes at a nominal stress of 125 MPa.

The replica cracks were measured by tracing enlarged (≈500×) images of the replicas on graph paper. The replicas were then reviewed at a resolution of ≈1μm taking note of: any reference features, abrupt changes in the crack path or scratches on the surface and the visible crack tip marked on the graph paper. The enlarged tracings could then readily be measured.

Growth rate is then calculated from the length measurement according to the following, secant formula:

$$\left.\frac{da}{dN}\right|_{N=i} = \frac{a_{i+1}-a_{i-1}}{N_{i+1}-N_{i-1}}$$

3.2.6 Compliance Measurement

The compliance curves are used to determine the opening load. If the cracks are small, the procedure for obtaining the opening load must be sensitive. Two different strain gauging techniques were employed on each crack as different strategies were found to be more appropriate during different regions of the life of the specimen. The basic concept involved electronically differencing two strain gauge readings (ε_1-ε_2): ε_1 (active gauge) situated so as to be influenced by the crack and ε_2 located such that it was not significantly influenced by the crack (far field). This difference provided a signal dependent upon the influence of the crack.

A dedicated far field gauge, axially in line with an active gauge, was found to improve results from each active gauge over using a common far field gauge situated on the back of the specimen. The reason better results were obtained is that it eliminates the effect, on the readings, of the inevitable bending of the specimen during loading. A dedicated far field gauge, ε_2, is subjected to the same strain field as the active gauge, ε_1, less the crack influence.

To further increase the response from the strain gauge a signal gain of 2000× was applied to the gauge output. This signal was then filtered to remove high frequency noise prior to being differenced electronically. Also, gauges of as small a size as was practical were used, the active region was 1.28mm wide by 0.75mm long.

The two strain gauge techniques employed were to place the active gauge, ε_1, either on top of the c-face crack or adjacent to the tip of the a-face crack. The location of the gauges are shown in Figure 17. In Figure 17a, the relative sizes of the gauges and the corner cracks have been exaggerated. In Figure 17b only the c-face gauges have been installed. During the early stages of the test the gauge on top of the c-face crack was found to give good results. A gauge so situated did not significantly effect crack length measurements as there is little increase in the length of this crack until well into the test (i.e. generally until a/c ≈0.4 - 0.5). As one would expect the gauges mounted on top of the crack were found to exhibit successively shorter lives as the crack increased in size. This gauge failure is attributed to the majority of the strain occurring in the region of crack mouth opening.

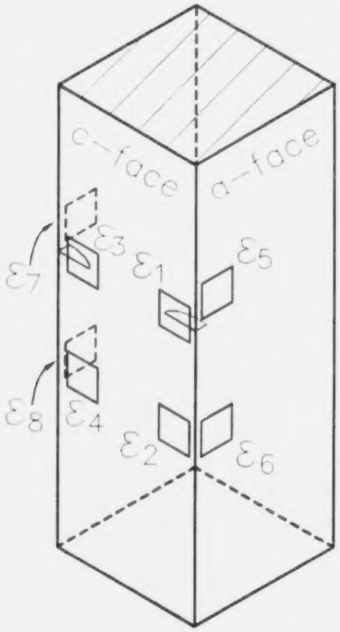
c-face
a-face
ε_7
ε_3
ε_1
ε_5
ε_8
ε_4
ε_2
ε_6

Figure 17: a) Location of the strain gauges

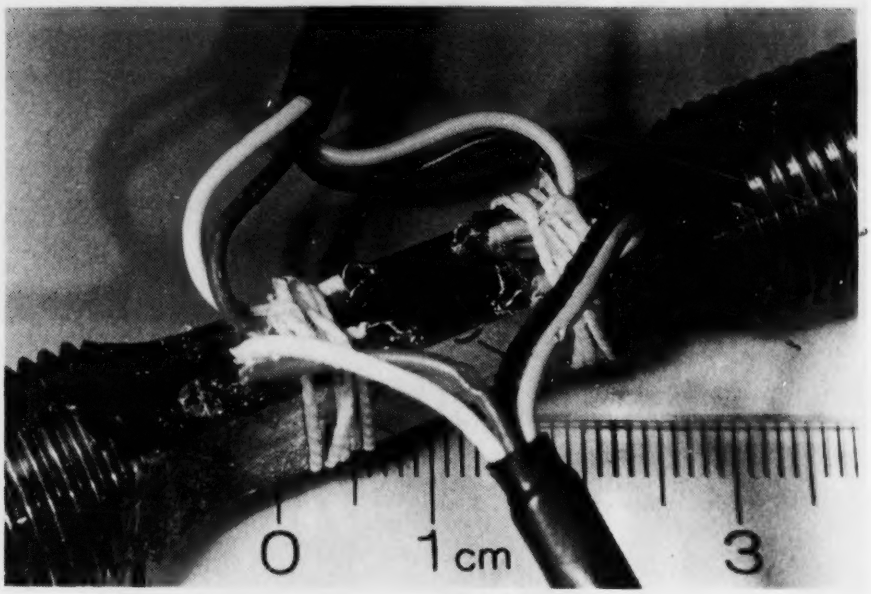

Figure 17: b) Location of the strain gauges

Due to the short life of the gauges mounted on the c-face crack, the method employing a gauge adjacent the tip of the a-face crack was also used to determine the opening load. That is, as the crack length increased, a strain gauge mounted adjacent to the crack tip on the a-face, approximately 0.3 - 0.5mm above the crack tip, was able to provide an indication of the opening load. There appears to be two competing effects which are revealed by a gauge so located:

- a strain greater than that shown by the corresponding far field gauge. This strain is due to the influence of the plastic zone surrounding the crack tip.
- a strain less than that shown by the corresponding far field gauge. Above and below the crack the stress and strain will be less than the nominal

values. When the crack is large enough this will effect the far field gauge and is referred to as shielding.

The first effect may not be detected as the calculated size of the plastic zone ahead of the crack tip is $r_p \approx 0.03$mm [56] and the observed plastically disrupted region at the surface was $r_p \approx 0.02$mm for a crack depth of about 0.15mm. Obtaining a response from a strain gauge adjacent to the crack tip, which is influenced by the crack, is dependant on gauge location relative to the current crack tip and the depth of the crack. To use a gauge adjacent the crack tip as a means of monitoring the opening load of a very small crack is difficult. The second effect, that of shielding, is larger than the first, masking the measured strain at the tip of the crack.

3.2.7 Opening Load Determination

Three procedures were investigated for determining the opening load measurements from the differential strain curves. Ideally the opening load determined from the curve will be that pertaining to the point where the crack is first open right to the tip.

The three methods were:

a) Linear intersection
b) Linear convergence
c) Curvilinear fit

Taking the differential strain curve from specimen B7 at N=5490 cycles as an example, the three methods are shown, Figure 18 and 19.

a) The linear intersection method involves fitting

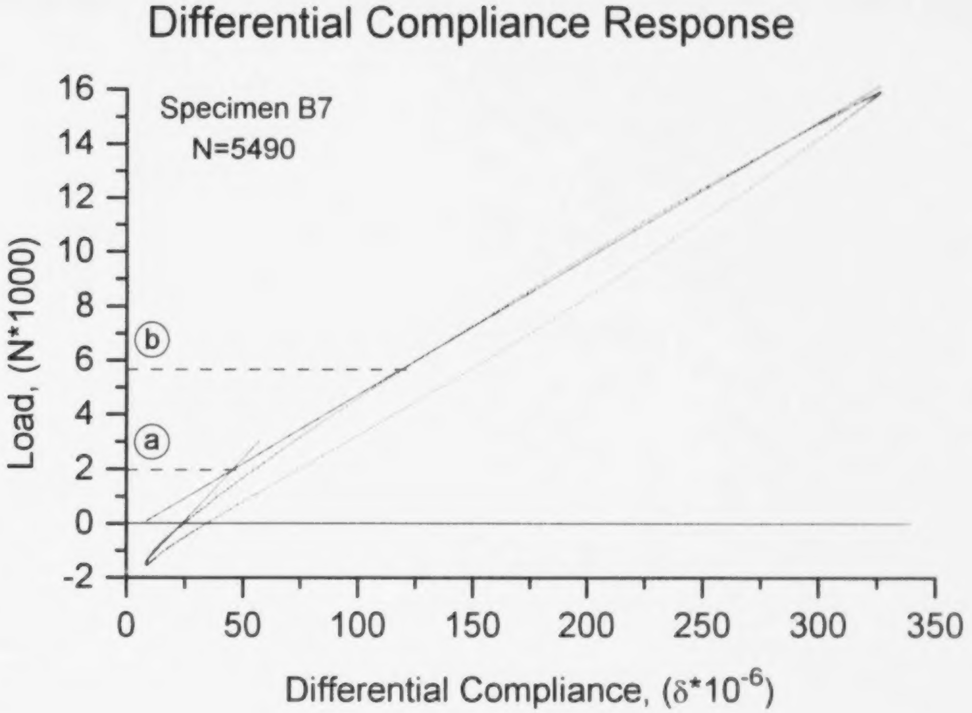

Figure 18: Linear fit methods

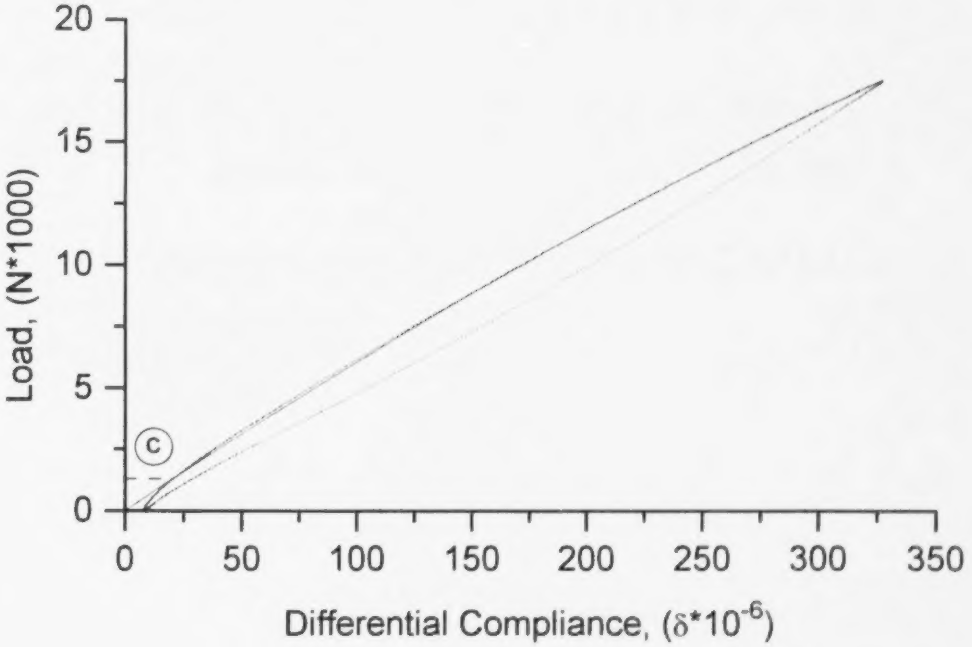

Figure 19: Curvilinear fit method

straight lines to the upper and lower parts of the loading branch. This results in an opening load value between the start of crack opening and the fully open condition. In looking at the differential strain curve the data points clearly do not fall on a straight line Figure 18, hence it is highly sensitive to which points are used in determining the 'best' linear fit. The shape of the curve changes slightly through the test due to a variety of influences. This means that effectively a different part of the curve is used to determine the opening load even when the same load range is employed for each loop analyzed.

b) Linear convergence, a modification to the intersection approach, involves taking the line fitted to the upper part of the loading branch and comparing it with the data[*]. When the linear fit and a curve fitted to the data are close together, that point is taken as being the opening load. This second approach is still sensitive to which part of the differential strain curve is utilized and so a third method was investigated.

c) The third method was to employ a curvilinear fit [57] to a Ramberg-Osgood type relation as in Figure 19. This relation is valid for materials which experience small amounts of plasticity.

$$\delta = (\varepsilon_1 - \varepsilon_2) = \frac{\Delta P}{M} + \left[\frac{\Delta P}{K'}\right]^{\frac{1}{n'}}$$ [§]

---

[*] To reduce the sensitivity of the analysis to noise, an incremental polynomial is fitted over 11 consecutive data points. When three consecutive points fall within the acceptance bandwidth, the first one is then taken as the opening load.

[§] Where ΔP is the load range and M, K' and n' are fitted constants.

From the above, δ must be zero at $\Delta P=0$. For the purpose of this analysis the loop is assumed to be symmetrical about $\Delta P/2$ and the origin shifted to the lower end of the loop. A further assumption is that it is the crack which brings about a divergence from the symmetry at the lower end. Further details of how this was programmed are given in Appendix B.

The fitted curve is compared to the data to evaluate the opening load by following up the loading branch of the compliance curve to the point where the data curve and the fitted curve come close together. This curvilinear fit was found to be more sensitive, and usually gives values close to those observed by others, that is close to zero in the early part of the test, and increasing as the test progresses.

Once the cracks became large (2 - 3mm) the test was terminated. The crack was then: photographed, etched, re-photographed, polished, re-etched and re-photographed. The final step was to cool the specimen in liquid nitrogen and break it to reveal the initial crack front and final fatigue crack growth region.

3.2.8 Summary of Experimental Details

There are two primary aspects to this investigation: initiating the small corner cracks and monitoring their subsequent behaviour under tension fatigue loading. The specimen fabrication and pre-cracking technique minimize residual stresses ahead of the crack tip and in the wake of the crack. The size of the crack is monitored using a thin film replica technique, having a resolution capability of 1μm. The crack opening load is measured by two differential strain gauge techniques. The two techniques employ the active gauge either on top of the mouth of the crack or adjacent the tip of the growing crack. The shape of the initial crack front is marked by heat coloration of the FT specimen prior to fatigue loading. Loading is conducted at a load ratio close to zero, with the maximum stress being 250 MPa. Microstructure photographs are made of the etched surface after the fatigue loading is completed. The final crack front is identified by fracturing the FT specimen at low temperature (-190°C).

In this experimental investigation, certain assumptions were made:

- a corner crack on a square, straight specimen was assumed to be a quarter ellipse.
- the initial damage in the FT specimens is negligible.
- the crack will not grow in length (along the c-face) until well into the test.
- the interaction of the two corner cracks will not be significant during the early part of the test.

4.0 Experimental Results

The majority of the data are presented in a graphical format. Numerical data are given in Appendix A.

4.1 Development of Crack Length and Depth

Initial crack length, c, and depth, a, have been measured using three different techniques. Replica measurements and SEM based measurements were presented in the Table 4 previously. Table 5 presents the initial and final dimensions of the fatigue cracks based on initial replica and, final direct measurement of the specimen after being cooled in liquid nitrogen and broken. Replica measurements are not available at the end of the test as the large amount of damage makes the readings difficult.

Table 5: Fracture measurement of initial and final crack size (mm).

	B4		B7		B8	
	Replica	Post-fract.	Replica	Post-fract.	Replica	Post-fract.
a_L	0.574	0.61	0.266	0.29	0.050	0.14
c_L	1.61	1.79	1.280	1.38	2.003	2.00
a_R	0.520	0.65	0.088	--	0.377	0.36
c_R	1.93	1.83	0.820	--	2.404	2.48
N_{EoT}	213,860		305,155		141,540	
a_L	Specimen broken in the testing machine. No final crack front available.		--	2.88	--	3.01
c_L			--	3.03	--	3.78
a_R			--	0.63	--	0.83
c_R			--	1.01	--	2.36

The shape of the initial and final crack fronts has been measured and is plotted in Figure 20 following for specimens B7 and B8.

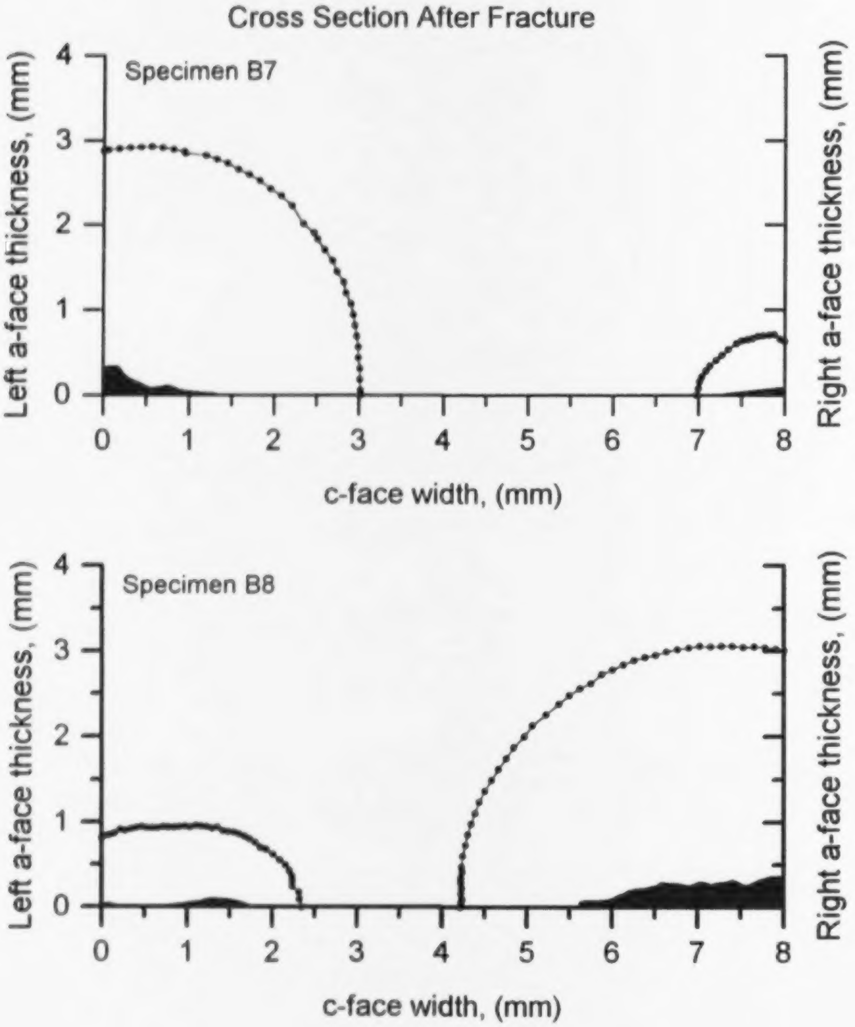

Figure 20: Crack fronts based on after fracture measurements

Figures 21 - 24 show the development of the size of the crack through the duration of each test. The test on specimen B6 was terminated early as it was primarily used to evaluate the technique being used to measure the opening load.

During those parts of the test for which the c-face crack was covered by a strain gauge for a significant part of the test, no data was collected. The data point given at N=0 was obtained prior to the strain gauge being mounted. In the figures a dashed line is used to show the estimated length of the c-face crack.

In Figure 24, pertaining to specimen B8, no length data is available for the c_L crack. This is due to the strain gauge being on top of this crack for the duration of the test. Though the strain gauge failed at N=55,900 cycles, it was not removed because this would have involved taking the specimen out of the testing machine. Given that one can sometimes detect events such as specimen removal in the growth rate and opening load data, every effort was made to avoid removing the specimen from the testing machine.

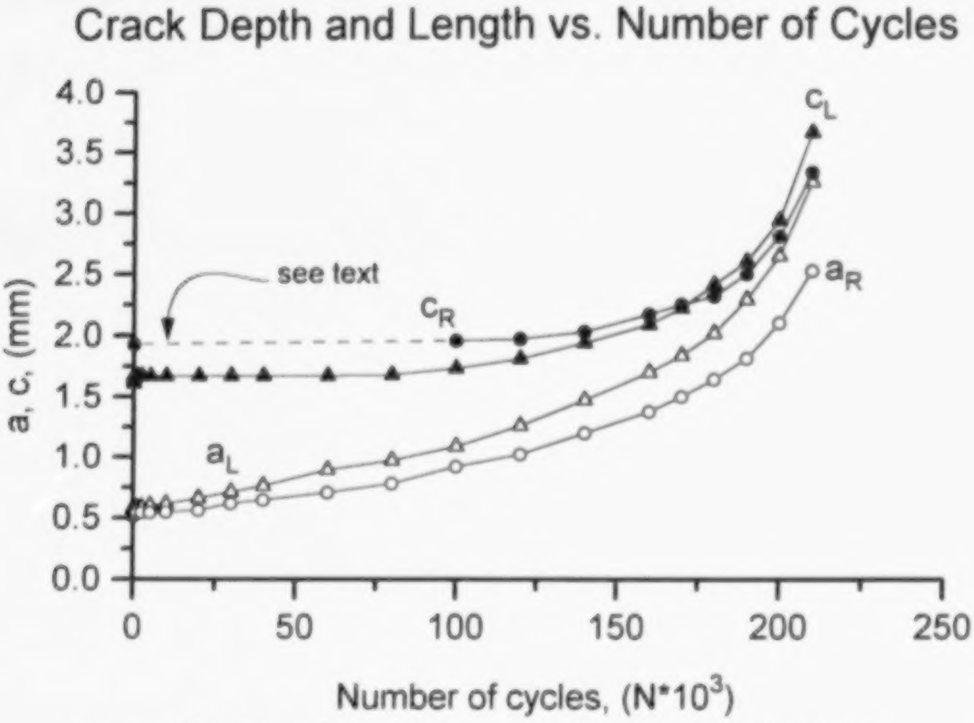

Crack Depth and Length vs. Number of Cycles

Figure 21: Specimen B4, crack size through the test

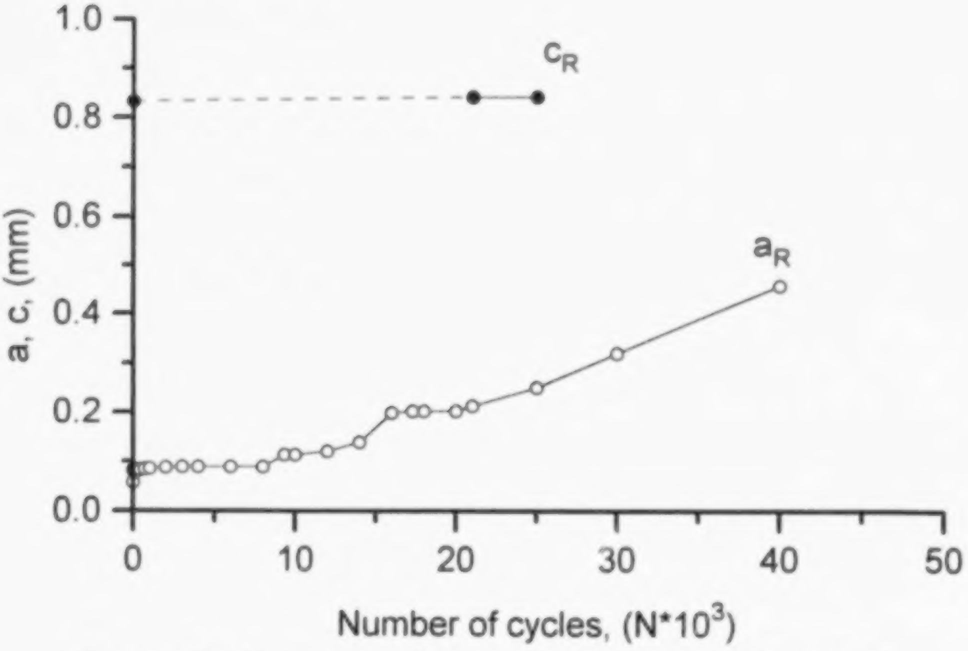

Figure 22: Specimen B6 crack size through the test

Crack Depth and Length vs. Number of Cycles

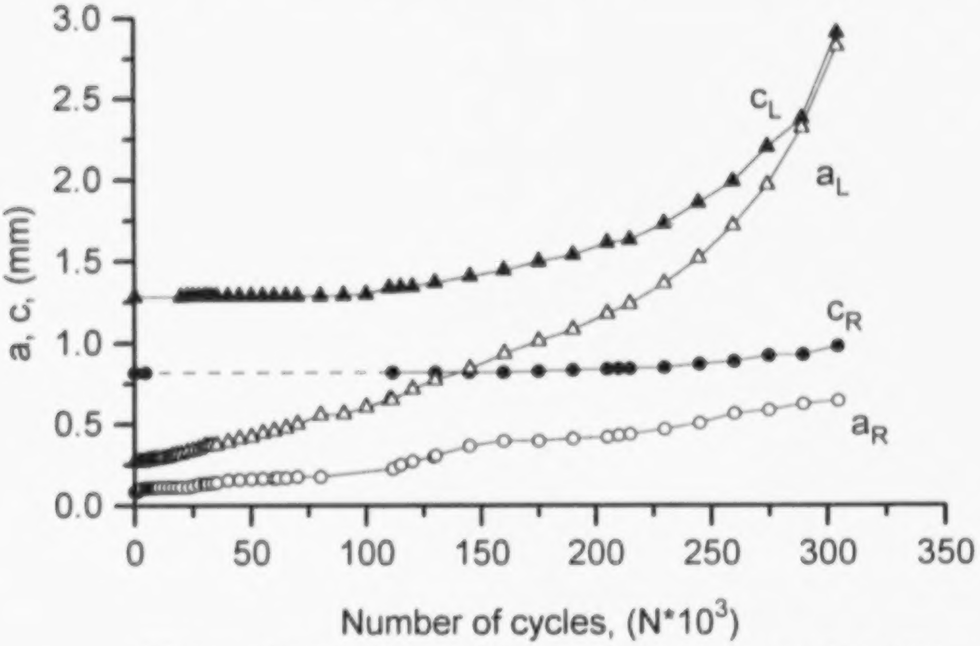

Figure 23: Specimen B7, crack size through the test

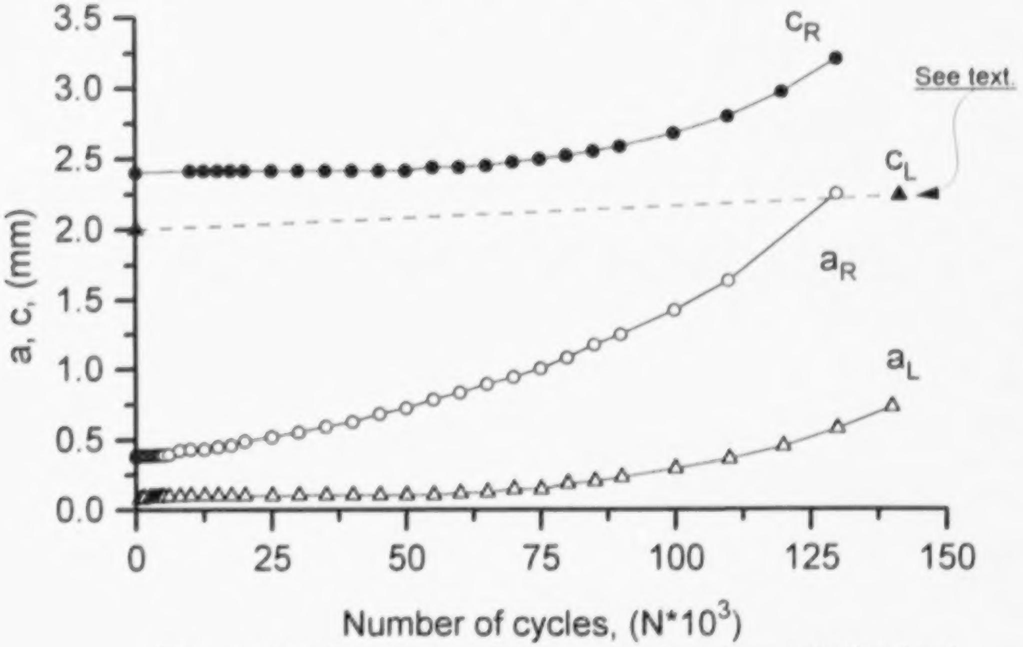

Figure 24: Specimen B8, crack size through the test

The change in the aspect ratio of the corner crack through the test is presented in Figures 25 and 26. One might normally plot the aspect ratio versus the number of cycles normalized with respect to the number of cycles until specimen failure. However, the tests conducted here were terminated once the crack was well into the long crack growth region, hence N_f is not available. Instead the aspect ratio has been plotted versus the crack depth normalized with respect to the initial crack size, a_0. The value of a_0 is included beside the corresponding curve.

There are a number of trends which can be identified:

- The aspect ratio of one of the corner cracks, on a given specimen converges towards a value greater than 0.9.
- The greater the initial aspect ratio, or larger the initial crack depth, the more quickly the aspect ratio will reach a maximum value (steeper slope).
- The maximum aspect ratio, saturation, is reached at a crack depth of ≈2mm.

The aspect ratio may not reach a value of 1.0 due to the geometry of the specimen. For example, on specimen B4, when saturation is reached the combined length of the two c-face cracks is 7mm, leaving a small uncracked region. With the specimens being 8mm wide the uncracked region will experience interaction of the two cracks, hence will serve to reduce a/c.

Evolution of the Aspect Ratio with Increasing Crack Depth

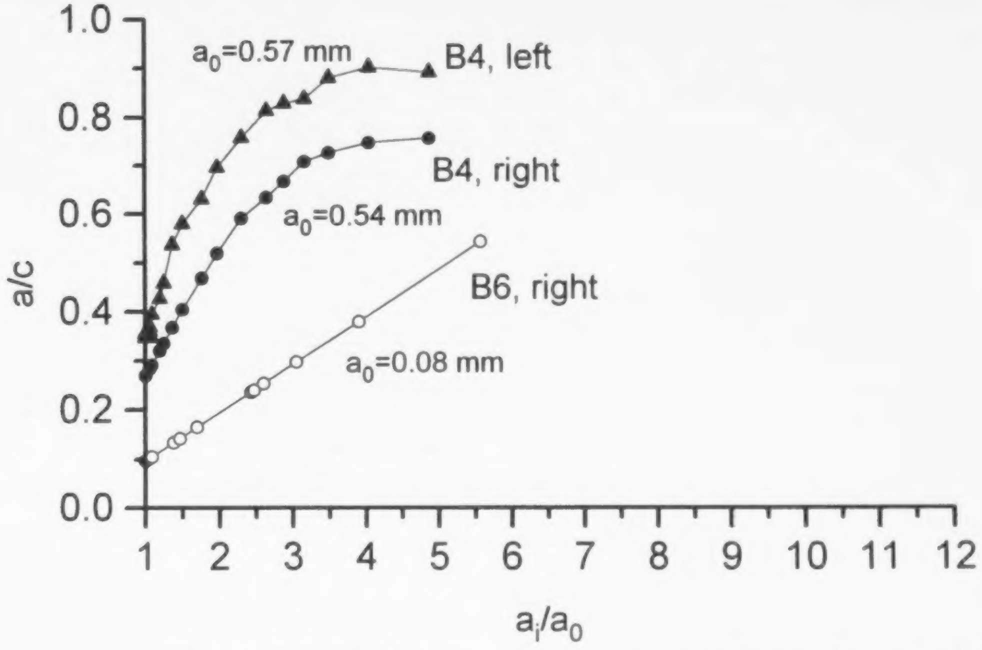

Figure 25: Shape development, specimen B4 and B6

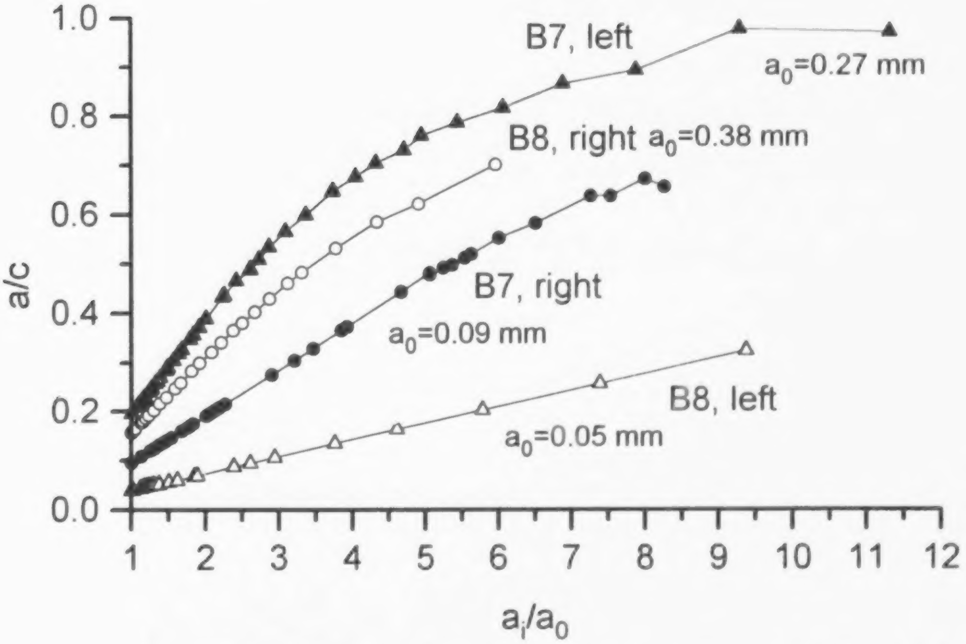

Figure 26: Shape development, specimen B7 and B8

4.2 Strain Gauge Responsiveness

4.2.1 Differential Compliance

The differential strain, $\delta=\varepsilon_1-\varepsilon_2$, of the strain gauge technique, and the change thereof, is presented in Figures 27 - 30. The difference in strain is divided by the applied load range, ΔP, for that particular cycle to reduce the influence of minor cycle-to-cycle load variations. The value of $\delta/\Delta P$ is referred to as the differential compliance.

These graphs demonstrate a number of phenomena:

a. A gauge situated on top of the c-face crack gives a greater signal than a gauge located adjacent to the tip of the a-face crack.

b. There is good reproducibility in the strain gauging technique. Care is necessary to obtain consistent results.

Figures 27 and 28 represent the left and right sides of specimen B7. Since the gauge life was found to be quite short, it was replaced several times in order to collect further data. Each gauge change is represented on the graph with a different symbol. The duration between the failure of one gauge and the installation of the next gauge, has been joined with a dotted line to aid in following the trend.

The sensitivity of the system is high. For example, there is a curvature in the early stages of the differential compliance curves based on the response of the c-face gauges. It could be that this represents a strain hardening. Conversely, this change in the curvature may be a replication effect in that the number of cycles between the loading associated with making successive replicas is gradually increased. The relaxation associated with the increased number of load cycles will then be more significant. This replication effect is clearly evident in the response of the a-face gauges (Figure 30, $N \approx 85,000$ cycles).

Figures 29 and 30 show the differential compliance of specimen B8. The left side c-face crack utilizes two far field gauges during the test. This is because the ε_4 gauge failed at $N \approx 17,560$ cycles and so the ε_8 gauge (around the corner from the ε_4 gauge) was used instead of the ε_4 gauge. This results in the discontinuity observed in Figure 29 at 17,575 cycles. The effect this has on the opening load calculations is within the scatter of the data points (see data table for the B8 left side crack in Appendix C).

The validity of values collected late in the test may be called into question, because during the later parts of the test the far field gauges experienced significant shielding due to the increasing size of the crack. This shielding, of the far field gauges, only affects data collected when the cracks are relatively large. Since the gauges situated on top of the c-face crack have a short life it will only be data from the adjacent side, or a-face, gauges that is affected. This is considered in greater detail in section 4.3.3. pertaining to the far field compliance.

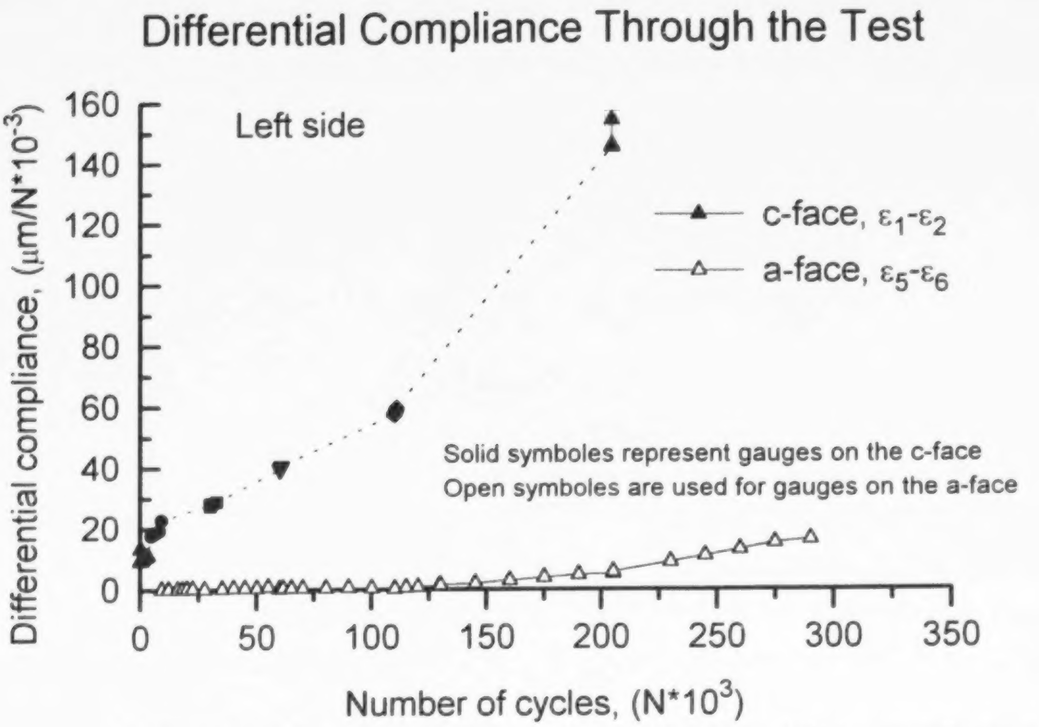

Differential Compliance Through the Test

Solid symboles represent gauges on the c-face
Open symboles are used for gauges on the a-face

Figure 27: Specimen B7, measured differential compliance

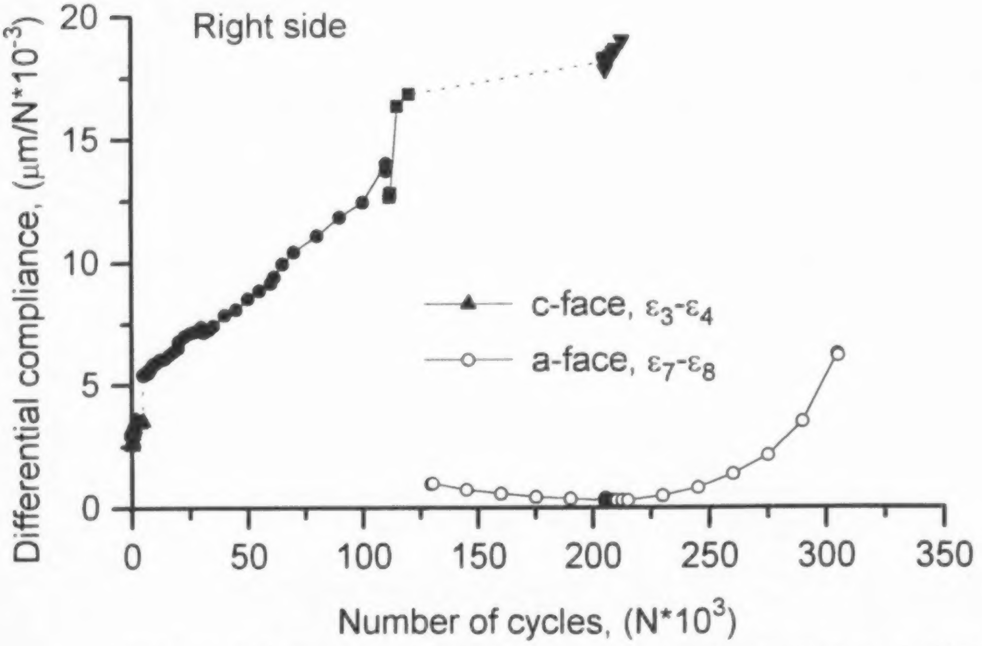

Figure 28: Specimen B7, measured differential compliance

Differential Compliance Through the Test

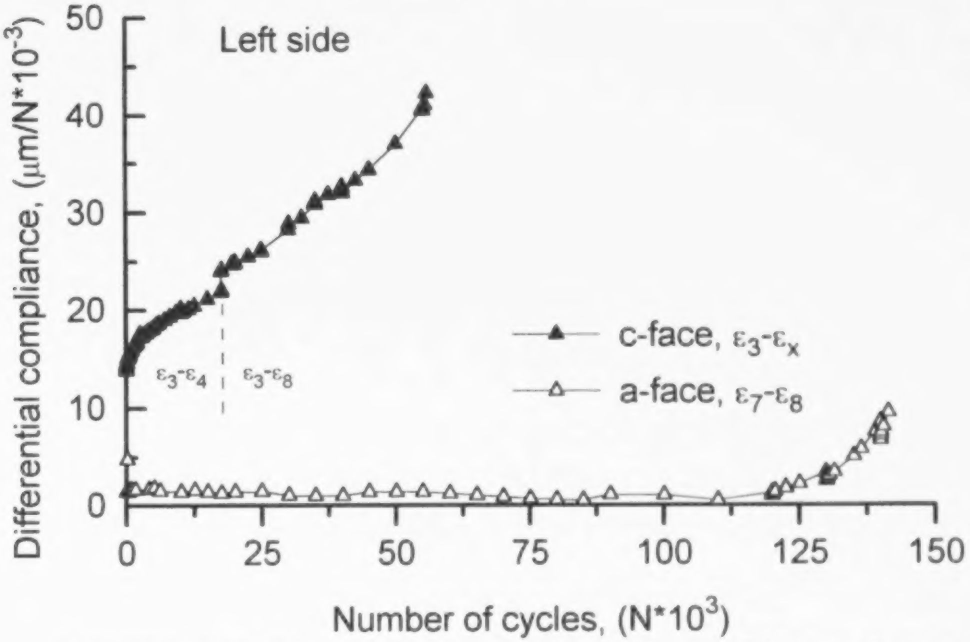

Figure 29: Specimen B8, measured differential compliance

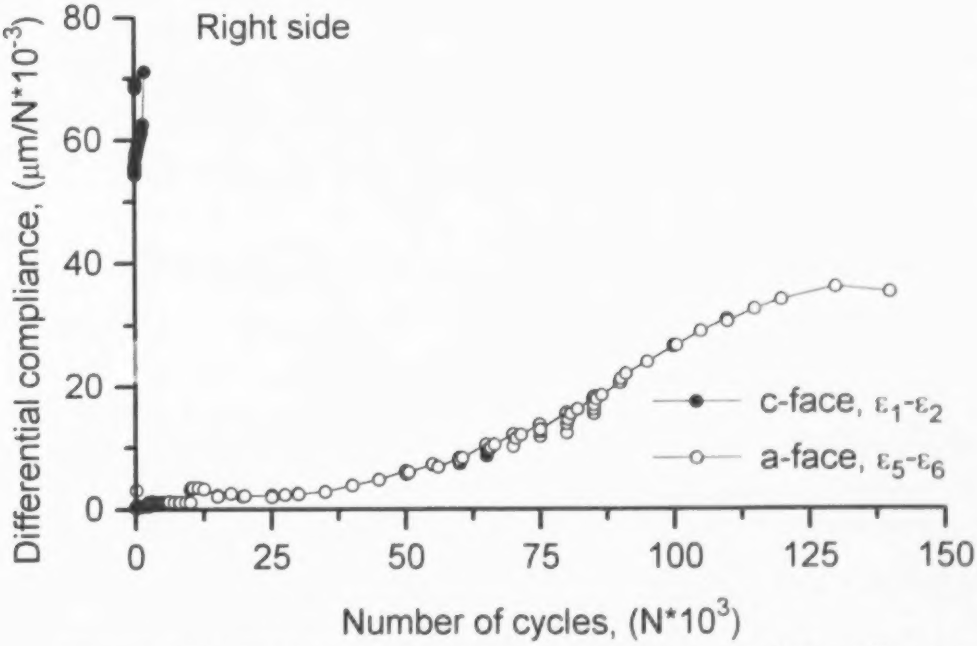

Figure 30: Specimen B8, measured differential compliance

The effectiveness of using strain gauges adjacent to the crack to determine the opening load is specifically presented in Figures 31 and 32 and later in section 4.3. This is done by separately plotting the compliance measured by the active and far field gauges. Theoretically the closer, or active gauge, should experience shielding to a greater extent than the far field gauge. However, in practice, the response of the active gauge does not differ appreciably from the far field gauge until the crack is of considerable size, a>0.6mm. It is not until the two curves separate that reasonable opening load calculations can be made.

As the crack continues to grow the far field gauge response may increase or decrease. Taking Figure 32 as an example, the far field gauge below the right side crack, ε_6, reveals a decrease in response as the crack increases in size, due to shielding. The far field gauge below the left side crack, ε_8, shows an increase in response, presumably due to bending of the specimen.

The influence that the crack has on the far field gauges cannot be discounted. Once a far field gauge response has been significantly affected, it is no longer appropriate to use it in assessing the opening load values, therefore such data are rejected.

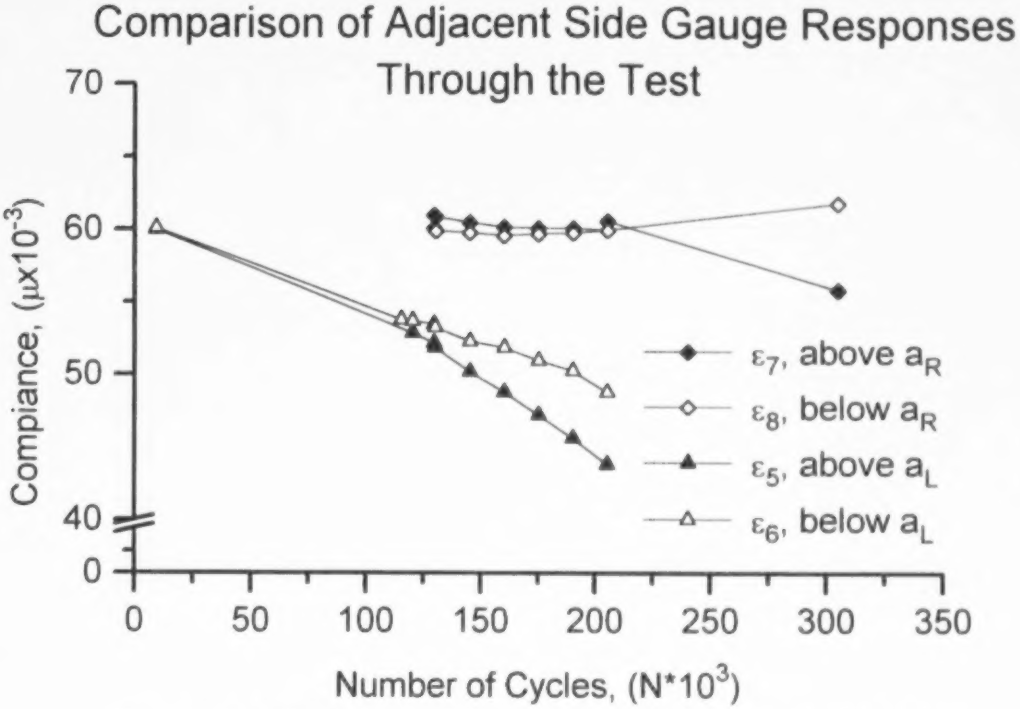

Figure 31: Specimen B7, adjacent side gauge response

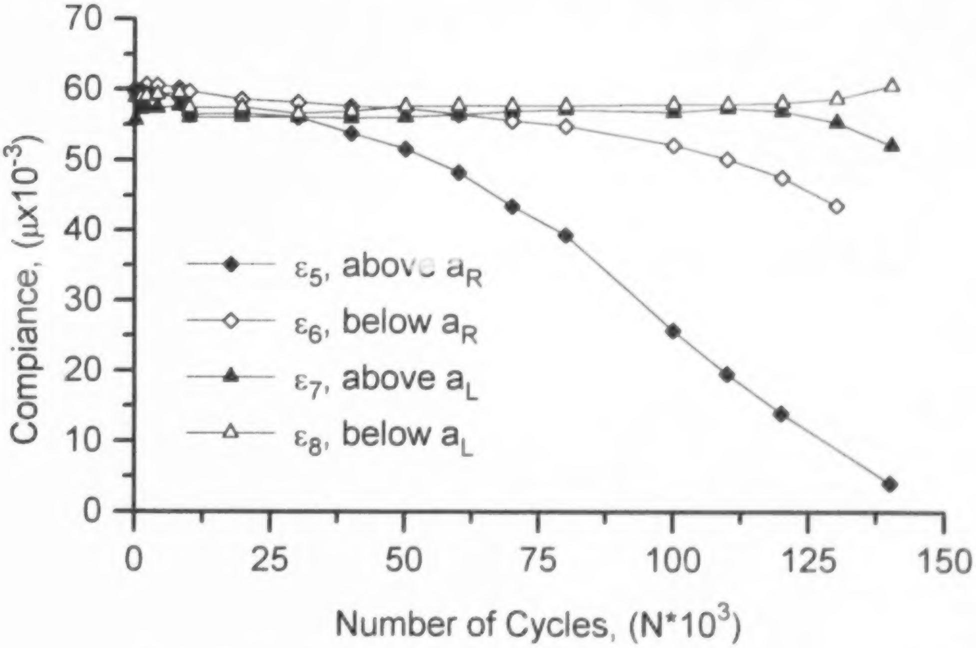

Figure 32: Specimen B8, adjacent side gauge response

4.2.2 Far Field Compliance

The far field gauges are located ≈2mm below the crack (a or c face). The compliance indicated by the far field gauges, $[(\varepsilon_{i,\,max}-\varepsilon_{i,\,min})/\Delta P]$[*], is shown in Figures 33 and 34. When the crack becomes large, they will be shielded from the full value of the nominal strain, the extent of the shielding increasing with the size of the crack. These figures can be used to identify the extent of shielding on the far field gauges and the point during the test when it occurs. Although these gauges are close to the crack, they are appropriately placed as it is the early part of the test which is of the greatest interest.

The primary purpose of monitoring the strain is to determine the opening load. When the response of the far field gauge has changed appreciably from its initial value, ±10%, then it will no longer be used in the calculation of the opening load. One can see from Figure 33, pertaining to specimen B7, that this corresponds to all cycles beyond 210,000 cycles for the right side and beyond about 120,000 cycles on the left side. Likewise in Figure 34 for specimen B8, data past 80,000 cycles can be rejected from the right side, and beyond 130,000 cycles for the left side. Clearly in this study, rejecting data due to shielding by the crack only becomes an issue for the strain gauges adjacent to the a-face crack.

---

[*] Where **i** is the location of the strain gauge.

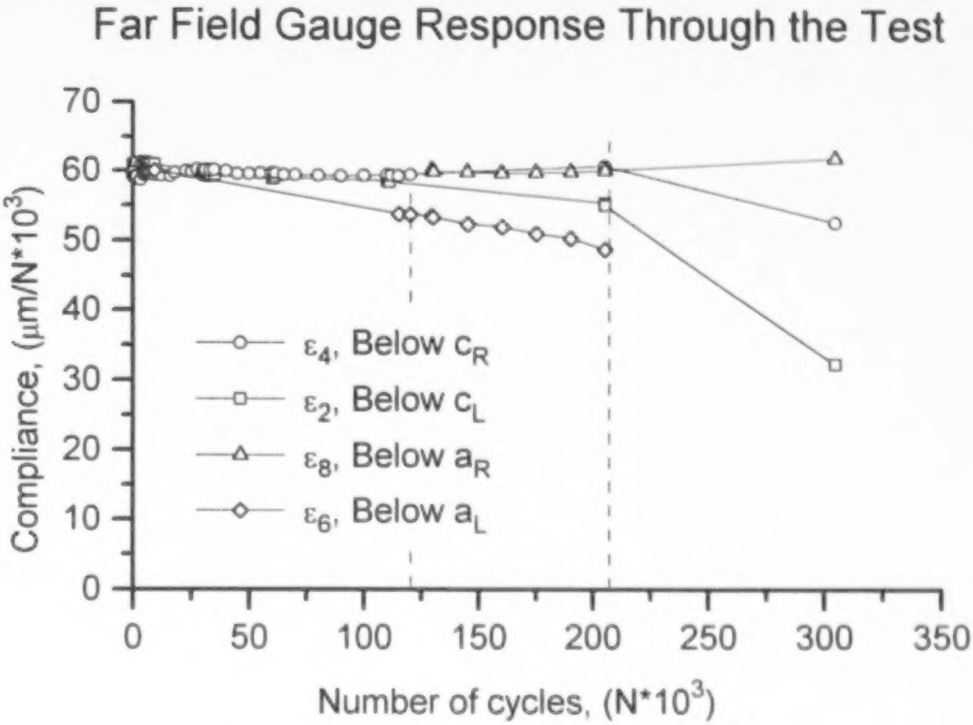

Figure 33: Specimen B7, far field gauge response

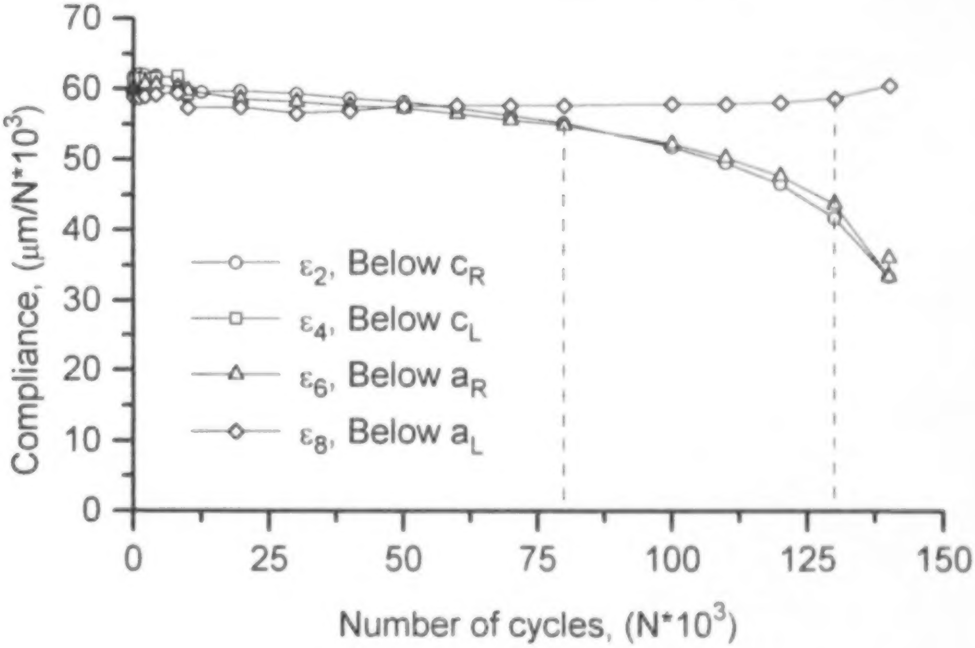

Figure 34: Specimen B8, far field gauge response

4.3 Opening Load Development

4.3.1 Opening Load Development, c-face Gauges

Opening load data, P_{open}/P_{max} versus the number of cycles, are presented in Figures 35 - 38 for specimens B7 and B8. In these graphs the active gauge is located on top of the c-face crack. There is no data available for the earlier specimens.

The result from each corner crack is presented separately, employing both the traditional linear intercept method, using solid symbols, and the curvilinear fit method, employing open symbols. This approach has been described earlier, (see section 3.2.7). When the far field gauges are no longer providing accurate far field strain values, as described in section 4.2.2, the resulting opening load data has not been included on the graphs. However, all data is tabulated in Appendix C.

The graphs are plotted using linear scales with an inset, where appropriate, showing the first two thousand cycles in greater detail. Replacement of the strain gauges is indicated by using a symbol of a different shape. The data points have been connected by straight lines. When no strain gauge was mounted over top the crack no connecting line is included. In Figures 35, 36 and 37, a dashed curve has been used to connect the average of each cluster of data points to assist in following the trend of the data.

These three figures also suggest there is a regular effect associated with the gauge replacement, since after the gauge is installed the indicated load decreases as further cycles are applied. This may be attributed to a number of factors; perhaps associated with removal of the specimen, mounting the gauge or collecting replicas. These same figures do not reveal as great an increase in the steady state opening load, based on the linear intercept technique. In fact, in Figures 35 and 37 the opening load interpretation is observed to decrease when the linear intercept method is used. This decrease is attributed to the inherent problems of the linear intercept method. As discussed in section 3.2.7, the actual compliance curve changes shape during the test, to greater curvature. However the same range of data points is used in the analysis through out the test. The linear intercept method has difficulty responding to this change in shape. The difficulty may be seen by the method indicating a decrease in the opening load.

Of the two methods used to calculate the opening load, both show the opening load increasing in the early part of the life of the specimen and subsequently converging towards a steady state value. In Figures 35 and 36 the results based on the curvilinear method identify an initial opening load close to zero, whereas the linear intersection technique is about 5% higher. As the test progressed the opening load using the curvilinear method showed a greater increase than did the linear intersection approach. Hence, the curvilinear technique used may be more sensitive to physical events which influence the closure, but will also be more sensitive to other effects.

Figures 37 and 38 present the opening load data for specimen B8. Again similar trends are observed. In Figure 37, pertaining to the left side crack, a significant drop can be seen at 10,000 cycles. This corresponds to the specimen being removed from the machine in order that the previously damaged c-face gauge on the right side crack could be removed. In this case the dashed trend line has also been interrupted so that it will more closely follow the data. As shown in Figure 38, the right side c-face gauge failed prior to 2000 cycles. In order to minimize interruptions in the test this gauge was not replaced, thus the development of the steady state conditions was not recorded.

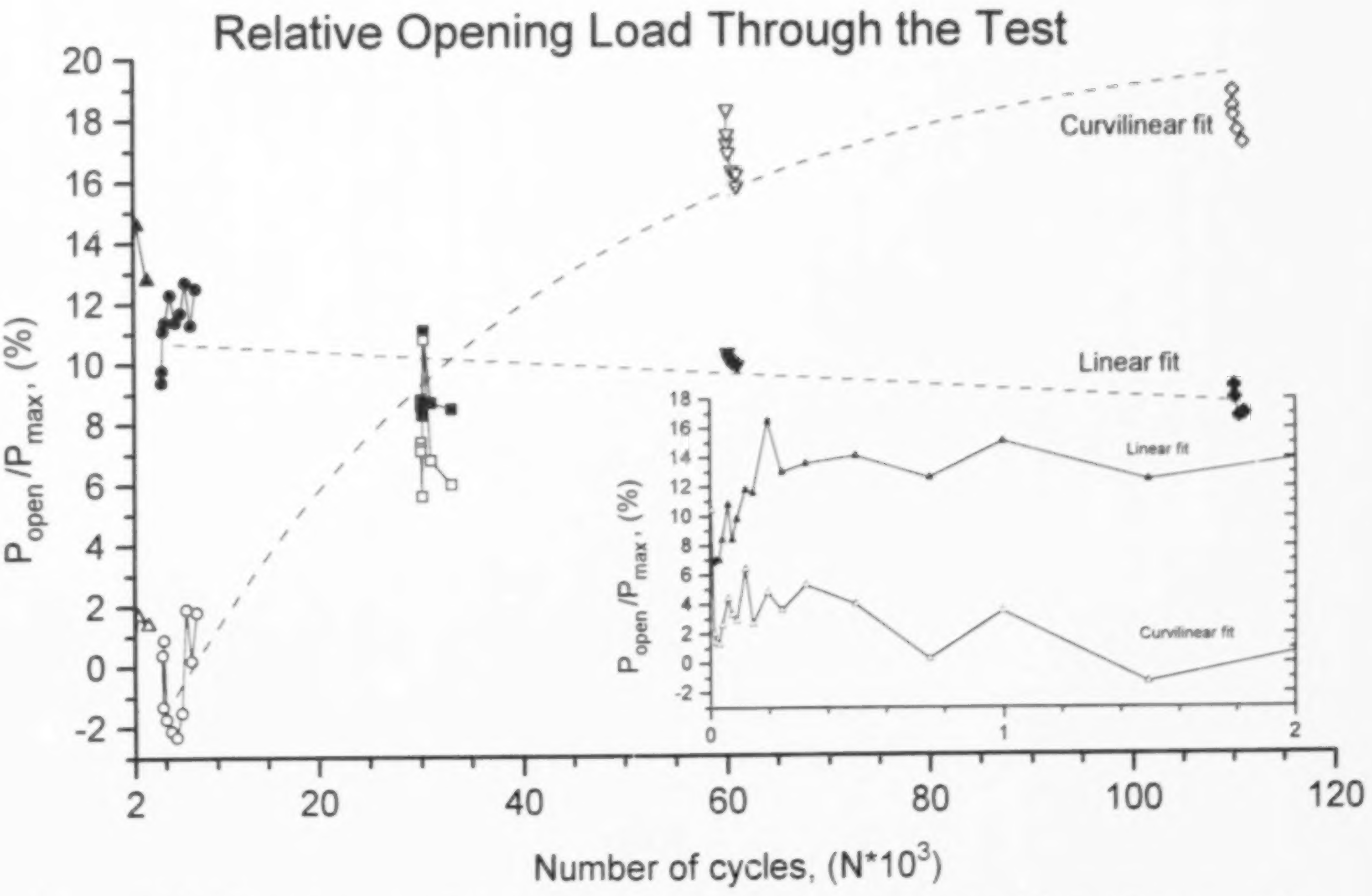

Figure 35: Specimen B7, left side, active gauge on top of the c-face crack

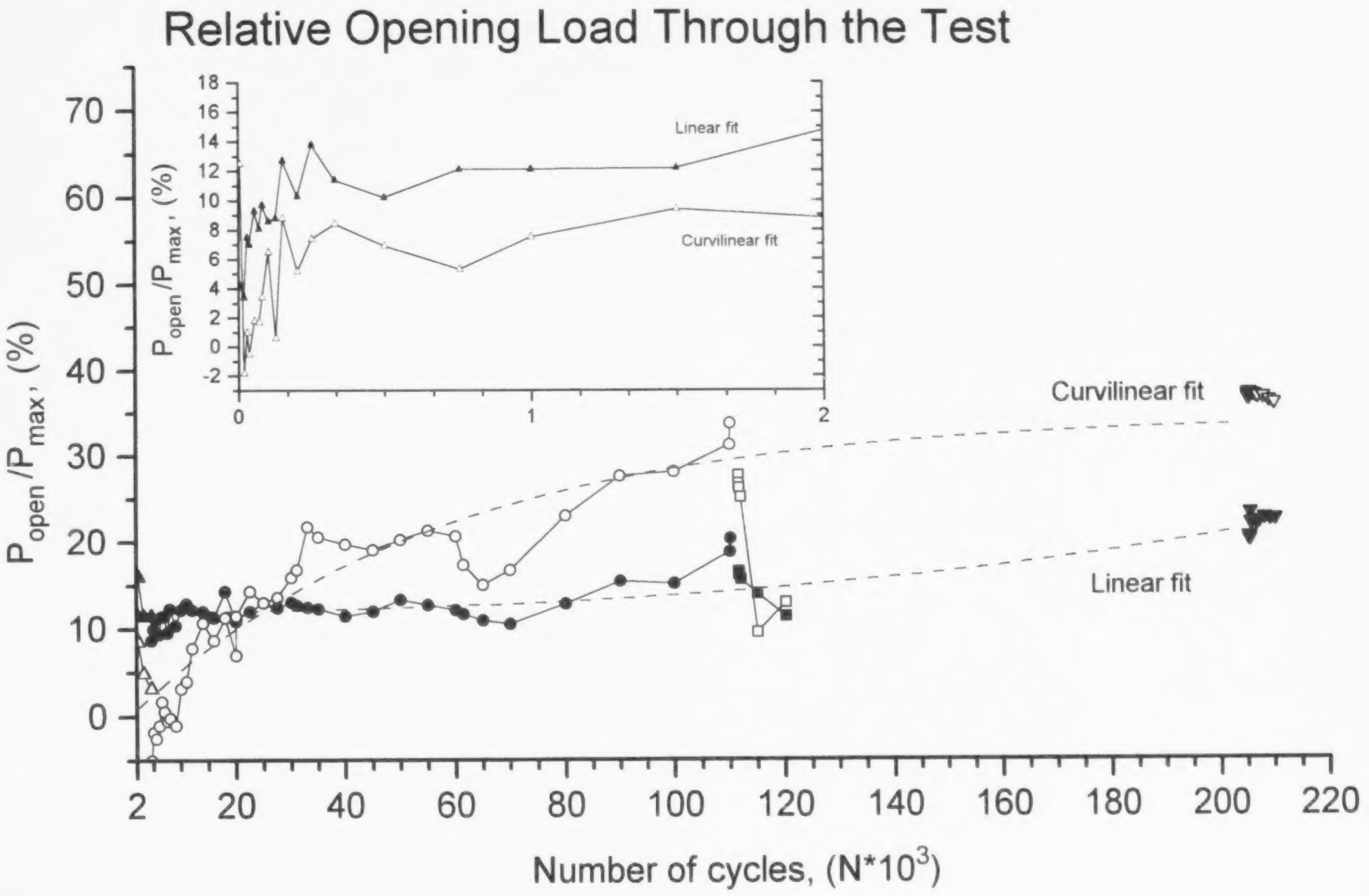

Figure 36: Specimen B7, right side, active gauge on top of the c-face crack

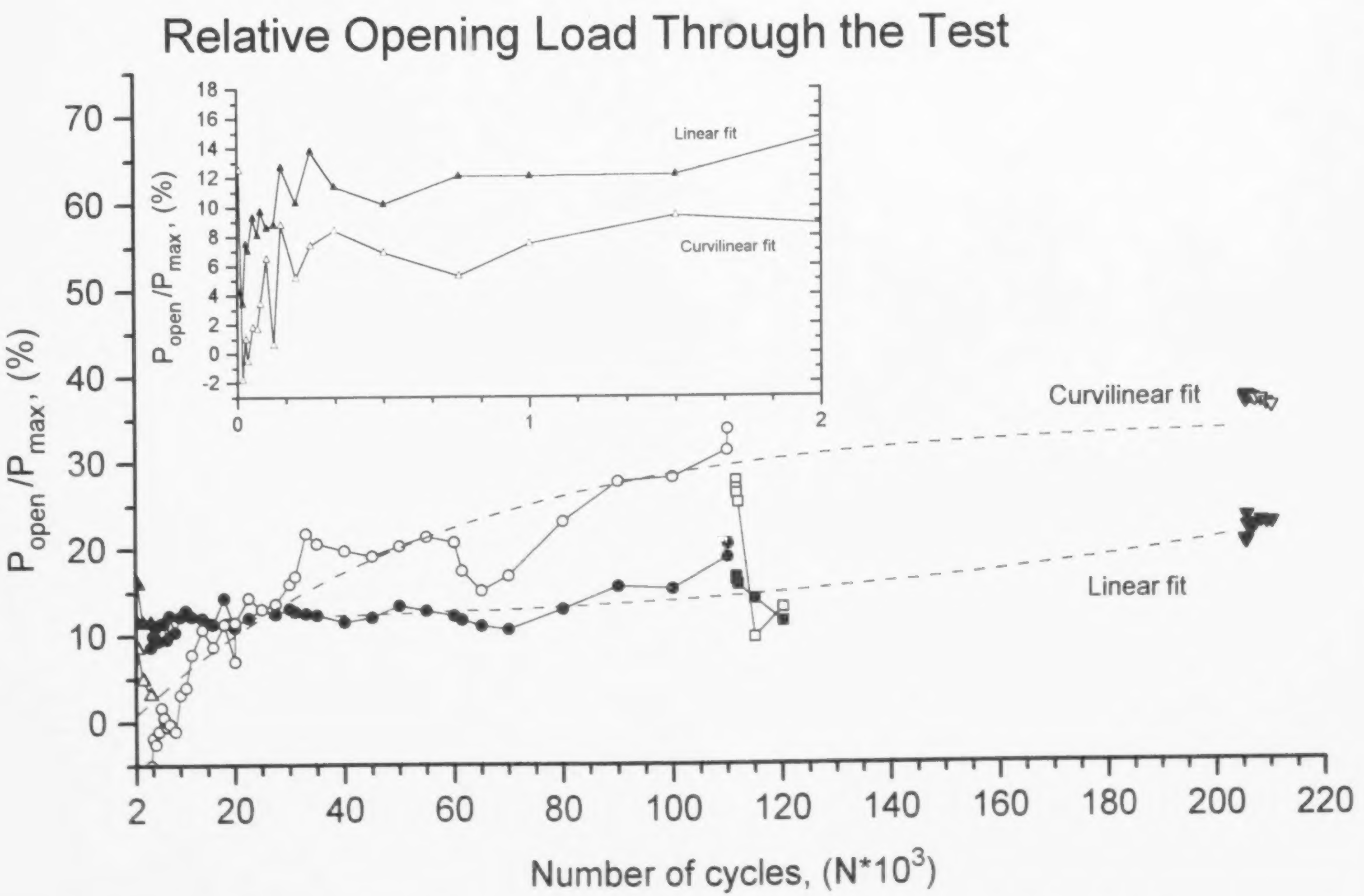

Figure 36: Specimen B7, right side, active gauge on top of the c-face crack

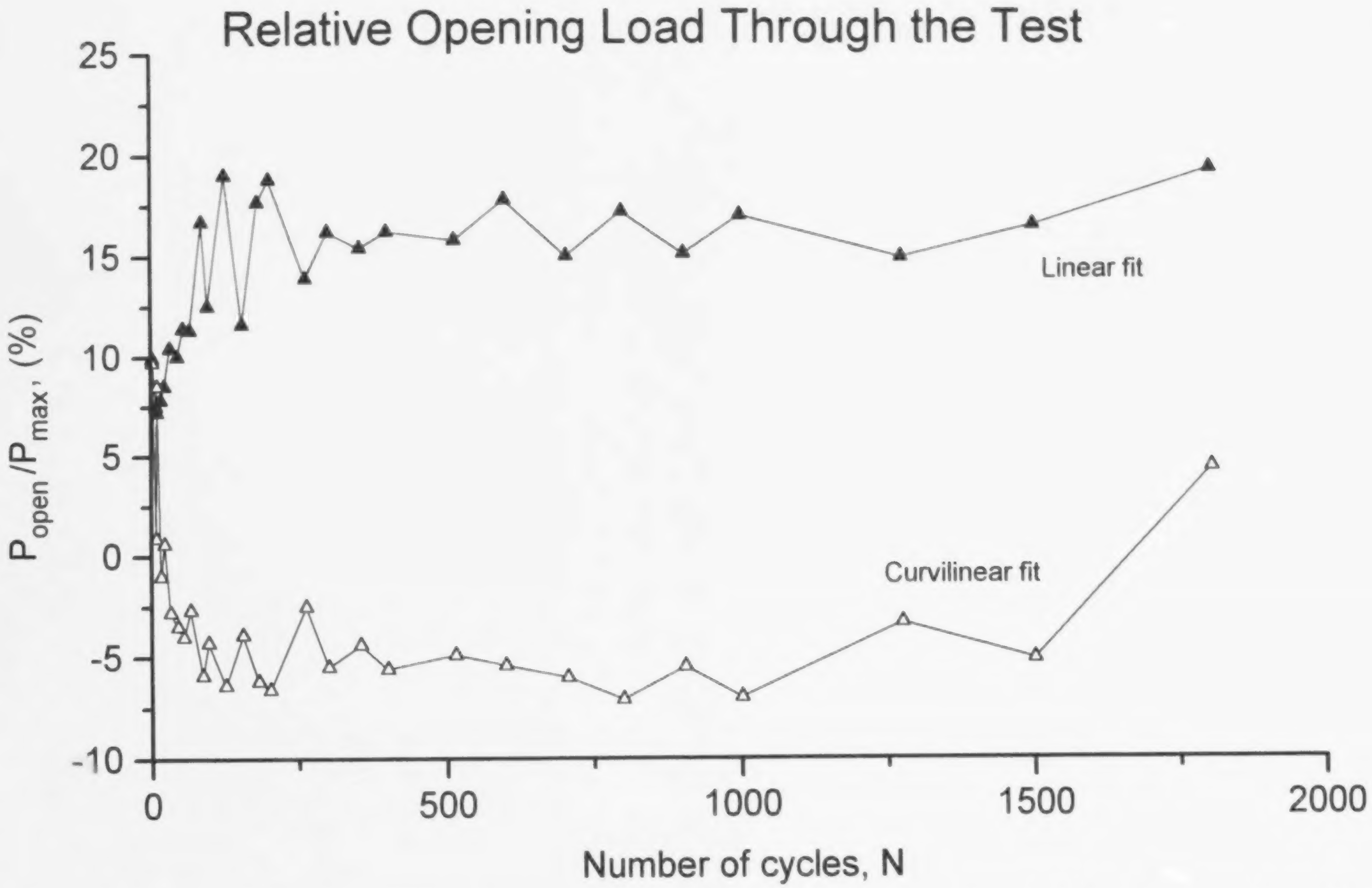

Figure 38: Specimen B8, right side, active gauge on top of the c-face crack

4.3.2 Opening Load Development, a-face Gauges

Opening load data, as recorded by active gauges located adjacent to the tip of the a-face crack, are given in Figures 39 and 40. Early in the test the response from the adjacent and far field gauges was very nearly the same. This results in the differential signal being small and hence sensitive to measurement noise. Therefore, the early life data has not been included on the graphs.

The compliance loops recorded showed considerable variability through the test. The analytic method presented on the graphs is the linear convergent approach described in section 3.2.7 under method b). In order to obtain more reasonable results, a different range of data points and accept bandwidth was used for the a-face data than for the c-face data.

The far field gauges are susceptible to shielding as the crack increases in size, as discussed in section 4.2.2. Applying the criteria presented in that section, opening load values cannot be calculated if the corresponding far field gauges are being shielded. Opening load values could not be obtained from the early life data as the signal from the active and far field gauges was similar. Thus, when the far field response was subtracted from that of the active gauges the resulting signal was extremely small. Since data are rejected from both the early and late parts of the test, the range of valid opening load data is narrow and differs with each crack investigated. This is shown in Table 6.

Table 6: Range of valid opening load data from the adjacent side gauges.

Specimen	Range of cycles
B7, right side	205,500 - 210,000
B7, left side	70,050 - 120,000
B8, right side	25,100 - 80,750
B8, left side	85,000 - 125,000

In the figures, the data collected late in the test are also included in an attempt to extend the trend revealed. This is justified in that rejecting data because the far field gauge is experiencing shielding might be an overly strict criteria. However, the connecting line between the points is given as dashed instead of solid. All opening load data are given in Appendix C.

A comparison of the two methods of determining the opening load, a-face and c-face strain gauges, can be made. Figures 39 and 40 utilize active gauges adjacent the tip of the crack, Figures 35 - 38 employ active gauges on top of the c-face crack. Since, the data from the adjacent gauges is only valid later in the test it provides information on the steady state opening load. Where overlap is present, the opening load data from the gauges located on top of the crack are from 0 to 10% lower than using the gauges adjacent the crack. Inconsistencies in collecting replicas or the influence of installing new strain gauges may account for fluctuations in opening load values in Figure 40.

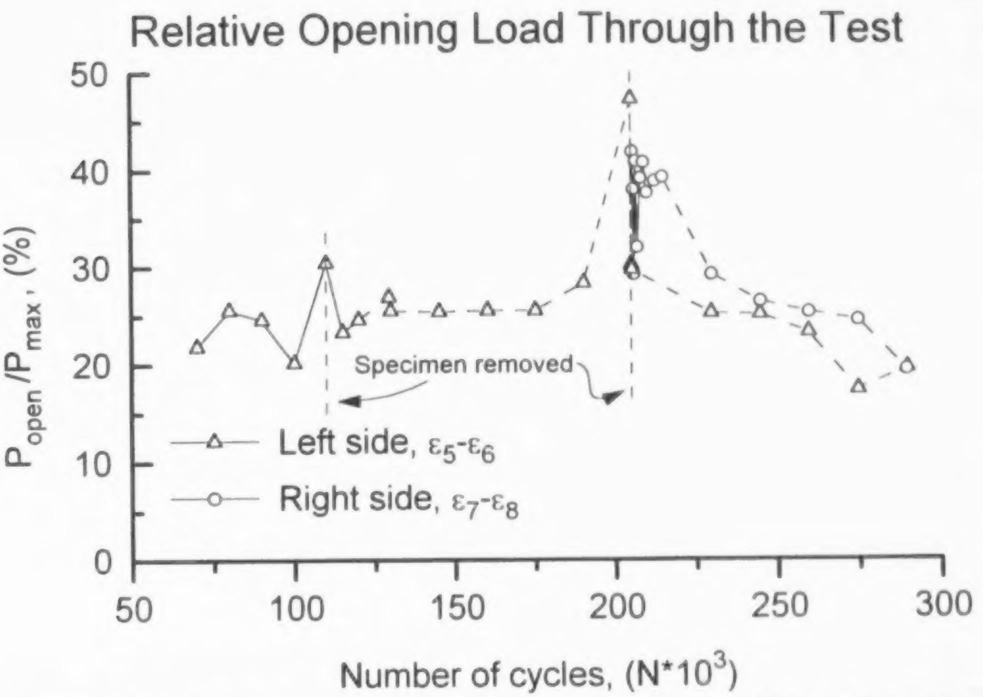

Figure 39: Specimen B7, active gauge adjacent the a-face crack

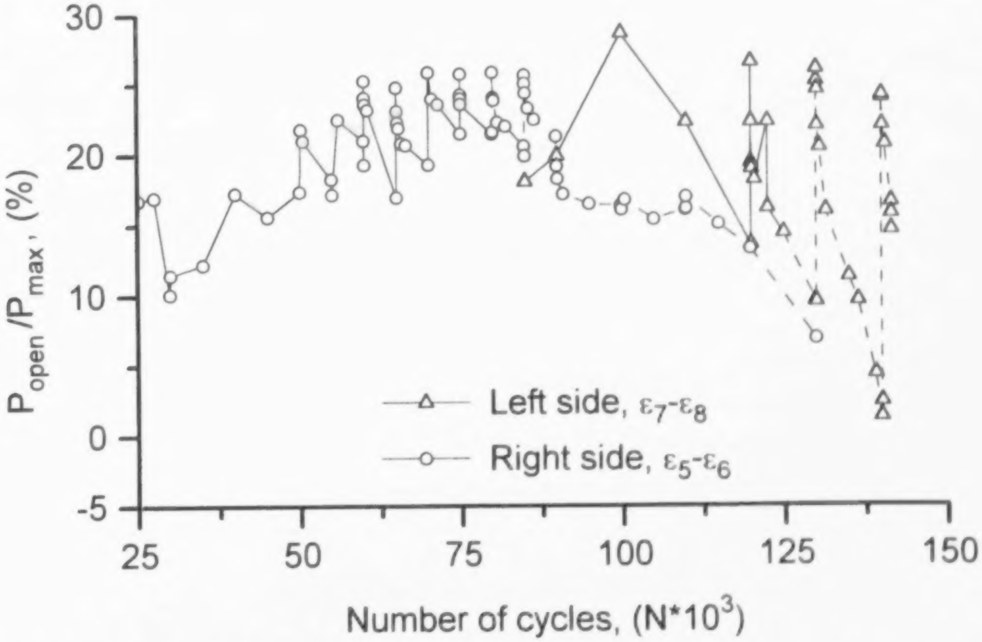

Figure 40: Specimen B8, active gauge adjacent the a-face crack

Additionally, Figure 40 shows an effect associated with collecting replicas of the cracks. This is presented in greater detail in Figure 41. On this figure, the cycle numbers at which the compliance loops were recorded are shown. It is clearly evident that an increase in the opening load and decrease in specimen compliance, see Figure 30, is identified after the replication procedure. This is followed by a gradual recovery of the compliance or opening load to the value prior to the replication event.

One may attribute this ≈5% increase in the opening load, to the specimen being subjected to a steady load of 8000N from which there may be plastic tensile strain at the crack tip bringing about residual tensile stresses upon release of the load. Such residual stresses would bring about the closure phenomenon of Figure 5. Alternately, the acetone might transport debris into the crack, effectively propping the crack open giving the appearance of an increase in the opening load (Figure 6).

This abrupt ≈5% increase in the opening load associated with collecting the replicas shows the system is quite sensitive. This reinforces the necessity of collecting opening load data in a consistent fashion. It also calls into question the procedure of applying a tensile load to the specimen as part of making replicas as there is clearly an identifiable effect. An effect from which the material does not recover for several thousand cycles, presenting a problem if one is particularly interested in the first few hundred cycles.

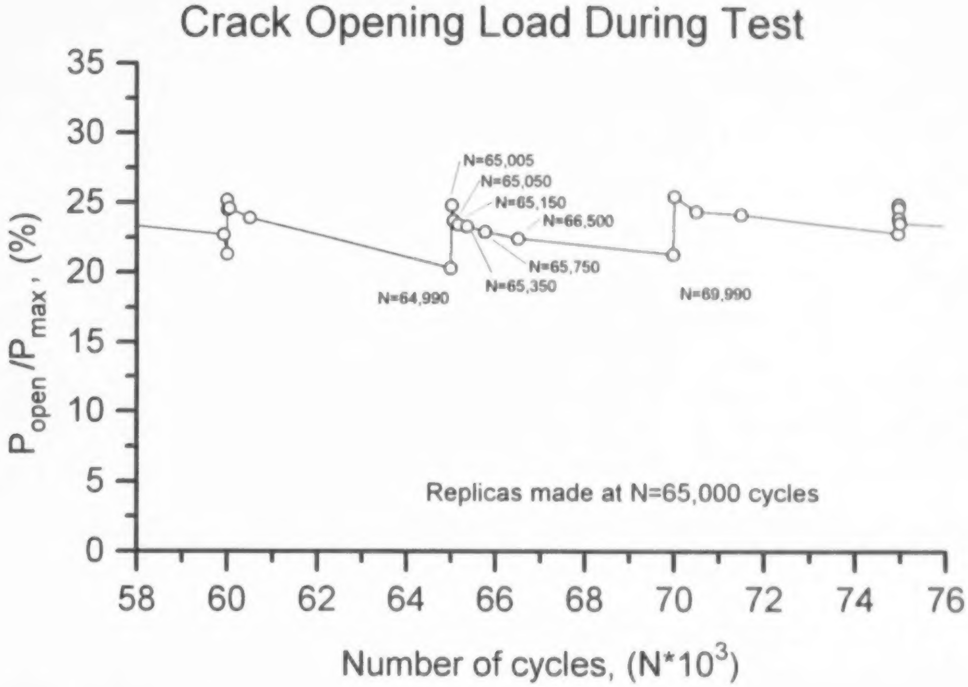
Crack Opening Load During Test

Figure 41: Active gauge adjacent to the crack,
Specimen B8, right side

4.4 Growth Rate Through the Test

Growth rate calculations, based on length measurements from the replicas, have been reduced according to the secant method presented in section 3.2.5. The growth rate results are plotted against the number of cycles in Figures 42 - 48 to show the growth rate changes during the test. The growth rate of both the a and c-face cracks are shown together in a similar fashion to the opening load data, on a linear scale with an insert figure for the early life.

When the calculated results indicate zero growth during a particular range of cycles, a vertical downward arrow is placed at the data point to indicate that the growth rate is below the scale of the graph. This description is also employed by Tokaji and Ogawa [58]. The next point which indicates growth is then connected with a dashed line. An upward arrow is also placed at this following data point indicating the growth rate prior to this point was below the scale of the graph.

There is a noticeable drop in the growth rate of the a-face crack, corresponding to the inception of steady growth of the c-face crack, particularly evident on specimen B7. Opening load data from c-face gauges are not available to coincide with this first growth of the c-face crack. In part because c-face length measurements cannot be made if a strain gauge is mounted on the mouth of the crack. On specimen B7 the opening load data from the c-face crack over laps with c-face growth results (Figure 35 and 36). This is because the gauges were replaced several times and removed promptly after gauge failure, permitting continued collection of the c-face replicas. However, by necessity such opening load results are intermittent, and so any influence the initial growth of the c-face crack might have on the crack opening load was not recorded.

If opening load values from the adjacent side gauges are considered, it is only the left side crack of specimen B7 (Figure 39) which can be compared to the growth rate, Figure 45. The c-face crack on this specimen begins to grow at about 70,000 cycles, the few opening load data points collected at this location do not permit significant interpretation.

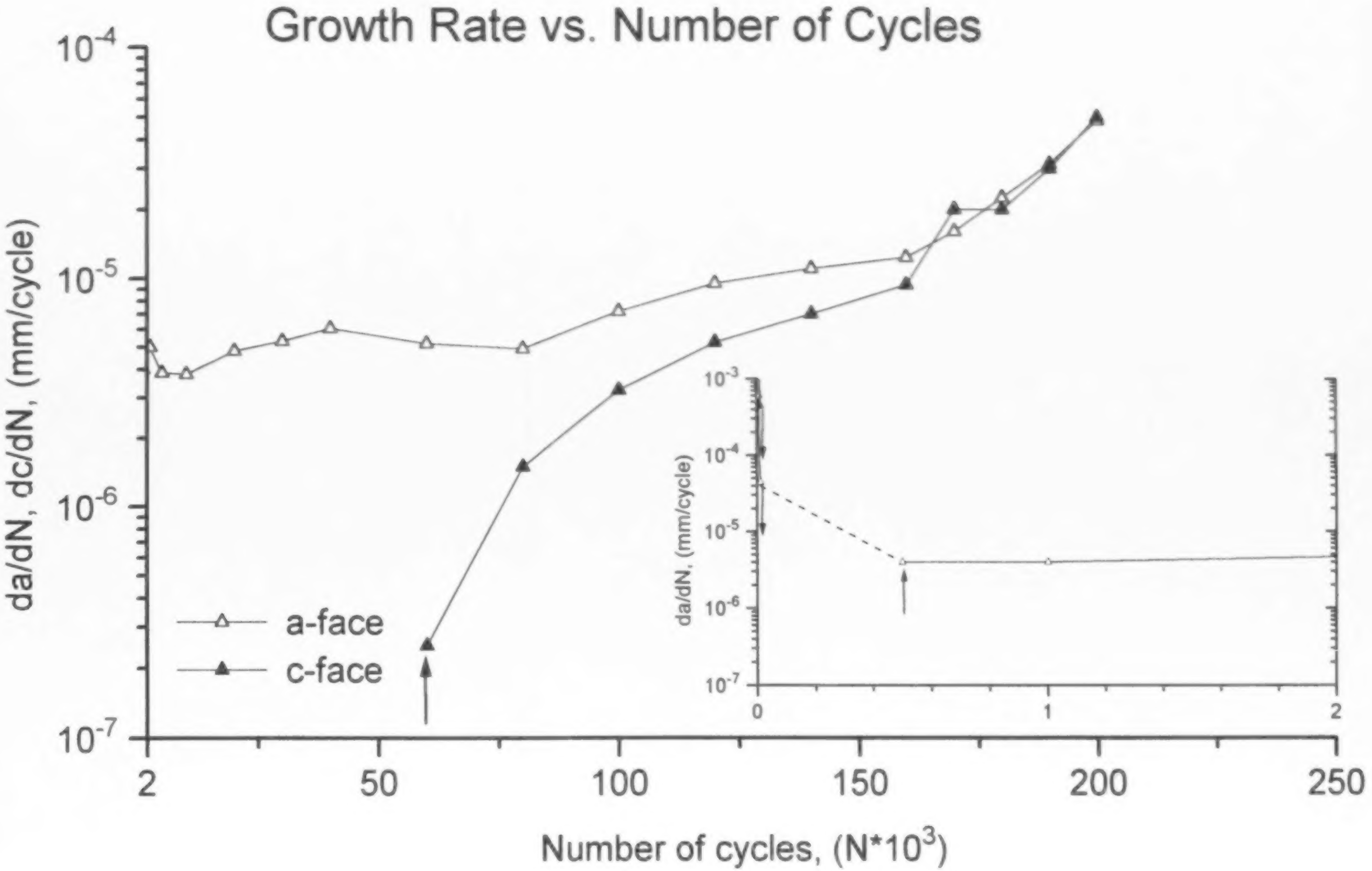

Figure 42: Specimen B4, left side

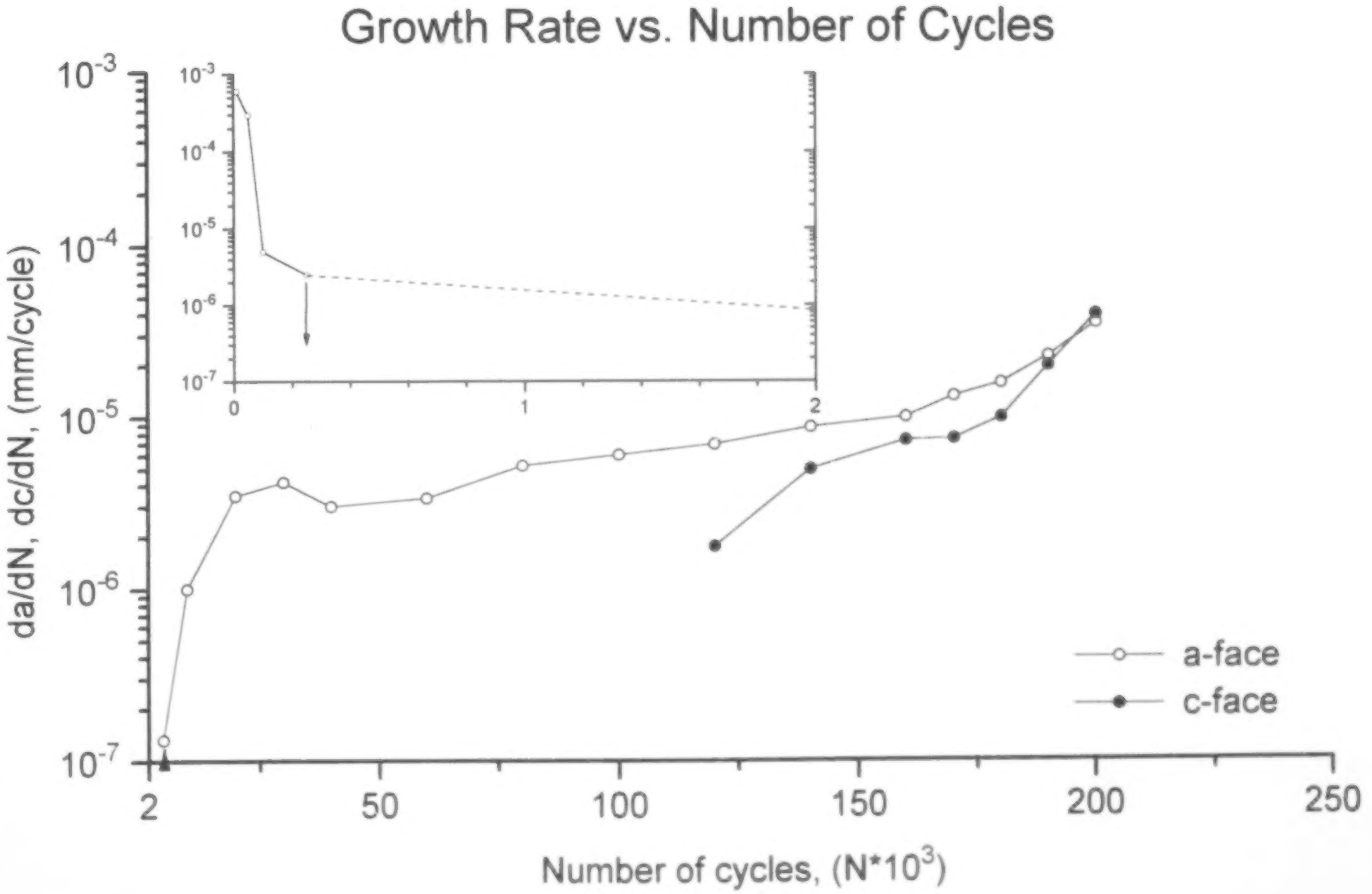

Figure 43: Specimen B4, right side

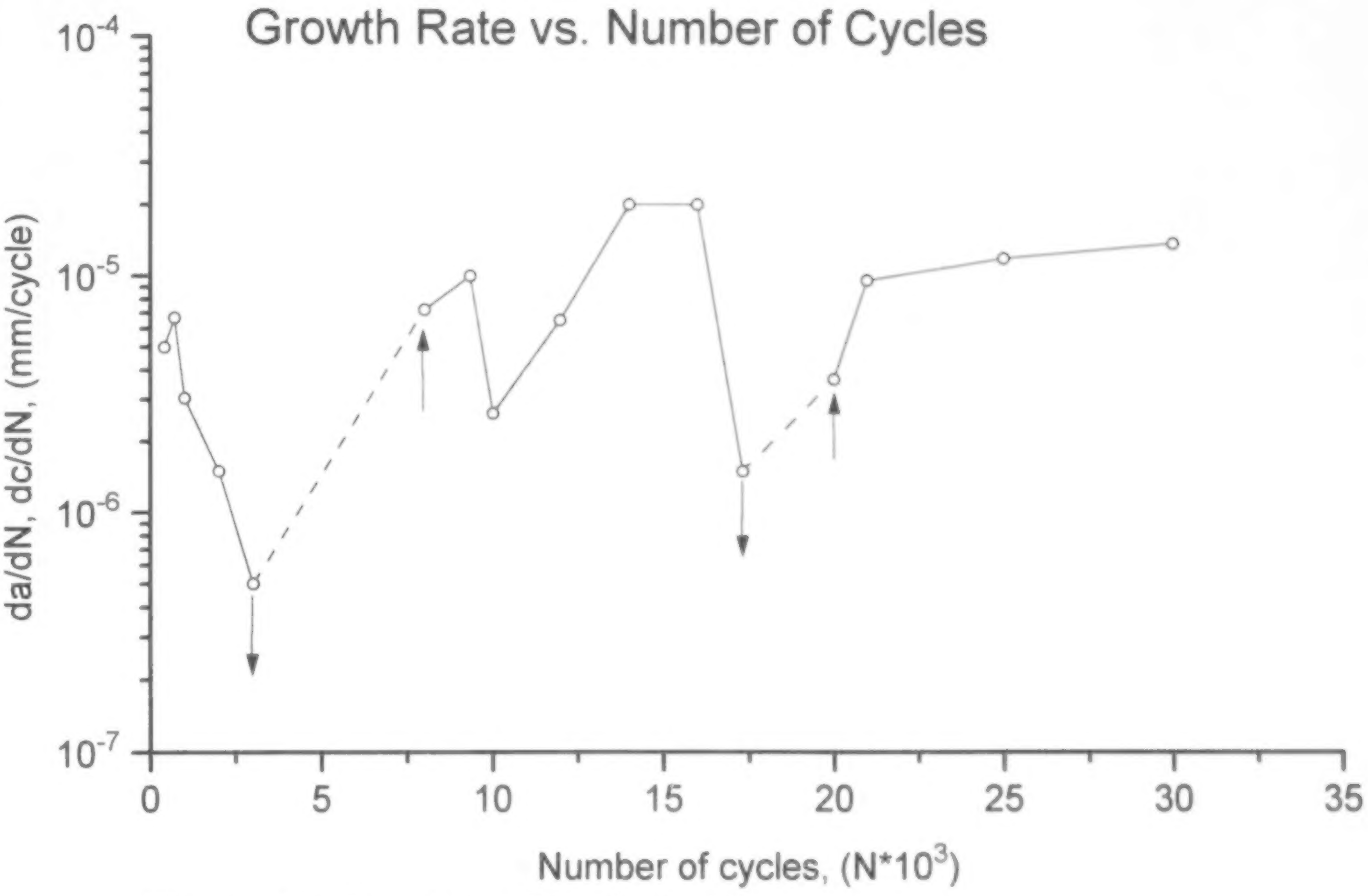

Figure 44: Specimen B6, right side

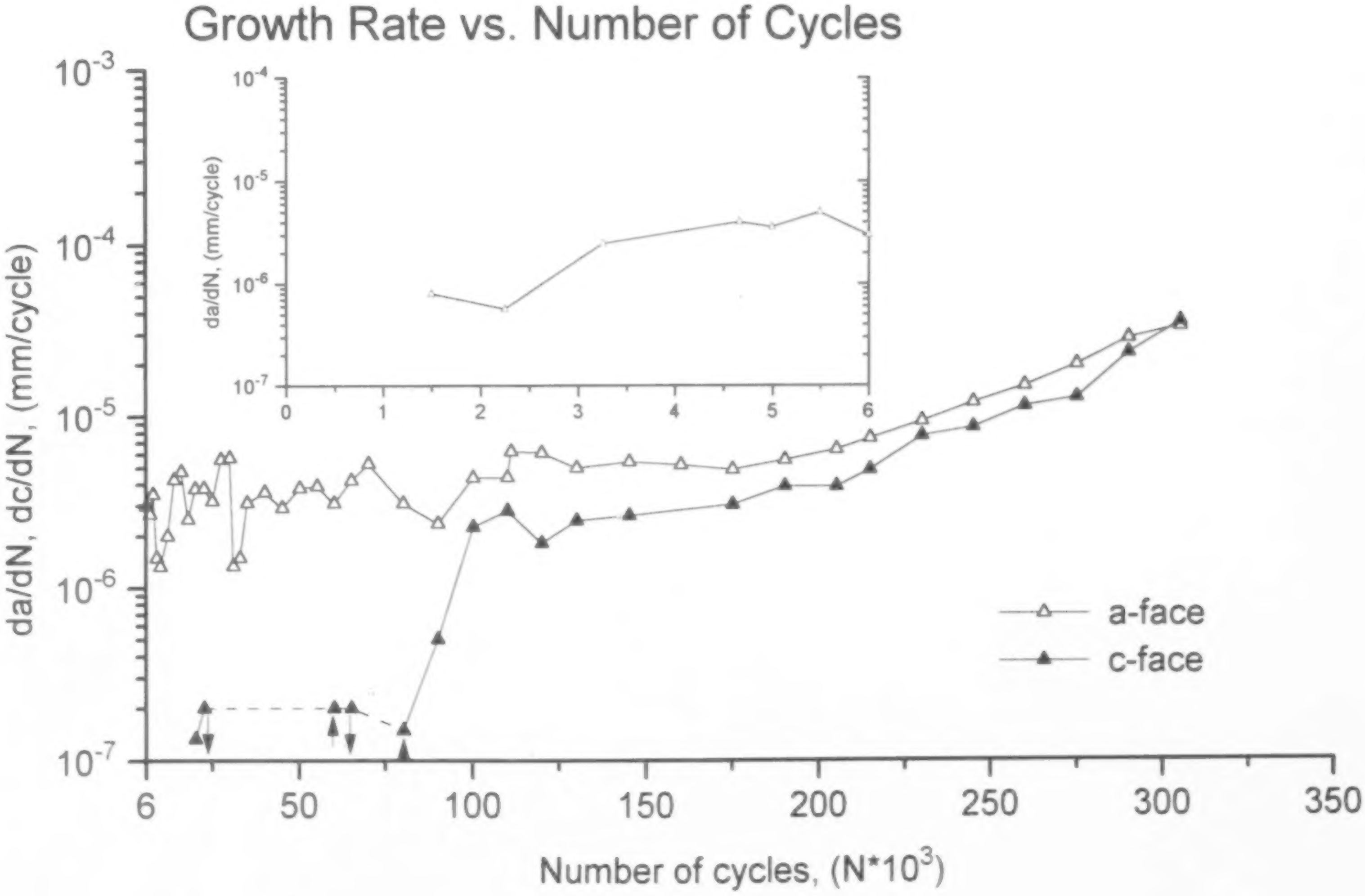

Figure 45: Specimen B7, left side

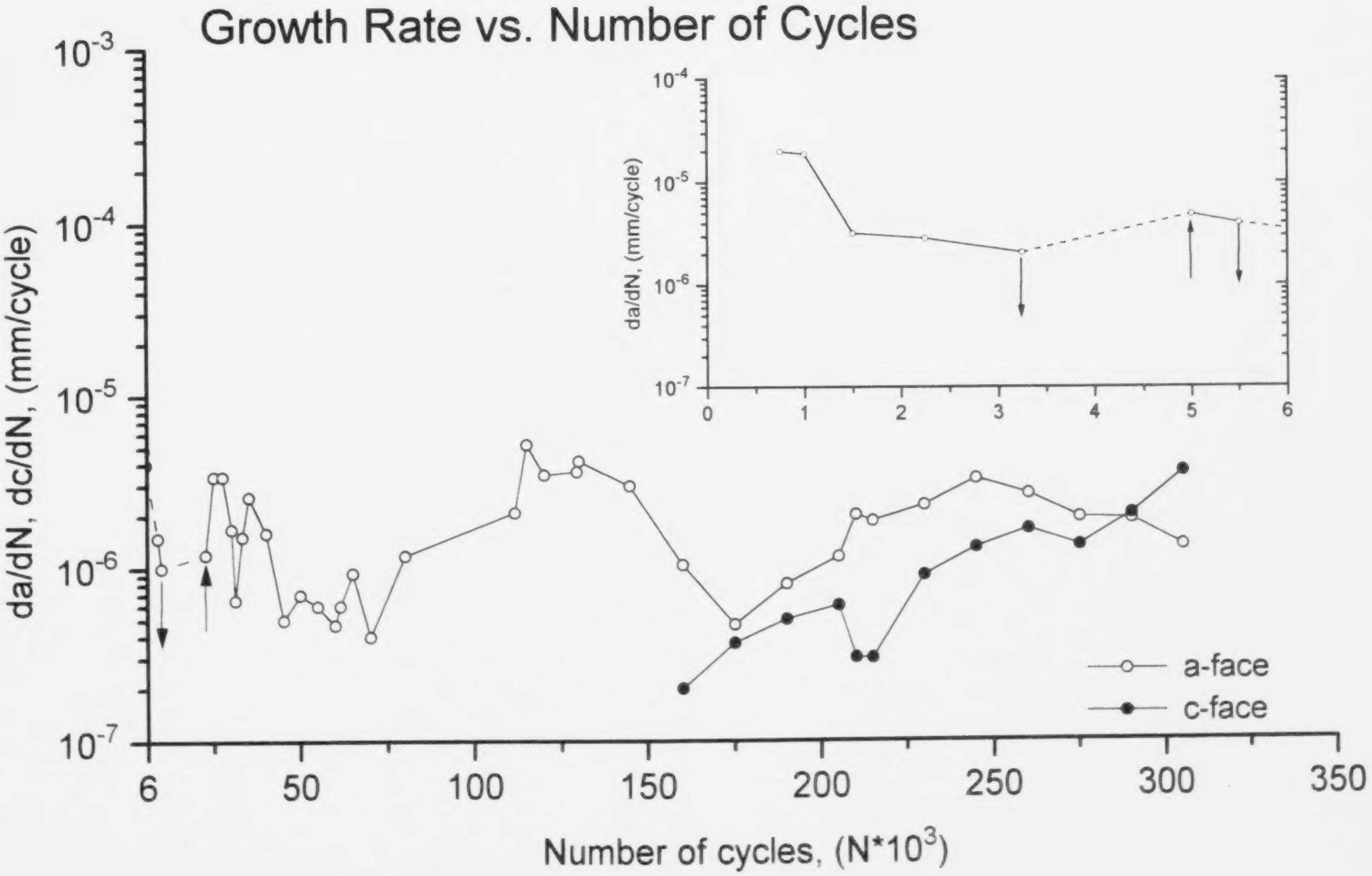

Figure 46: Specimen B7, right side

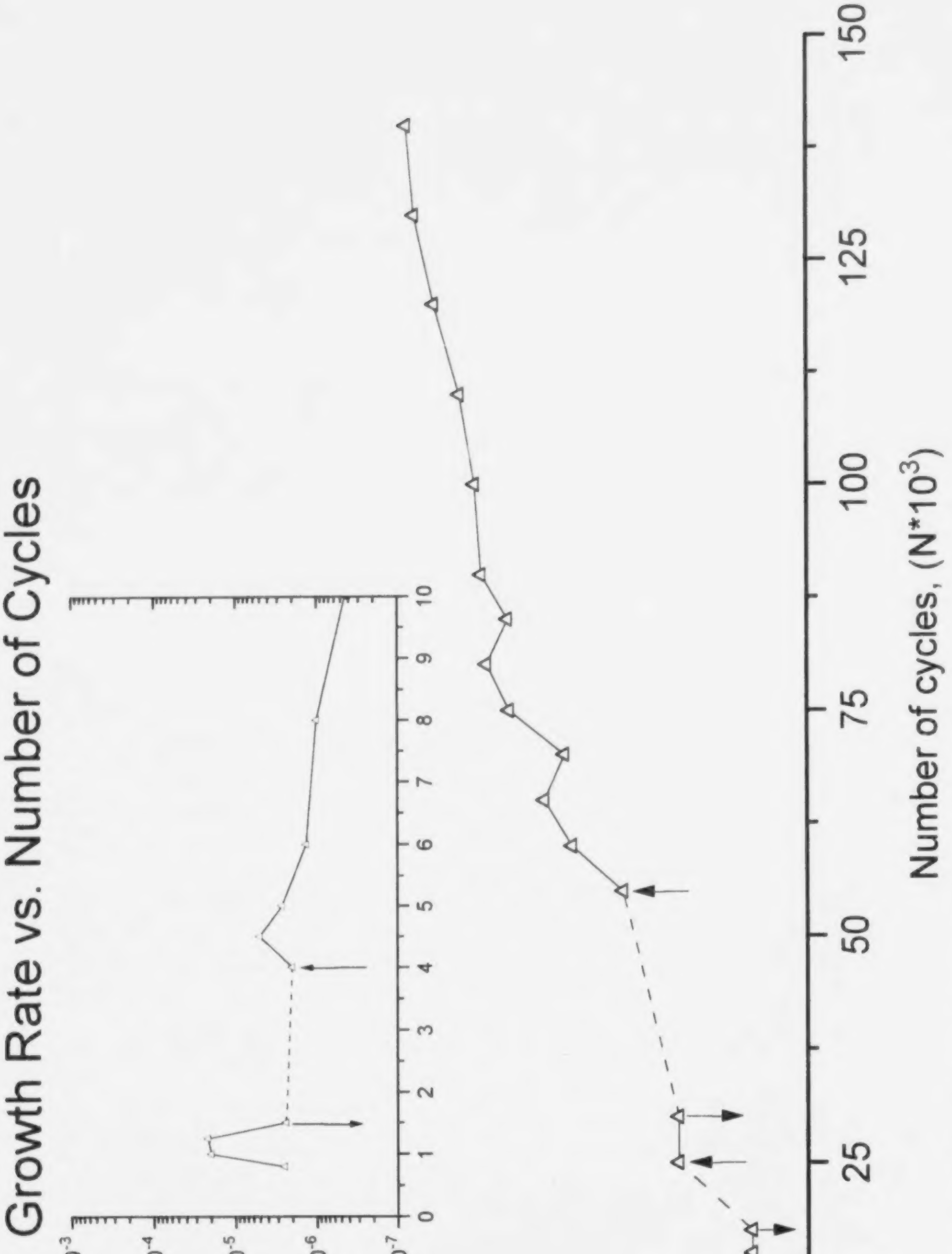

Figure 47: Specimen B8, left side

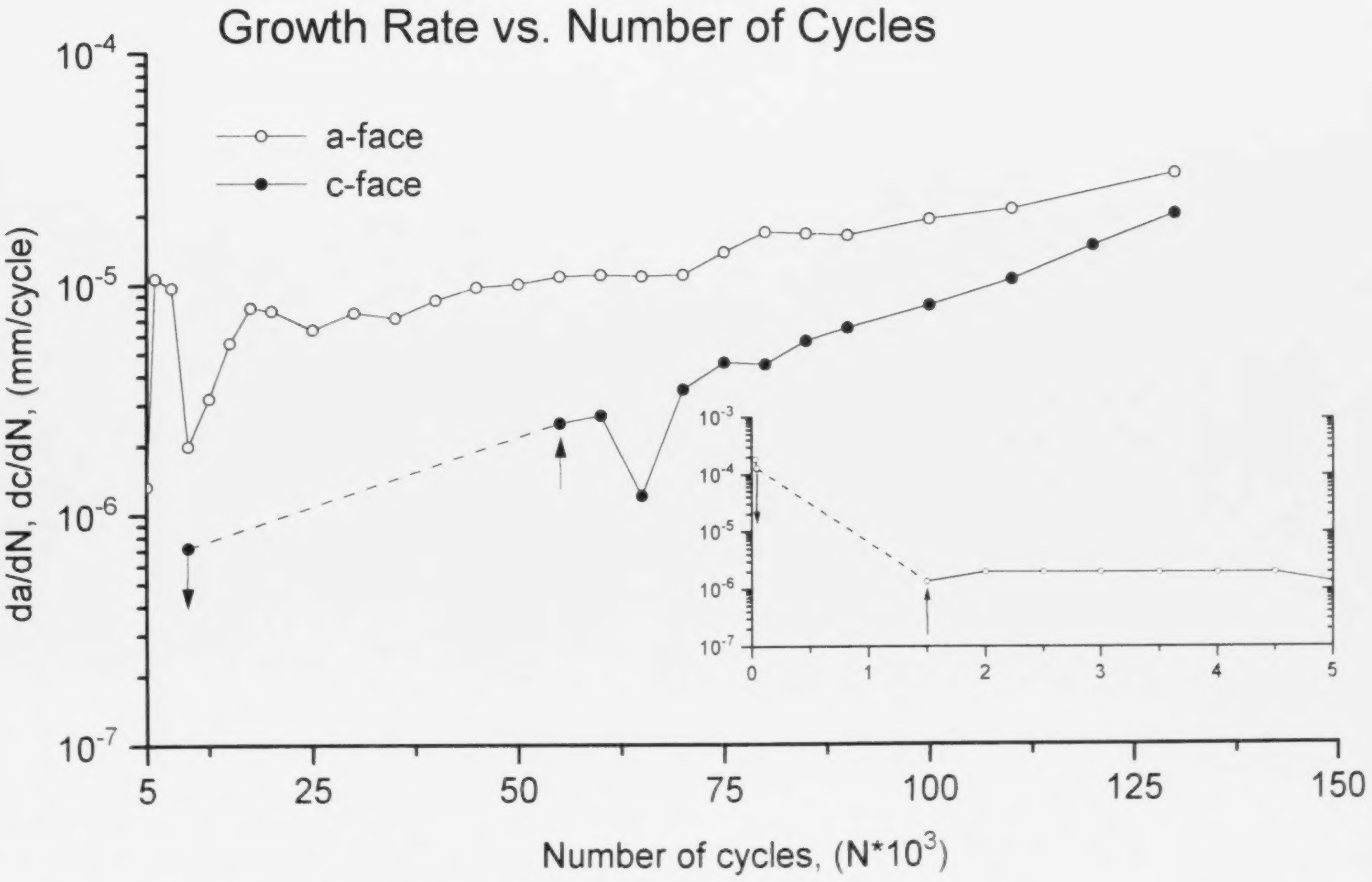

Figure 48: Specimen B8, right side

4.5 Growth Rate versus Crack Depth

Growth rate on both the a and c faces versus the depth, a, of the crack are presented on Figures 49 - 52. When the calculated growth rate is less than the scale of the graph, a vertical downward arrow is placed at that data point. A vertical upward arrow is placed at the next point which does show growth and is connected with a dotted line to aid in following the data set. There is no growth data for the left side c-face crack of specimen B8 as there was a strain gauge on top of the crack for the duration of the test.

Figure 52 combines the growth rate data of the a-face crack for specimens B4, B7 and B8. Once the crack is well developed, the slopes of the growth rate curves pertaining to depth and length appear to converge towards a common value. In order to reduce congestion in this figure, the upward arrows, used to indicate that the recorded growth was below the scale of the graph, have been omitted.

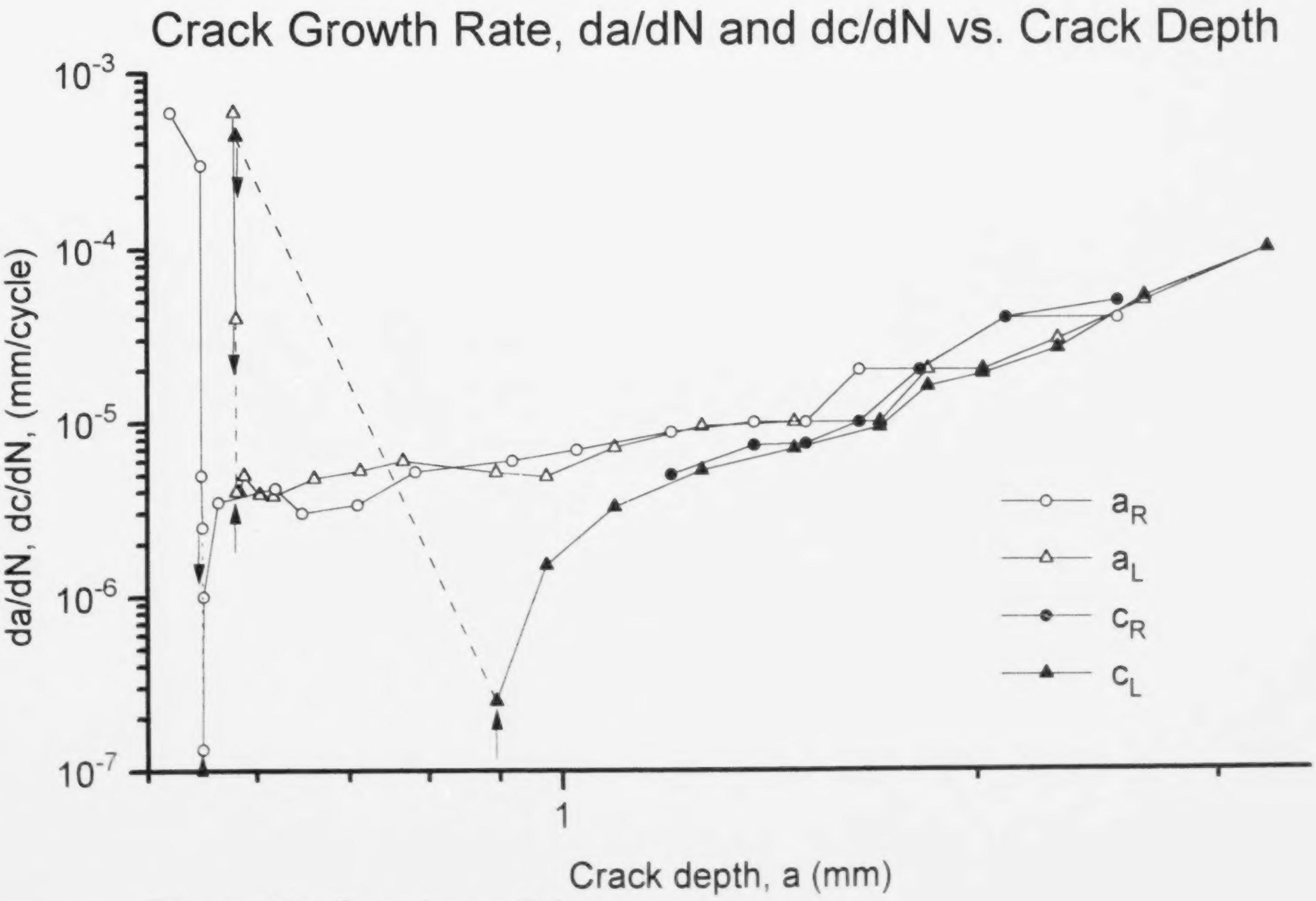

Crack Growth Rate, da/dN and dc/dN vs. Crack Depth

Figure 49: Specimen B4

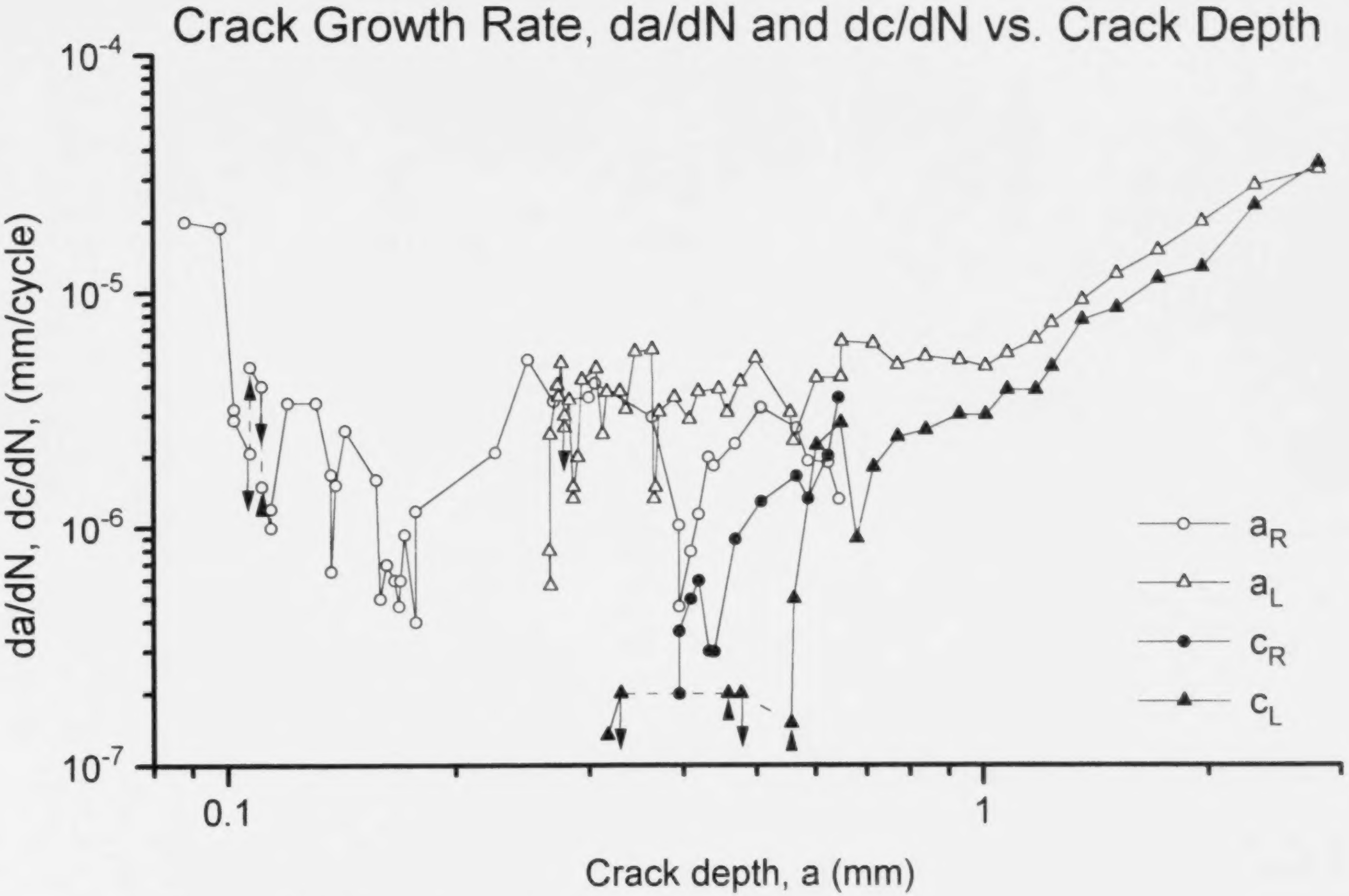

Figure 50: Specimen B7

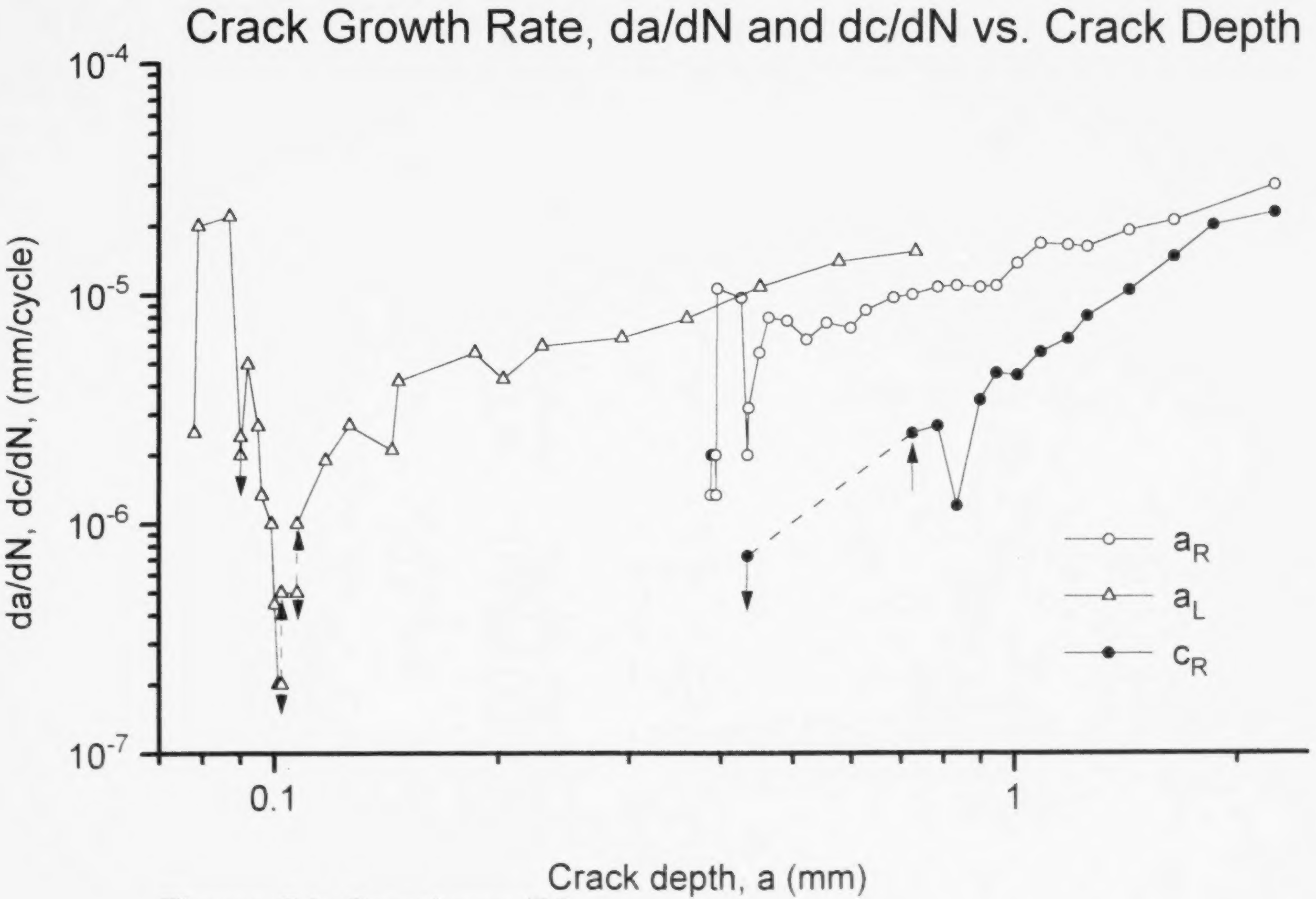

Figure 51: Specimen B8

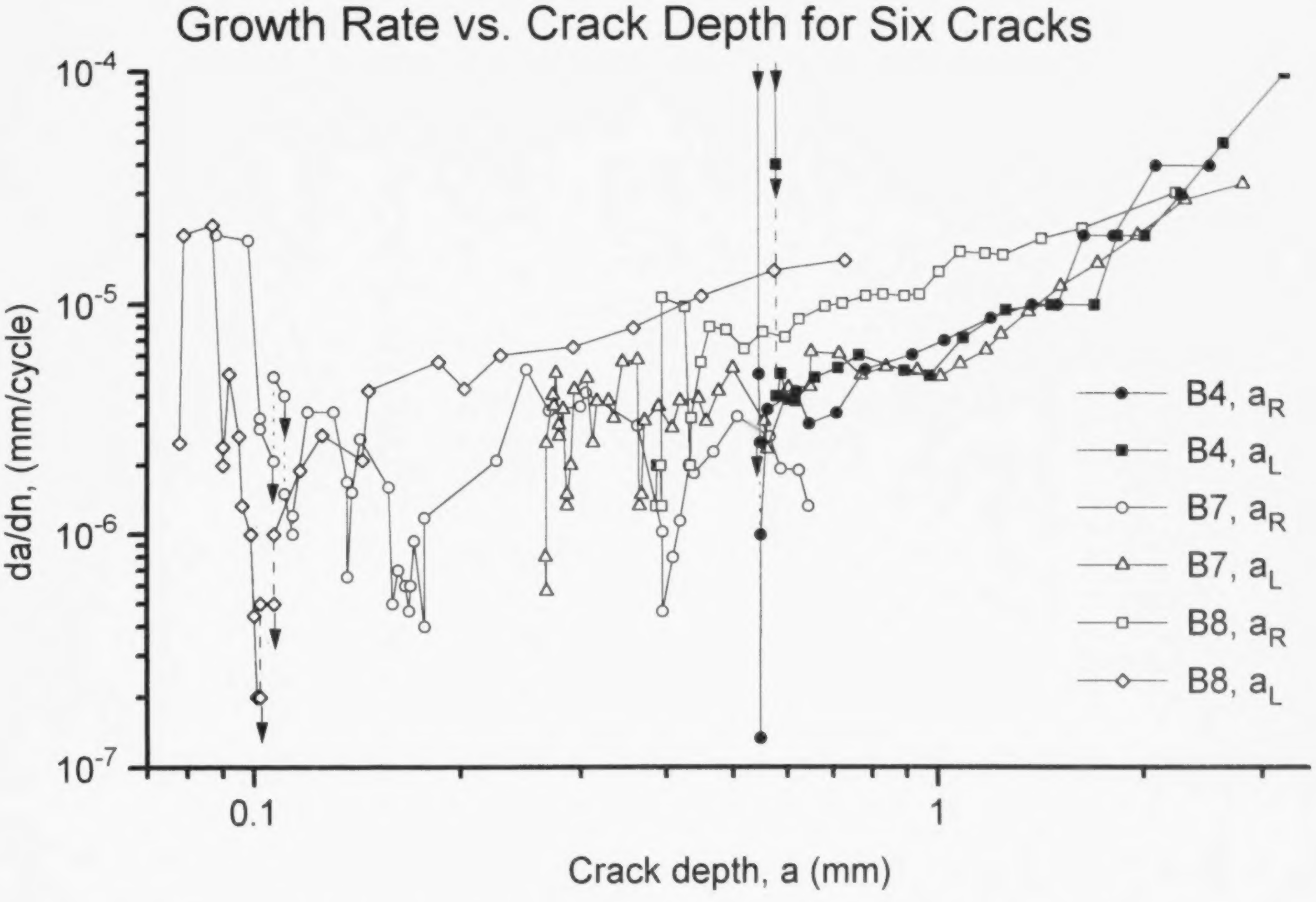

Figure 52: Specimen B4, Specimen B7 and Specimen B8

4.6 Opening Load versus Crack Extension

The opening load measurements for given crack extensions are presented in Figure 53, for those specimens where opening load data are available (B7 and B8). The opening load information is that which is obtained using the curvilinear approach presented in section 3.2.7. Two points to bear in mind are: this assessment does not take into consideration growth below the surface, and that it is difficult to accurately determine a_0. An error in a_0 would effectively shift the result slightly to the left or right.

The values for the left side crack of specimen B7 extend beyond the horizontal axis of the graph, hence the connecting line is truncated at the right side of the figure. No data are included for the a_L crack of specimen B8 as the gauge on the corresponding c-face failed prior to any detectable crack extension. Hence P_{open}/P_{max} cannot be presented relative to crack extension.

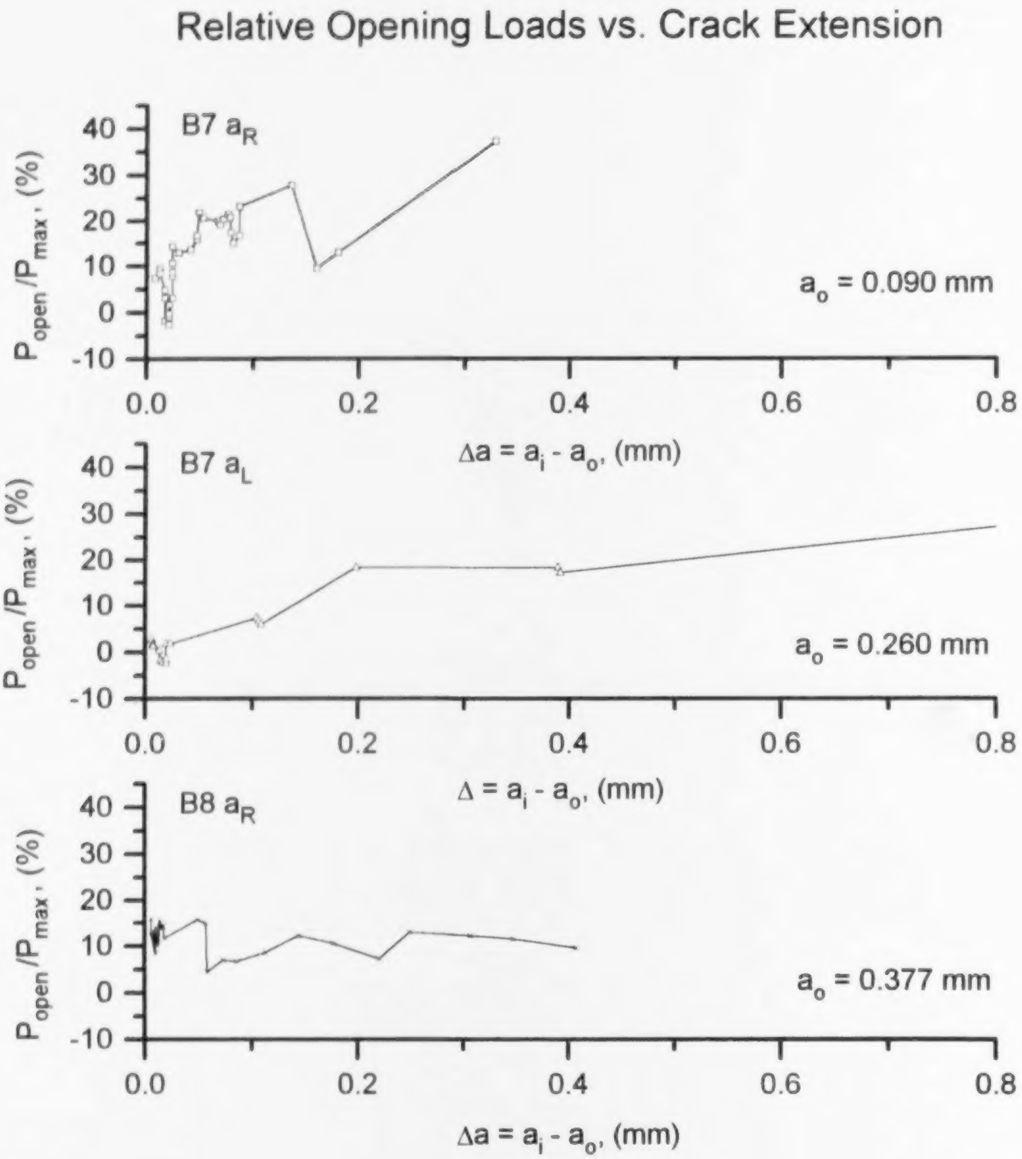

Figure 53: Development of the opening load

4.7 Growth Rate versus Aspect Ratio

As part of investigating the influence the shape of the crack will have on the growth rate, both da/dN and dc/dN are plotted versus the aspect ratio (Figures 54 - 56). From these figures, one can conclude that growth on the c-face usually begins when the a/c ratio is between 0.43 - 0.53. In the case of larger initial cracks this coincides with $a \approx 2a_0$, however this does not always hold. For example, in the case of the much smaller a_R crack of specimen B7, growth on the c-face occurs at $a \approx 4a_0$.

The calculated ΔK at the tip of the c-face crack at the time it begins to grow is presented in Table 7. In the calculation of ΔK, the full range of the applied stress was used. The use of this approach will be discussed in greater detail in section 5.2 which deals with the growing crack.

Table 7: ΔK corresponding to initial growth of the c-face crack.

B4	Left	9.2 $\mathrm{MPa\sqrt{m}}$
	Right	8.6 $\mathrm{MPa\sqrt{m}}$
B7	Left	7.5 $\mathrm{MPa\sqrt{m}}$
	Right	6.5 $\mathrm{MPa\sqrt{m}}$
B8	Left	- -
	Right	8.2 $\mathrm{MPa\sqrt{m}}$

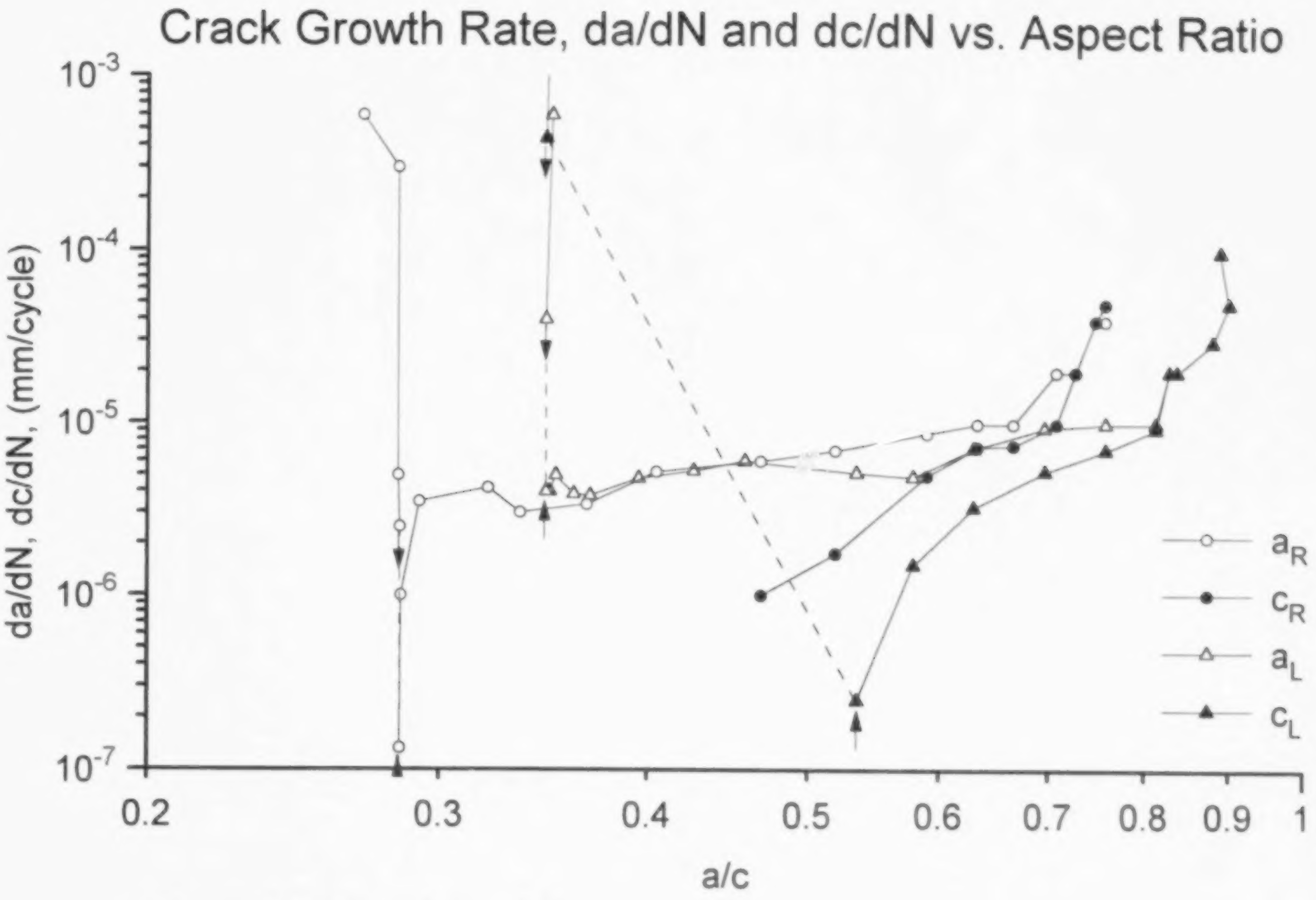

Figure 54: Specimen B4

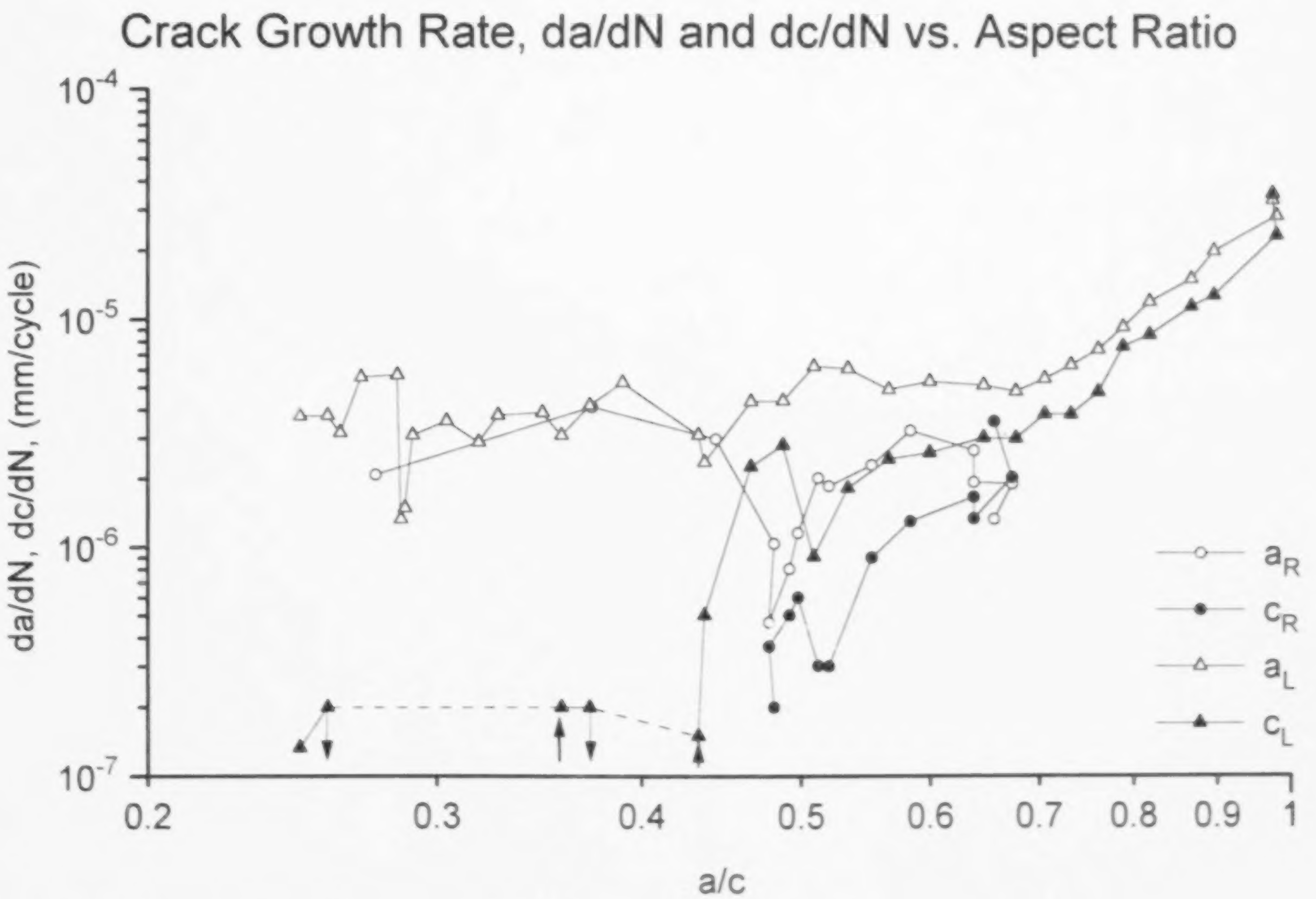

Figure 55: Specimen B7

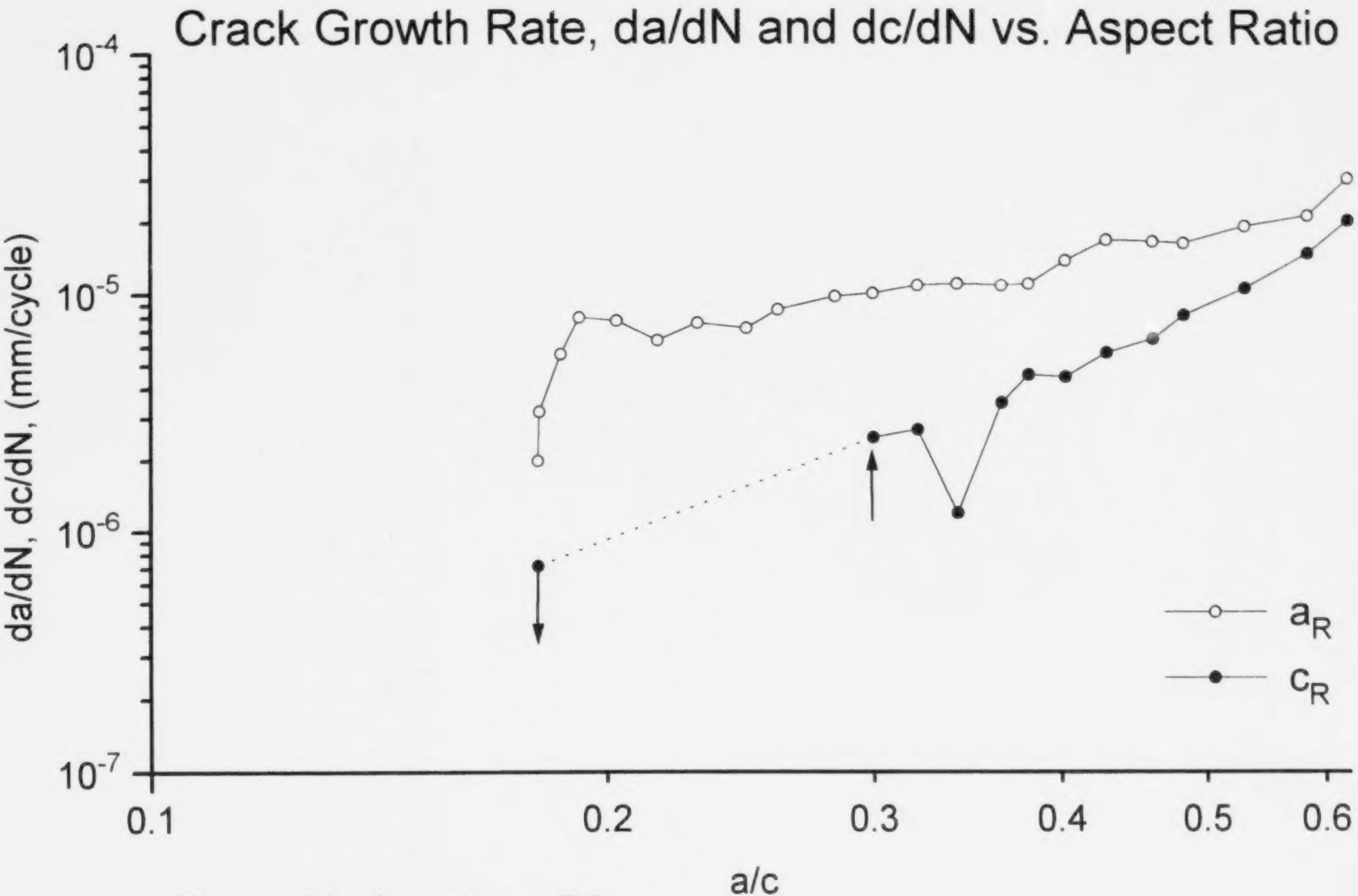

Figure 56: Specimen B8

4.7 Microstructural Observations

The material used in this investigation exhibits a dual phase structure, ferrite and pearlite. As shown in Figure 9 the microstructure of the c-face reveals a banded ferritic/pearlitic structure. This is as one would expect with a rolled, low carbon steel product. The a-face does not show this banded structure, instead there are irregularly dispersed pearlite regions within the ferrite, Figure 57.

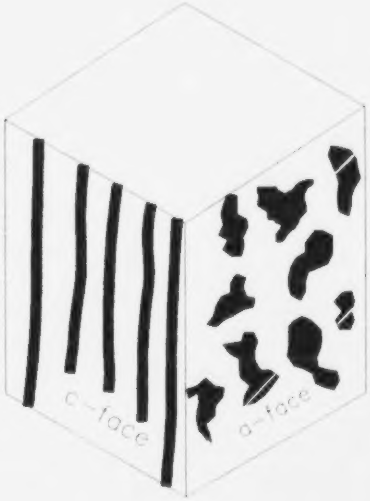

Figure 57: Microstructure of the a and c faces

It is mainly the early growth stages that are of interest, and since the c-face cracks do not grow until well into the test, it is only the effect on the a-face that has been investigated here. The most significant microstructural influence can be observed in the growth rate data. The growth rate versus crack depth data have been lined up with microstructure photographs of the crack, Figures 58, 59 and 60.

When the crack is small there is a reduction in growth rate corresponding to the crack passing through a region of pearlite. This may come as no surprise as the pearlite is a harder, stronger material than the ferrite. A similar behaviour has been observed by other investigators.

In a similar fashion the opening load results can be compared with the microstructure. Figures 61 and 62 compare P_{open}/P_{max} to the microstructure. In the early stages of growth, the crack opening load fluctuates as it passes through ferrite/pearlite regions.

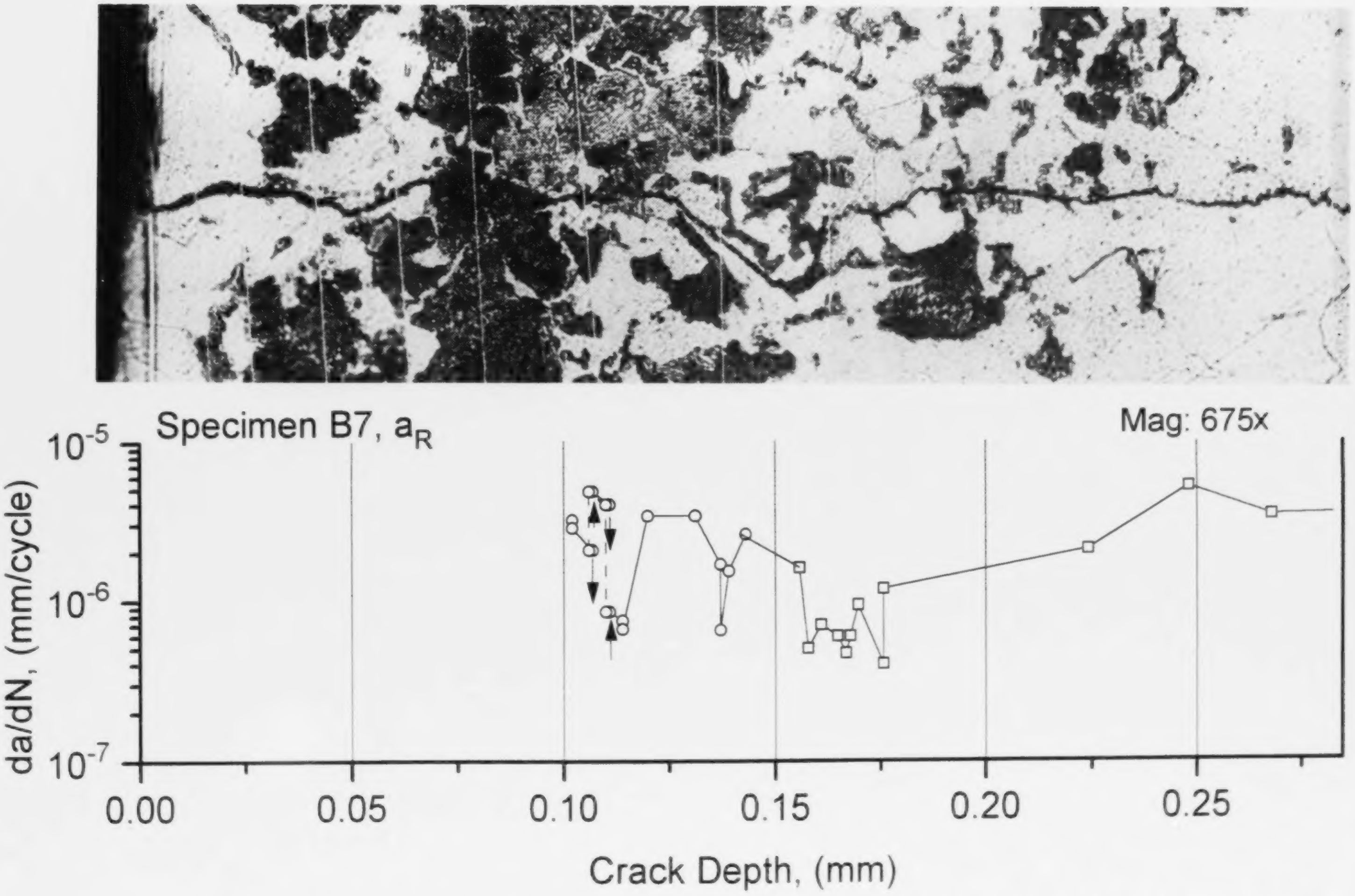

Figure 58: Comparison of growth rate to microstructural features

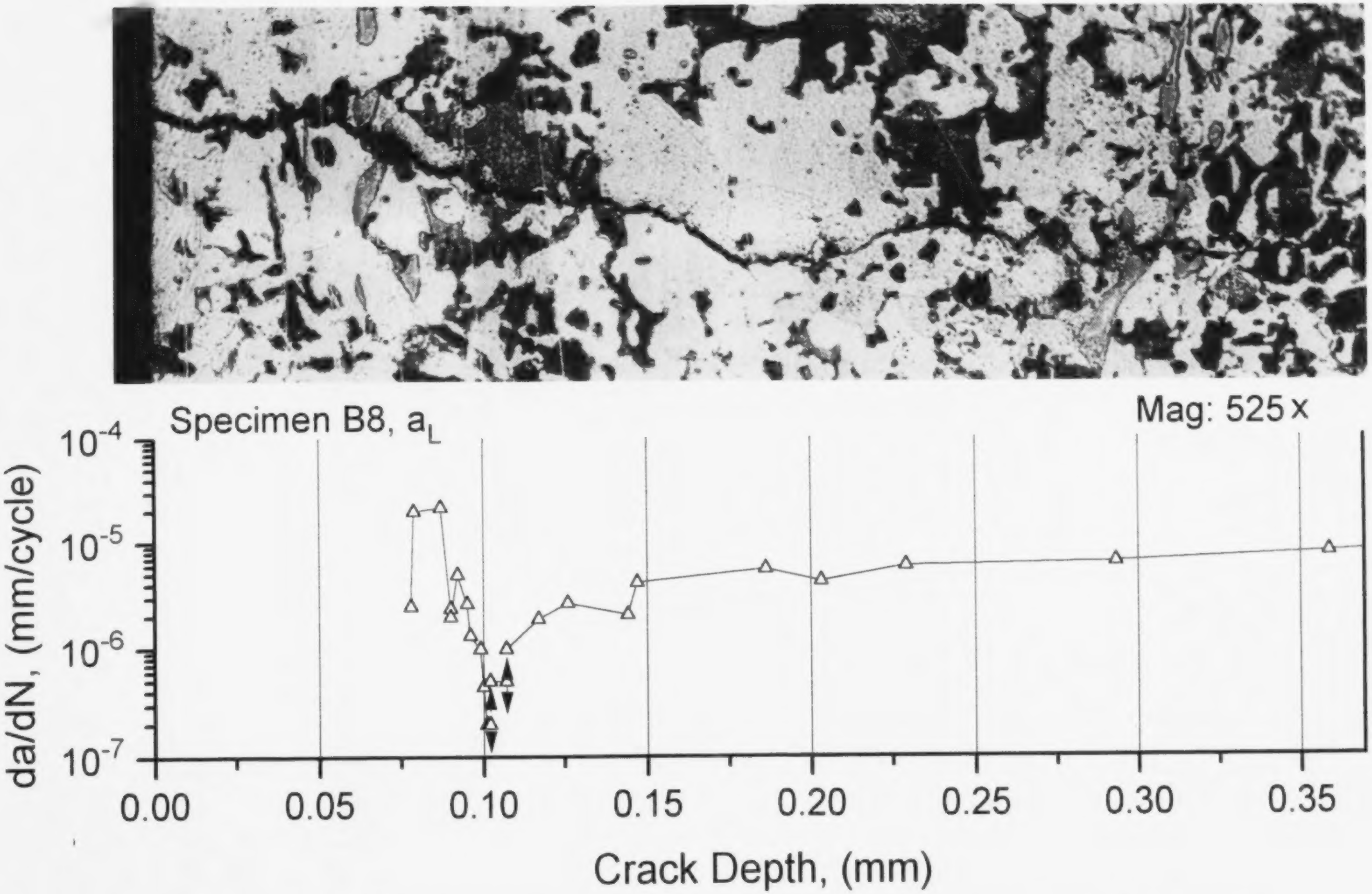

Figure 59: Comparison of growth rate to microstructural features

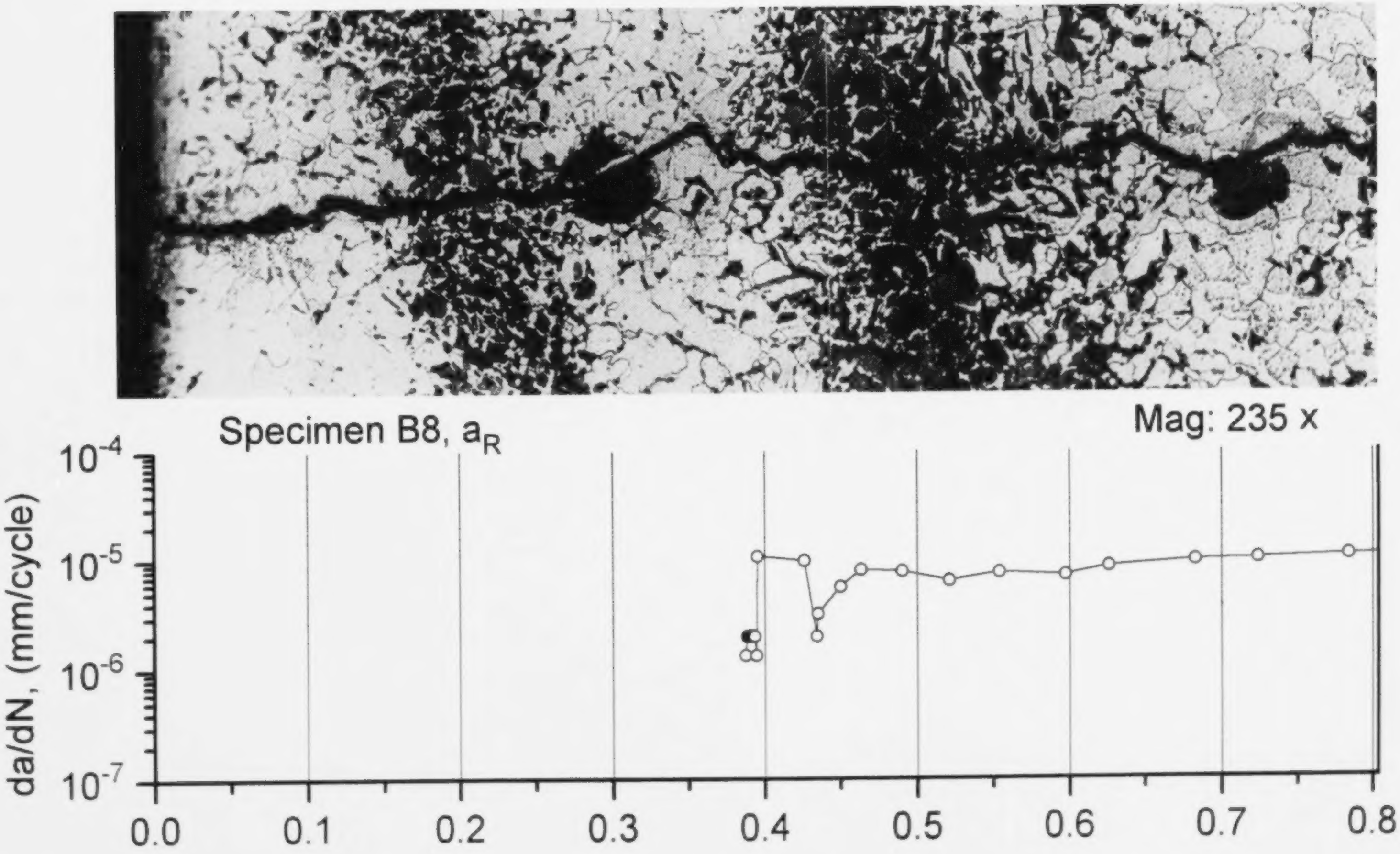

Figure 60: Comparison of growth rate to microstructural features

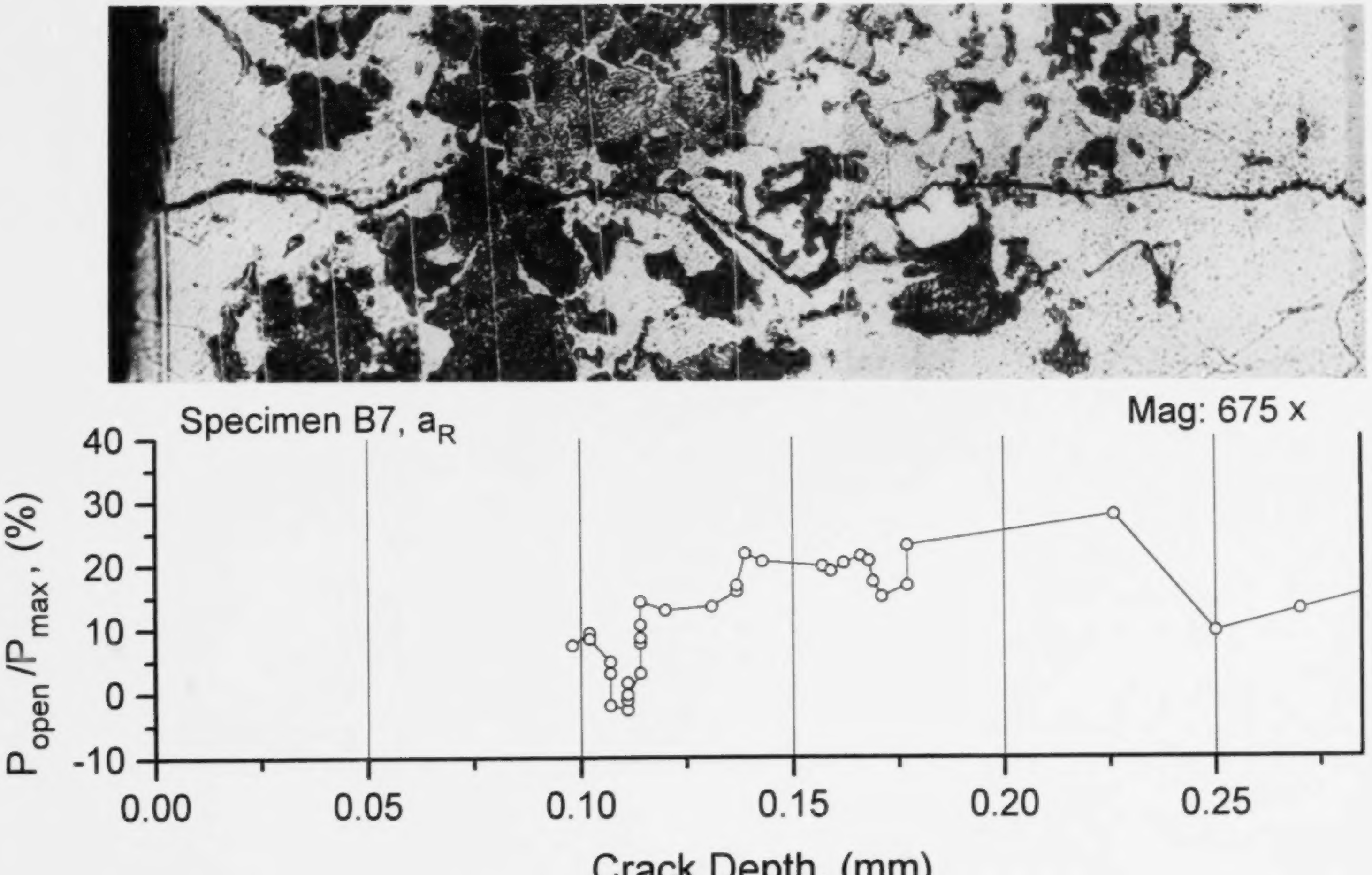

Figure 61: Comparison of opening load to microstructural features

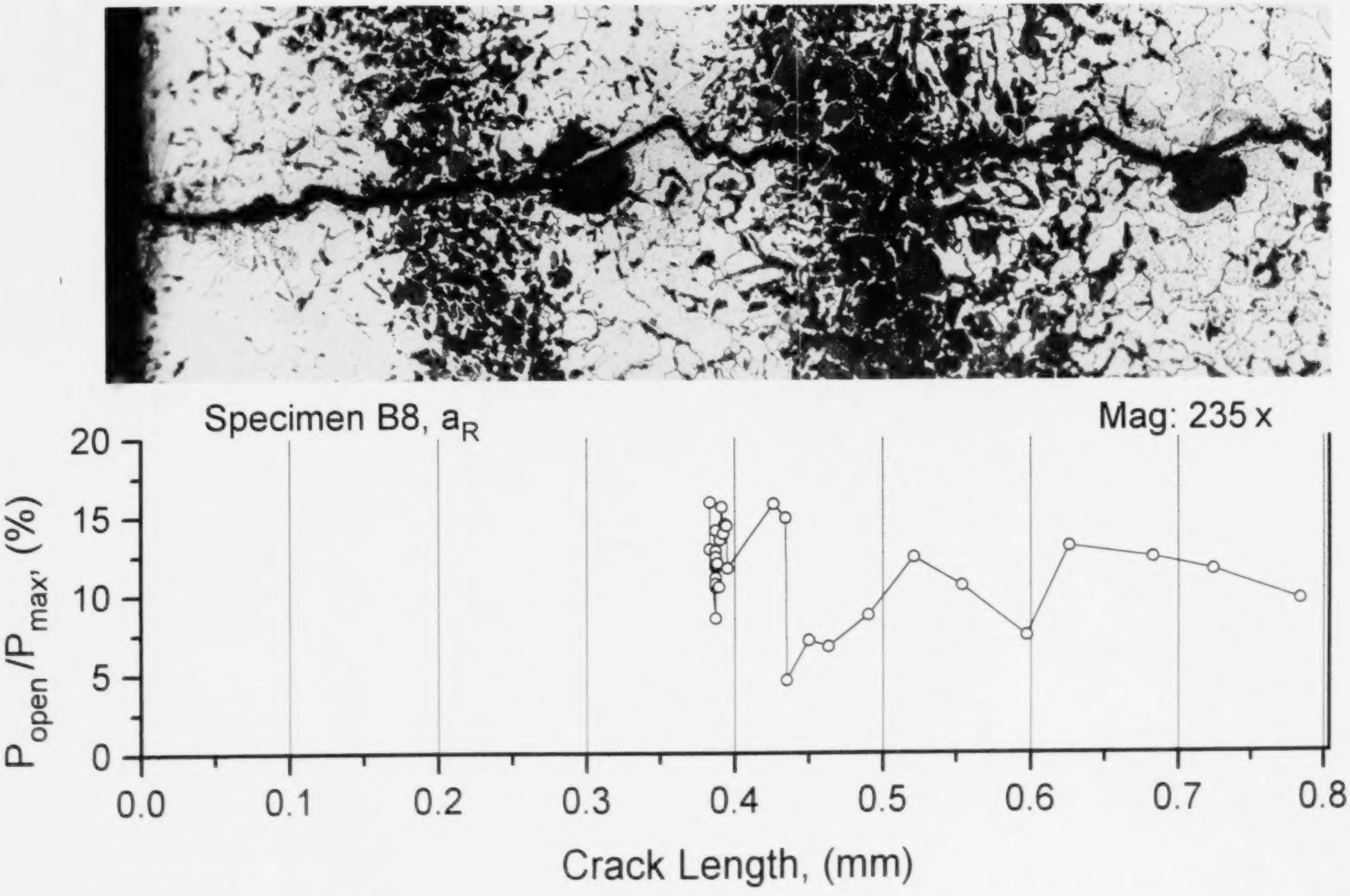

Figure 62: Comparison of opening load to microstructural features

5.0 Data Interpretation

The data presented in Chapter 4 provides the basis for an understanding of the growth and closure behaviour of short cracks. The analysis of the data can be simplified by considering two stages of crack behaviour: the stationary crack and the growing crack. The separation of the two stages is made at the point where growth begins on the a-face. Prior to this there appears to be activity, based on fluctuations in the opening load measurements, but no visible growth. The growing crack provides behaviour information in terms of growth rates, opening load and the aspect ratio.

5.1 Stationary Crack

The stationary crack is present in the early stages of each of the tests. Following the first few loading cycles the crack does not exhibit growth, perhaps for several thousand cycles. During the initial cycles, the opening load results exhibit an initial decrease, followed by a gradual increase. There is generally a drop in the opening load which corresponds to the first growth events that follow the first period of self arrest.

Given that the measurement resolution of the equipment is 1μm, growth rates of 10^{-6} mm/cycle will only be detected with an elapse of 1,000 cycles, which is no longer the very early stages of the test. This is further complicated in that the replication inspection technique employed was not able to detect the extreme tip of the crack, particularly early in the test. As the crack develops, the technique's ability to record the tip region improves. Hence some of the indicated growth may have been due to the crack being more clearly defined.

The opening load data are shown in Figures 63 and 64, up to the point where there is growth detected on the a-face. An arrow is placed on the graph indicating the first a-face growth event recorded, beyond the initial 35 cycles, for that crack. The curvilinear approach as presented in section 3.2.7 was used in determination of the opening load for these figures.

It should be stressed that the term "Stationary Crack" used here means the absence of apparent growth on the a-face (in every case the growth along the c-face started later than on the a-face). There may be growth below the surface. The shape of the crack front is assumed to be a partial ellipse. Based on observations of the initial crack front after specimen fracture, the shape varies from crack to crack and can only be approximated by a partial ellipse. The possible evolution of the shape of the crack front with no surface growth was not part of this investigation.

Nominally the greatest crack driving force will be at the tip of the crack on the a-face. This statement is based on calculations of the initial ΔK (see Figure 16 in section 3.2.3) and the unconstrained nature of the crack at the free surface. However, if the initial crack front geometry, which is determined by the pre-crack specimen, is not favourable, then the crack tip driving force may be greater at some point below the surface. There may be growth and damage development which will not show up in the surface observations but which will have an impact on the strain gauge readings.

Opening Load Prior to Crack Extension

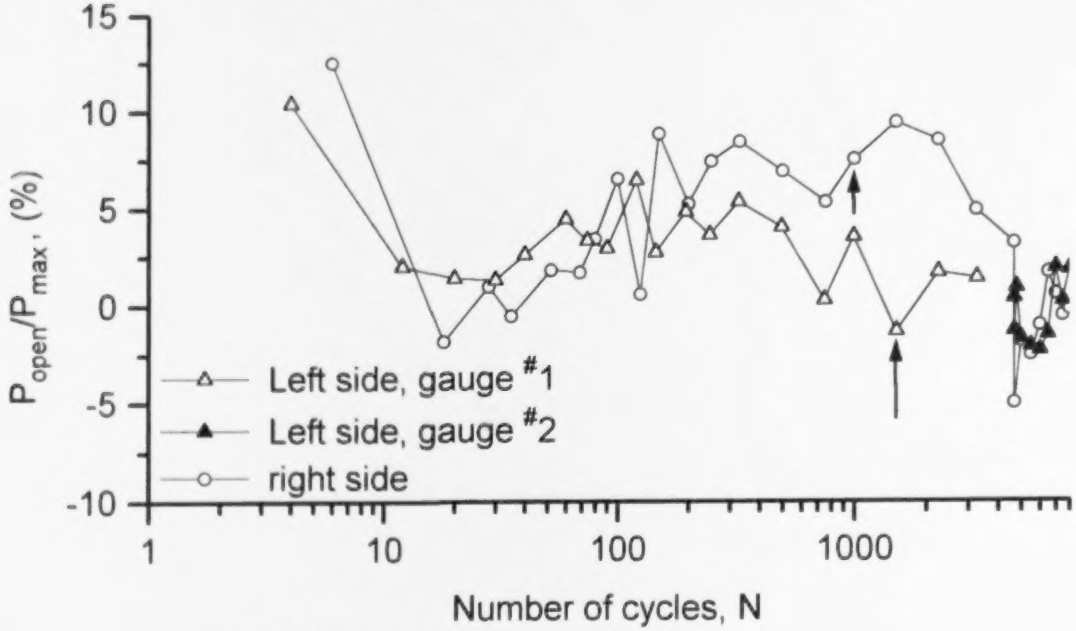

Figure 63: Specimen B7

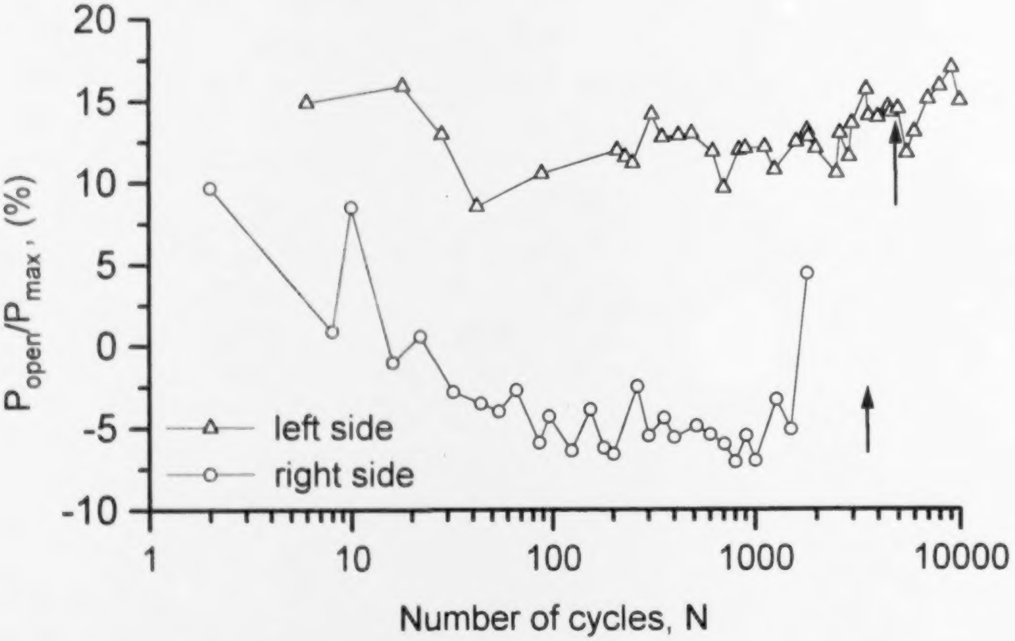

Figure 64: Specimen B8

The crack tip stress intensity range, ΔK, corresponding to the initial growth of seven of the cracks, has been plotted in Figure 65 against the number of cycles when the a-face crack begins to grow. The early indications of growth, $N<35$ cycles, have not been included. One might expect that those cracks having a higher ΔK would begin to grow earlier than those with a lower ΔK. This does not appear to be the case; the data suggest an irregular pattern. No improvement is observed if one calculates a ΔK_{eff} based on the opening load value when growth begins (see Figures 63 and 64). Conducting such a calculation on the ΔK result simply lowers the value of ΔK by 0.3 - 1.0 $MPa\sqrt{m}$.

The threshold stress intensity factor as predicted by Ellyin and Fakinlede [59] is also included in Figure 65. All the cracks presented here have a calculated initial ΔK close to, or below, this threshold. In every case the cracks propagated to such a size that ΔK was greater than this threshold, though, initially all displayed the anomalous behaviour characteristic of short cracks. Thus ΔK_{th} as presented by Ellyin and Fakinlede [59] can reasonably be regarded as the lower threshold for the growth of long cracks.

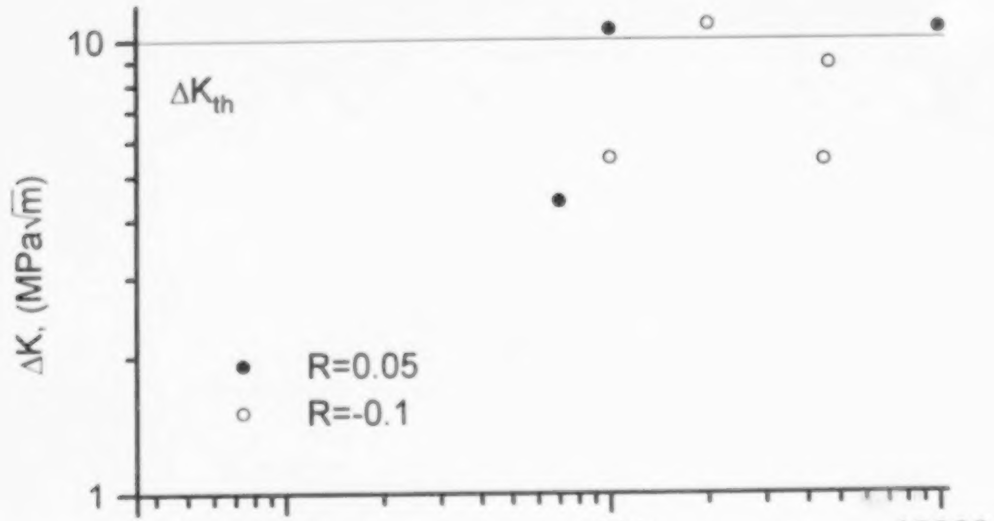

Number of cycles prior to crack growth, N_s

Figure 65: Applied stress intensity factors for the stationary crack

5.2 Growing Crack

An understanding of the behaviour of a growing crack is the most important part of this study. An examination of the results of the crack growth rate through the test (section 4.4) or with increasing depth (section 4.5) reveals irregular behaviour of short cracks. The growth results can be further separated into two regions:

- a-face growing and c-face stationary
- a-face and c-face both growing.

The point at which the c-face crack begins to grow is noted as part of interpreting the results.

The c-face crack begins to grow when the aspect ratio reaches 0.43 - 0.53. The rate at which the aspect ratio increases is dependant on the size of the initial cracks. Larger initial cracks result in the aspect ratio increasing more quickly than for smaller cracks. It was also observed that the when the c-face crack begins to grow there is usually a drop in the growth rate of the a-face crack.

A common technique in interpreting long crack growth rate data is to graph such data with respect to ΔK on a log-log scale. This has an advantage over plotting growth rate versus the crack depth (section 4.5) by giving consideration to the shape of the crack. The standard procedure is to consider the full range of stress ($\Delta\sigma$) for $R>0$ and only σ_{max} in the case of $R<0$. The reason this is done is that the crack is assumed to be closed during compressive loading. However, during this investigation, the full stress range, $\Delta\sigma$, was considered because it, nominally, remains constant through the test, whereas the closure level is not consistent. Certainly in the short crack region, the

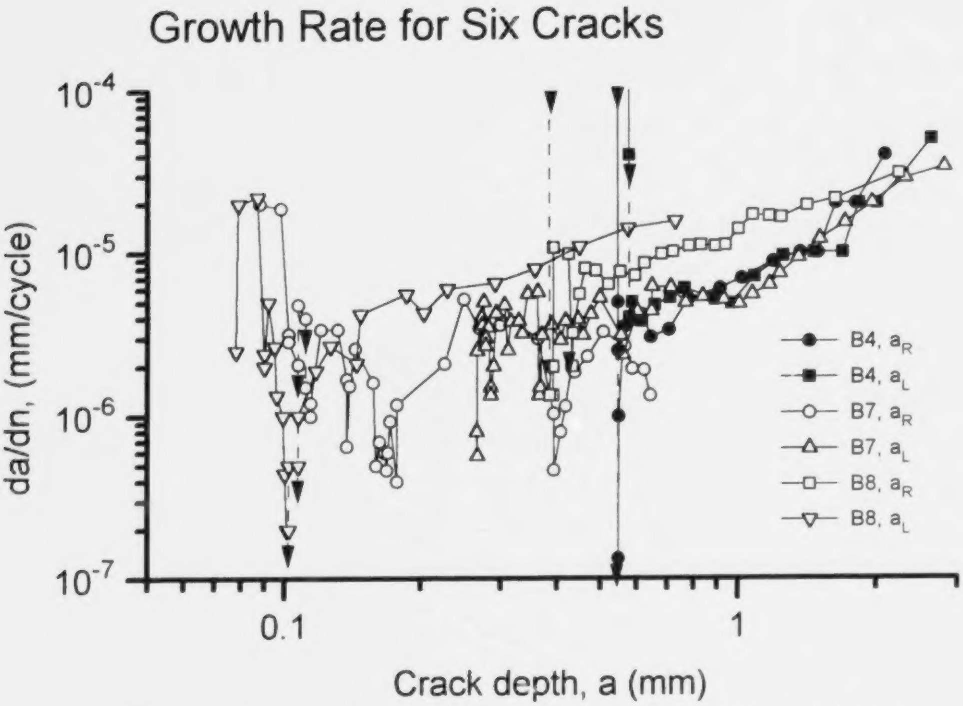

Figure 66: Specimens B4, B7 & B8 vs crack depth

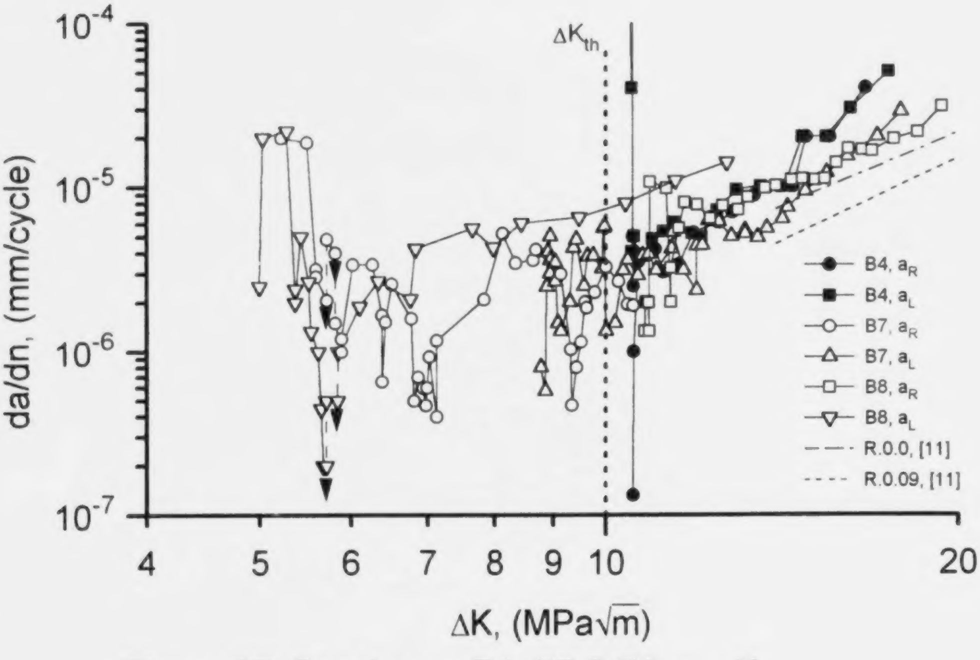

Figure 67: Specimens B4, B7 & B8 vs ΔK

closure will not be fully developed. The extent of compressive loading relative to the tensile load is small, hence the error introduced is not likely to be great.

The following three figures present some of the standard means of reducing long crack data. Figure 66 shows the same data as Figure 52 and is included here for the purpose of comparison. Figure 67 represents the growth rate data plotted against ΔK. Both of these figures show that the longer crack growth data will fall into a fairly narrow scatter band. Figure 67, da/dN versus ΔK, permits comparison to other fracture mechanics investigations. Included in Figure 67 is growth data, obtained by Ellyin and Li [11], for the same material. The threshold stress intensity factor as predicted by Ellyin and Fakinlede [59] is also included as being the lower threshold for growth of long cracks.

The experimentally obtained growth rates for a given ΔK are above the curves obtained by Ellyin and Li [11]. One may be able to attribute this difference to the closure effect not being fully developed along the entire front of the crack. Hence, the effective driving force will be slightly higher and therefore the growth rate will also be higher. Alternatively, it being late in the test there may be some interaction between the two cracks on the specimen, resulting in a higher actual ΔK than the value calculated.

It is often considered that any load applied when the crack is closed is non-damaging. Hence, in the calculation of the effective stress intensity, ΔK_{eff}, only $P_{max}-P_{open}$ should be considered. Figure 68 also shows the growth rate data, except in this figure it is plotted versus ΔK_{eff}. The determination of ΔK_{eff} is dependent on the values obtained for P_{open}[*]. In this investigation, opening load data are only available for the early part of the test, principally because of the short gauge life. The data are further diminished since opening load data which corresponds to regions of no detectable growth can not be included on a diagram such as Figure 68. The growth rate curves of reference [11] have been included in this figure. The results presented in the reference have been modified, assuming a fully developed opening load of 20% (20% being an average value, e.g. Figure 35).

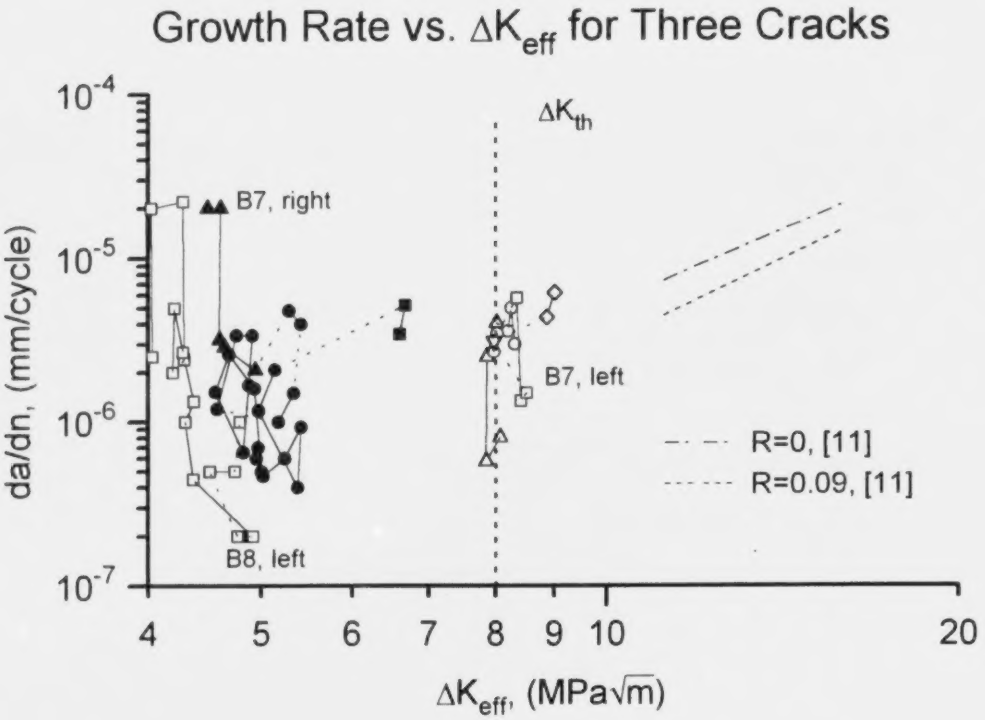

Figure 68: Specimens B7 and B8 vs ΔK_{eff}

---

[*] Instead of using the full load range, ΔP to calculate $\Delta\sigma$, only $P_{max}-P_{open}$ is used to obtain $\Delta\sigma_{eff}$.

Each of the cracks presented in figures 66 - 68 reveals a decrease in growth rate when the cracks are small. Using ΔK_{eff} based on the opening loads measured did little to bring about a regular, or steadily increasing, trend in the growth rate results.

5.3 Discussion

The only information available for the stationary crack is the opening load. There are two principal trends exhibited in this data. The first is a decrease in the recorded opening load of 5 - 15% within the first 50 cycles. An explanation for the initial drop in the opening load is that there may be some surface residual stresses induced during specimen preparation. These residual stresses will wash out during the first few cycles, bringing about a decrease in the opening load. The second trend follows the first with a gradual increase in the opening load through the next several thousand cycles. In most cases there is a temporary drop in the opening load which coincides with the beginning of detectable crack growth.

This trend, of an increase in the crack opening load, has been noted by numerous investigators right back to Elber [25], and is also observed here. There may be several means to investigate this more closely; such as to utilize microstructural barriers which are less significant relative to the crack. This could be accomplished either by looking at a larger crack (one loses the small crack aspects), or by investigating a material which has lower, or at least uniform, microstructural barriers (single phase or even single crystal material). An obvious drawback would be that the study would no longer pertain to common, practical engineering problems such as one encounters with A516 Grade 70.

All the cracks investigated displayed a high growth rate in the during the first few cycles (N<35)[*]. The crack may be growing slowly, but because the measurement resolution is ≈1μm, no change in length is recorded until there is an extension of 1μm. Attributing the full 1μm extension to that replication interval (perhaps 20 cycles) results in a very high growth rate, 50×10^{-6}mm/cycle. Yet another reason for the apparently high growth rate may be that the maximum depth of the crack is not be at the surface corresponding to the a-face. Hence the small uncracked region, may grow quickly, until the deepest point is at the surface.

Considering the influence the aspect ratio (a/c) has on the growth rate, one can see a general trend that there is a drop in the growth rate of the a-face crack which coincides with the inception of steady growth at the tip of the c-face crack (section 4.7, specimen B7). The initial growth of the c-face crack can be anticipated beginning at an aspect ratio of 0.43 - 0.53. This permits one to place a strain gauge on top of the c-face crack and later remove it in time to make length measurements.

A significant aspect of this investigation is the recognition that some of the early fluctuations in growth rate involve the tip of the crack interacting with significant inhomogenaities in the microstructure. The most important of these features appears to be the pearlite regions that result in a decrease in the growth rate. It is not possible to correlate all fluctuations in growth rate as being due to the microstructure. However, one must bear in mind that microstructure varies in depth. A significant microstructural feature present below the surface cannot be seen, yet it may effect the crack growth rate.

---

[*] In this study these high initial growth rates are considered to be prior to the stationary crack stage and are not specifically included. The increase in crack depth may be the crack is simply becoming more clearly defined due to the first few loading cycles.

5.4 Conclusion

The conclusions coming out of this investigation can be divided into two categories: interpretive results of the behaviour of short cracks and assessment of the experimental techniques. The purpose of this study was to examine the behaviour of short cracks. It has significantly corroborated the investigations of others. In conducting this study, a number of experimental methods had to be developed, refined or were found to be, in some way, undesirable.

The cracks investigated ranged in initial size from $a \approx 0.1 - 0.6$mm in depth. Considering the behaviour of the cracks, it was observed that the opening load of a stationary crack increases, suggesting material plasticity and damage accumulation. Then at the point where growth begins there is a decrease in the opening load, likely due to the crack propagating through the damaged region, effectively relieving residual stresses ahead of the crack tip, resulting in a decrease in the opening load. As the test progresses the opening load was found to increase gradually, though at times irregularly. These irregularities were generally a decrease in the crack opening load, some of which corresponded to the crack tip passing through a region of pearlite. As a crack increased in depth, it was found that the opening load approached a steady state value in the range between 10 and 30% of P_{max}.

Growth rate fluctuations (Figure 66), at crack depths of less than 0.2mm, observed on the right side crack of specimen B7 and the left of side specimen B8, were shown to correspond to the crack tip passing through a region of pearlite. When the crack is less than 0.12mm, it was seen that the crack may temporarily self arrest.

The growth rate was plotted versus the applied stress intensity factor range to account for the shape of the crack. This approach was found to provide agreement with the work of other investigators, including the anomalous aspects of short crack behaviour. The growth rate was then plotted against the effective applied stress intensity factor range and was not found to resolve the short crack effect.

The two principal variables measured were crack size (depth and length) and the opening load. The most successful means of measuring crack size investigated herein was the thin film plastic replica technique. However, the application of mean load as part of collecting the replica was shown to have an influence on the opening load measurements. It would be desirable to have a means of measuring the crack size which did not require this application of tensile load for a long period of time.

Perhaps a thick replica technique[*] would permit sufficient resolution, using an SEM, without requiring significant tensile load being applied to the specimen.

The opening load measurement techniques concentrated on two strain gauge method: an active gauge adjacent the tip of the growing crack or an active gauge on top of the mouth of the crack. An increase in event sensitivity was obtained by taking the difference between the strain measured by a far field gauge and the active gauge. However, because of the sensitivity of the system to unavoidable specimen bending, more consistent results could be obtained by using a dedicated far field gauge axially in line with the active gauge.

The procedure involving an active gauge adjacent the tip of a small growing crack, is intended to detect plasticity associated with the tip of the crack. In this investigation, such an approach was found to be ineffective. Instead, crack shielding was found to be the more prominent gauge response than detecting plasticity at the crack tip. This method did not work for either the early or late stages of crack growth.

The opening load measurement technique wherein the active gauge was placed on top of the crack mouth was found to perform well for small cracks. It has the disadvantage of a short gauge life, particularly as the crack increases in size (i.e. half a millimetre). Greater consistency in the interpretation of the opening load from the differential compliance curve was obtained by fitting a Ramberg-Osgood type relation to the curve and comparing this fitted curve to the data.

---

[*] Using a replica 5mm thick would permit the replica to be pressed against the surface of the specimen while curing. The replica would then be gold coated and conductive backing applied, prior to the actual replica material being dissolved away.

6.0 References

1. Wöhler, A., Zeitschrift für Bauwesen, Vol. 16, pp. 67, 1866.

2. Paris, P. and Erdogan, F., "A Critical Analysis of Crack Propagation Laws." ASME Journal of Basic Engineering, Vol. 85, p. 528-534, 1963.

3. Suresh, S. and Ritchie, R. O., "Propagation of Short Fatigue Cracks," International Metals Review, Vol. 29, No. 6, p. 445-476, 1984.

4. Tokaji, K., Ogawa, T. and Harada, Y., "The Growth of Small Fatigue Cracks in a Low Carbon Steel; and the Effect of Microstructure and Limitations of Linear Elastic Fracture Mechanics," Fatigue and Fracture of Engineering Materials and Structures, Vol. 9, p. 205-217, 1986.

5. Taylor, D., "Fatigue Thresholds," Publ. Butterworths & Co., p. 27-37, 1989.

6. Kujawksi, D. and Ellyin, F., "Propagation of Small Corner Cracks Initiated in Cyclic Compression," Engineering Fracture Mechanics, Vol. 43, No. 4, p. 657-662, 1992.

7. Kujawski, D. and Ellyin, F., "Fatigue Growth of Physically Small Inclined Cracks," Fatigue and Fracture of Engineering Materials and Structures, Vol. 16, No. 7, p. 743-752, 1993.

8. Hussey, I. W., Roche, J. and Grabowski, L., "A Fully automated System for Monitoring Short Crack Growth," Fatigue and Fracture of Engineering Materials and Structures, Vol. 14, No. 2/3, p. 309-315, 1991.

9. Lankford, J., "The Influence of Microstructure on the Growth of Small Cracks," Fatigue and Fracture of Engineering Materials and Structures, Vol. 8, p. 161-175, 1985.

10. de los Rios, E. R., Tang, Z. and Miller, K. J., "Short Crack Behaviour in a Medium Carbon Steel," Fatigue and Fracture of Engineering Materials and Structures, Vol. 7, No. 2, p. 97-108, 1984.

11. Ellyin, F and Li, H.-P., "Fatigue Crack Growth in Large Specimens with Various Stress Ratios," Journal of Pressure Vessel Technology, Vol. 106, August 1984, p. 255-260.

12. Wanhill, R. J. H., "Short Cracks in Aerospace Structures," *The Behaviour of Short Fatigue Cracks*, EGF Pub. 1, Ed. K. J. Miller & E. R. de los Rios, 1986, Mechanical Engineering Publications, London, p. 27-36, 1986.

13. Gangloff, R. P., Slavik, D. C., Piascik, R. S. and Van Stone, R. H., "Direct Current Electrical Potential Measurement of the Growth of Small Cracks, " *Small Crack Test Methods*, ASTM STP 1149, Ed. J. M. Larsen & J. E. Allison, American Society for Testing and Materials, p. 116-168, 1992.

14. Donald, J. K. and Ruschau, J., "Direct Current Potential Difference Fatigue Crack Measurement Techniques," *Fatigue Crack Measurement: Techniques and Applications*, Ed. K. J. Marsh, R. A. Smith & R. O. Ritchie, Engineering Materials Advisory Service, Ltd., p. 11-37, 1991.

15. Collins, R. and Lugg, M. C., "Use of A.C. Field Measurements for Non-destructive Testing," *Fatigue Crack Measurement: Techniques and Applications*, Ed. K. J. Marsh, R. A. Smith & R. O. Ritchie, Engineering Materials Advisory Service, Ltd., p.39-67, 1991.

16. ASTM E 647 - 91, "Standard Test Method for Measurement of Fatigue Crack Growth Rates," Annual Book of ASTM Standards, Volume 3.01, p. 654-681, 1991.

17. Beevers, C. J. Editor, "Advances in Crack Length Measurement," Engineering Materials Advisory Service Ltd., 1982.

18. de los Rios, E. R. and Brown, M. W., "Microscopic Techniques," *Fatigue Crack Measurement: Techniques and Applications*, Ed. K. J. Marsh, R. A. Smith & R. O. Ritchie, Engineering Materials Advisory Service, Ltd., p. 289-313, 1991.

19. Larsen, J. M., Jira, J. R. and Ravichandran, K. S., "Measurement of Small Cracks by Photomicroscopy: Experiments and Analysis," *Small Crack Test Methods*, ASTM STP 1149, Ed. J. M. Larsen & J. E. Allison, American Society for Testing and Materials, p. 57-80, 1992.

20. Blom, A. F., Hedlund, A., Zhao, W., Fathulla, A. Weiss, B. and Stickler, R., "Short Fatigue Crack Growth Behaviour in Al 2024 and Al 7475," *The Behaviour of Short Fatigue Cracks*, EGF Pub. 1, Ed. K. J. Miller & E. R. de los Rios, 1986, Mechanical Engineering Publications, London, p. 37-66, 1986.

21. Fathulla, A., Weiss, B. and Stickler, R., "Short Fatigue Cracks in Technical pm-Mo Alloys," *The Behaviour of Short Fatigue Cracks*, EGF Pub. 1, Ed. K. J. Miller & E. R. de los Rios, 1986, Mechanical Engineering Publications, London, p. 115-132, 1986.

22. Yi, L., Smith, R. A. and Grabowski, L., "An Automated Image Processing System for the Measurement of Short Fatigue Crack Growth," *Fatigue Crack Measurement: Techniques and Applications*, Ed. K. J. Marsh, R. A. Smith & R. O. Ritchie, Engineering Materials Advisory Service, Ltd., p. 375-387, 1991.

23. Davidson, D. L., "The Experimental Mechanics of Microcracks," *Small Crack Test Methods*, ASTM STP 1149, Ed. J. M. Larsen & J. E. Allison, American Society for Testing and Materials, p. 81-91, 1992.

24. Stephens, R., Grabowski, L. and Hoeppner, D. W., "In-Situ/SEM Fatigue Studies of Short Crack Behaviour at Ambient and Elevated Temperature in a Nickel-Base Superalloy," *Short Fatigue Cracks*, ESIS 13, Ed. K. J. Miller & E. R. de los Rios, 1992, Mechanical Engineering Publications, London, p. 335-348, 1992.

25. Elber, W., "Fatigue Crack Closure under Cyclic Tension," Engineering Fracture Mechanics, Vol. 2, p. 37-45, 1970.

26. de Lange, R. G., "Plastic Replica Methods Applied to a Study of Fatigue Crack Propagation," Transactions of the AIME, Vol. 230, p. 644-648, 1964.

27. Swain, M. H., "Monitoring Small-Crack Growth by the Replication Method," *Small Crack Test Methods*, ASTM STP 1149, Ed. J. M. Larsen & J. E. Allison, American Society for Testing and Materials, p. 34-56, 1992.

28. Silk, M. G., "Ultrasonics," *Fatigue Crack Measurement: Techniques and Applications*, Ed. K. J. Marsh, R. A. Smith & R. O. Ritchie, Engineering Materials Advisory Service, Ltd., p. 95-145, 1991.

29. Resch, M. T., Nelson, D. V. Shyne, J. C. and Kino, G. S., "Surface Acoustic Wave Monitoring of Growth of Small Fatigue Cracks," *Advances in Crack Length Measurements*, Ed. C. J. Beevers, Engineering Materials Advisory Services Ltd., p. 473-504, 1982.

30. Resch, M. T. and Nelson, D. V., "An Ultrasonic Method for Measurement of Size and Opening Behaviour of Small Fatigue Cracks," *Small Crack Test Methods*, ASTM STP 1149, Ed. J. M. Larsen & J. E. Allison, American Society for Testing and Materials, p. 169-196, 1992.

31. Park, Y., De Vadder, D. and François, D., "Crack Tip Closure Measurements by Means of a Focused Ultrasonic Beam," 10th Congress on Material Testing, Budapest, October 1991.

32. Jenkins, P. J. and Briggs, G. A. D., "Acoustic Microscopy," *Fatigue Crack Measurement: Techniques and Applications*, Ed. K. J. Marsh, R. A. Smith & R. O. Ritchie, Engineering Materials Advisory Service, Ltd., p. 147-172, 1991.

33. Stephens, R., Grabowski, L. and Hoeppner, D. W., "In-Situ/SEM Fatigue Studies of Short Crack Behaviour at Ambient and Elevated Temperature in a Nickel-Base Superalloy," *Short Fatigue Cracks*, ESIS 13, Ed. K. J. Miller & E. R. de los Rios, 1992, Mechanical Engineering Publications, London, p. 335-348, 1992.

34. Swain, M. H., "Monitoring Small-Crack Growth by the Replication Method," *Small Crack Test Methods*, ASTM STP 1149, Ed. J. M. Larsen & J. E. Allison, American Society for Testing and Materials, p. 34-56, 1992.

35. Gangloff, R. P., Slavik, D. C., Piascik, R. S. and Van Stone, R. H., "Direct Current Electrical Potential Measurement of the Growth of Small Cracks, " *Small Crack Test Methods*, ASTM STP 1149, Ed. J. M. Larsen & J. E. Allison, American Society for Testing and Materials, p. 116-168, 1992.

36. Järvine, A. K., "The Effect of Compressive Overloads on Crack Growth Rates and Crack Closure for 2024-T351 Aluminum," MSc. Thesis, University of Waterloo, Waterloo, Ontario, Canada, 1992.

37. Sharpe, W. N. and Su, X., "Closure Measurements of Naturally Initiating Small Cracks," Engineering Fracture Mechanics, Vol. 30, No. 3, p. 275-294, 1988.

38. Pearson, S., "Initiation of Fatigue Cracks in Commercial Aluminium Alloys and the Subsequent Propagation of Very Short Cracks," Engineering Fracture Mechanics, Vol. 7, pp. 235-247, 1975.

39. Ogura, K., Miyoshi, Y. and Nishikawa, I., "Fatigue Crack Growth and Closure of Small Cracks at the Notch Root," *Current Research on Fatigue Cracks*, Ed. T. Tanaka, M. Jono & K. Komai, Current Japanese Materials Research - Vol. 1, Elsevier Applied Science, p. 67-91, 1987.

40. Kendall, J. E. and King, J. E., "Short Fatigue Crack Growth behaviour: Data Analysis Effects," International Journal of Fatigue, Vol. 10, No. 3, p. 163-170, 1988.

41. Berens, A. P. "Fatigue Crack Growth Data Analysis," *Metals Handbook*, 9th Edition, Vol. 8: Mechanical Testing, p. 678-684, 1978.

42. Chen, D. L., Weiss, B. and Stickler, R., "Application of a New Evaluation Method for Near-Threshold Closure Effects of Small Surface Fatigue Cracks," *Proceedings of the 10th Congress on Materials Testing, Budapest, Hungary*, Ed. E. Czoboly, Vol. 2, p. 466-471, 1991.

43. DuQuesnay, D. L., "Fatigue Damage Accumulation in Metals subjected to High Mean Stress and Overload Cycles," University of Waterloo, Ph. D. thesis, 1991.

44. ASM Committee on Fatigue Crack Propagation, "Fatigue Crack Propagation," *Metals Handbook*, 9th Edition, Vol. 8: Mechanical Testing, p. 377-402, 1978.

45. Fleck, N. A., "Compliance Methods for Measurement of Crack Length," *Fatigue Crack Measurement: Techniques and Applications*, Ed. K. J. Marsh, R. A. Smith & R. O. Ritchie, Engineering Materials Advisory Service, Ltd., p. 69-93, 1991.

46. Jenkins, M. G., Kobayashi, A. S. and Bradt, R. C., "Crack Length Measurements of Ceramics at Elevated Temperatures Using the Laser Interferometric Displacement Gauge," *Fatigue Crack Measurement: Techniques and Applications*, Ed. K. J. Marsh, R. A. Smith & R. O. Ritchie, Engineering Materials Advisory Service, Ltd., p. 335-373, 1991.

47. "*Mechanics of Fatigue Crack Closure*," Ed. by J. C. Newman Jr. and Wolf Elber, ASTM STP 982, American Society for Testing and Materials, 1988.

48. "*The Behaviour of Short Fatigue Cracks*," EGF Pub, Ed. by K. J. Miller and E. R. de los Rios, Mechanical Engineering Publications, London, 1986.

49. "*Short Fatigue Cracks*," ESIS 13, Ed. by K. J. Miller and E. R. de los Rios, Mechanical Engineering Publications, London, 1992.

50. Proceedings of the Fifth International Conference on Fatigue and Fatigue Thresholds, "*Fatigue 93*," Ed. J.-P. Bailon and J. I. Dickson, Volume 1, Engineering Material Advisory Services, Ltd., 3-7 May 1993.

51. Ellyin, F. and Kujawski, D., "Plastic Strain Energy in Fatigue Failure," ASME Journal of Pressure Vessel Technology, Vol. 106, p. 342-347, 1984.

52. Pippan, R., "The Length and the Shape of Cracks Under Cyclic Compression: The Influence of Notch Geometry," Engineering Fracture Mechanics, Vol. 31, p. 715-718, 1988.

53. Newman, J. C., Jr. and Raju, I. S., "Stress-Intensity Factor Equations for Cracks in Three-Dimensional Finite Bodies," Fracture Mechanics: Fourteenth Symposium - Volume I: Theory and Analysis, ASTM STP 791, Eds. J. C. Lewis and G. Sines, American Society for Testing and Materials, p. I-238 - I-265, 1983.

54. Pickard, A. C., "The Application of 3-Dimensional Finite Element Methods to Fracture Mechanics and Fatigue Life Prediction," Rolls-Royce Ltd., Engineering Materials Advisory Services, Ltd., 1986.

55. Newman, J. C. Jr., "Modelling Small Fatigue Crack Behaviour," Fatigue 93, Volume 1, Ed. J.-P. Bailon and J. I. Dickson, Proceedings of the Fifth International Conference on Fatigue and Fracture Thresholds, Engineering Materials Advisory Services, Ltd., p. 33-44, 3 - 7 May 1993.

56. Lam, Y. C., Kujawski, D. and Ellyin, F., "The Development of Crack Closure with Crack Extension," Scripta Metallurgica et Materialia, Vol. 25, Pergamon Press plc, p. 2313-2318, 1991.

57. Press, W. H., Flannery, B. P., Teukolsky, S. A. and Vetterling, W. T., "Numerical Recipes in C," Cambridge University Press, p. 542, 1990.

58. Tokaji, K. and Ogawa, T., "The Growth Behaviour of Microstructurally Small Fatigue Cracks in Metals," *Short Fatigue Cracks*, ESIS 13, Ed. K. J. Miller and E. R. de los Rios, , Mechanical Engineering Publications, London, p. 85-99, 1992.

59. Ellyin, F. and Fakinlede, C.O., "Probabilistic Simulation of Fatigue Crack Growth by Damage Accumulation," Engineering Fracture Mechanics, Vol. 22, No. 4, p. 697-712, 1985.

Appendix A

Data for specimens B4, B6, B7 and B8:

- Specimen specific data
- Loading information
- Growth rate
- Stress intensity factor range
- Crack opening load results

Data title: Left side corner crack. Data filename: b4−left.dat

Specimen ID Number: B4 Number of Points: 25

Width: 7.96 mm Thickness: 7.95 mm P_{min}: 791 N P_{max}: 15820 N

R: 0.05 S_{min}: 12.5 MPa S_{max}: 250 MPa N_{EoT} = 213,860 cycles

Cycles	a_L (mm)	c_L (mm)	delta K	da/dN
0	0.574	1.61	MPa(m)$^{1/2}$	mm/cycle x 10^{-6}
5	0.578	1.65	10.49	600.0
10	0.580	1.67	10.52	44.4
50	0.580	1.67	10.52	0.0
101	0.580	1.67	10.52	0.0
251	0.580	1.67	10.52	0.0
500	0.580	1.67	10.52	4.0
1000	0.583	1.67	10.54	4.0
2500	0.588	1.67	10.57	5.0
5000	0.603	1.67	10.65	3.9
10000	0.617	1.67	10.73	3.8
20000	0.660	1.67	10.96	4.8
30000	0.713	1.67	11.21	5.3
40000	0.766	1.67	11.43	6.0
60000	0.894	1.67	11.86	5.2
80000	0.973	1.68	12.09	4.9
100000	1.090	1.73	12.46	7.2
120000	1.26	1.81	12.95	9.5
140000	1.47	1.94	13.58	11.0
160000	1.70	2.09	14.24	12.3
170000	1.84	2.22	14.75	16.0
180000	2.02	2.41	15.46	22.5
190000	2.29	2.60	16.21	31.5
200000	2.65	2.94	17.47	48.5
210000	3.26	3.66		

Filename: B4L−DK.WK3

Using the secant method for determining da/dN.

Data title: Right side corner crack. Data filename: b4−right.dat

Specimen ID Number: B4 Number of Points: 25

Width: 7.96 mm Thickness: 7.95 mm P_{min}: 791 N P_{max}: 15820 N

R: 0.05 S_{min}: 12.5 MPa S_{max}: 250 MPa N_{EoT} = 213,860 cycles

Cycles	a_R (mm)	c_R (mm)	delta K	da/dN
0	0.520	1.93	MPa(m)$^{1/2}$	mm/cycle x 10^{-6}
5	0.520	1.93	10.35	0.0
10	0.520	1.93	10.35	600.0
50	0.547	1.93	10.55	296.7
101	0.547	1.93	10.55	5.0
251	0.548	1.93	10.55	2.5
500	0.548	1.93	10.55	0.0
1000	0.548	1.93	10.55	0.0
2500	0.548	1.93	10.55	0.0
5000	0.548	1.93	10.55	0.1
10000	0.549	1.93	10.56	1.0
20000	0.563	1.93	10.66	3.5
30000	0.619	1.93	11.03	4.2
40000	0.647	1.93	11.20	3.0
60000	0.710	1.93	11.55	3.4
80000	0.782	1.93	11.90	5.2
100000	0.919	1.96	12.50	6.1
120000	1.024	1.97	12.85	7.0
140000	1.198	2.03	13.41	8.8
160000	1.375	2.17	14.08	10.1
170000	1.500	2.25	14.49	13.4
180000	1.642	2.32	14.86	15.9
190000	1.817	2.50	15.56	22.9
200000	2.100	2.81	16.70	35.7
210000	2.530	3.34		

Filename: B4R−DK.WK3

− Light shaded regions represent estimated values.

Using the secant method for determining da/dN.

Data title: Right side corner crack. Data filename: b6−right.dat

Specimen ID Number: B6 Number of Points: 30

Width: 7.986 mm Thickness: 7.977 mm P_{min}: 794 N P_{max}: 15880 N

R: 0.05 S_{min}: 12.5 MPa S_{max}: 250 MPa N_{EoT} = 40,000 cycles

Cycles	a_R (mm)	c_R (mm)	delta K	da/dN
0	0.082	0.833	MPa(m)$^{1/2}$	mm/cycle x 10^{-6}
2	0.058	0.84	3.69	0.0
4	0.082	0.84	4.35	4000.0
8	0.082	0.84	4.35	0.0
25	0.082	0.84	4.35	0.0
35	0.082	0.84	4.35	0.0
50	0.082	0.84	4.35	0.0
101	0.082	0.84	4.35	0.0
199	0.082	0.84	4.35	0.0
300	0.082	0.84	4.35	0.0
400	0.082	0.84	4.35	5.0
700	0.084	0.84	4.40	6.7
1000	0.086	0.84	4.45	3.1
2010	0.088	0.84	4.50	1.5
3000	0.089	0.84	4.53	0.5
4000	0.089	0.84	4.53	0.0
6000	0.089	0.84	4.53	0.0
8000	0.089	0.84	4.53	7.2
9335	0.113	0.84	5.05	12.0
10000	0.113	0.84	5.05	2.6
12000	0.120	0.84	5.19	6.5
14000	0.139	0.84	5.54	19.8
16000	0.199	0.84	6.45	19.0
17310	0.202	0.84	6.48	1.5
18000	0.202	0.84	6.48	0.0
20010	0.202	0.84	6.48	3.7
21000	0.213	0.842	6.62	9.6
25000	0.250	0.842	7.03	11.9
30000	0.320	0.84	7.62	13.8
40000	0.457	0.84		

Filename: B6R−DK.WK3

− Light shaded regions represent estimated values.

Using the secant method for determining da/dN.

Data title: Left side corner crack. Data filename: b7−left.dat

Specimen ID Number: B7 Number of Points: 73

Width: 7.965 mm Thickness: 7.998 mm P_{min}: −1593 N P_{max}: 15926 N

R: −0.10 S_{min}: −25 MPa S_{max}: 250 MPa N_{EoT} = 305,155 cycles

Cycles	a_L (mm)	C_L (mm)	delta K MPa(m)$^{1/2}$	da/dN mm/cycle x 10^{-6}	Pop/Pmax (%)	delta K_{eff} MPa(m)$^{1/2}$
0	0.250	1.280				
1	0.266	1.280	8.77	8000.0		
2	0.266	1.280	8.77	0.0		
4	0.266	1.280	8.77	0.0	10.4	7.14
6	0.266	1.280	8.77	0.0	8.3	7.31
12	0.266	1.280	8.77	0.0	2.0	7.81
18	0.266	1.280	8.77	0.0	1.6	7.85
20	0.266	1.280	8.77	0.0	1.4	7.86
30	0.266	1.280	8.77	0.0	1.3	7.87
40	0.266	1.280	8.77	0.0	2.6	7.76
60	0.266	1.280	8.77	0.0	4.4	7.62
75	0.266	1.280	8.77	0.0	3.3	7.71
90	0.266	1.280	8.77	0.0	2.9	7.74
120	0.266	1.280	8.77	0.0	6.4	7.46
145	0.266	1.280	8.77	0.0	2.7	7.76
195	0.266	1.280	8.77	0.0	4.8	7.59
245	0.266	1.280	8.77	0.0	3.6	7.68
325	0.266	1.280	8.77	0.0	5.3	7.55
495	0.266	1.280	8.77	0.0	4.0	7.65
750	0.266	1.280	8.77	0.0	0.3	7.95
995	0.266	1.280	8.77	0.0	3.5	7.69
1494	0.266	1.280	8.77	0.8	−1.3	8.07
2245	0.267	1.280	8.78	0.6	1.7	7.85
3250	0.267	1.280	8.78	2.5	1.4	7.87
4658	0.273	1.280	8.86	4.0	0.4	8.02
4994	0.274	1.280	8.88	3.6	−1.7	8.21
5490	0.276	1.281	8.90	5.0	−2.1	8.26
5994	0.279	1.281	8.94	3.0	−2.3	8.32
6494	0.279	1.281	8.94	0.0	−1.5	8.25
6990	0.279	1.281	8.94	2.7	1.9	7.98
7990	0.283	1.281	9.00	3.5	1.8	8.03
8994	0.286	1.281	9.03	1.5		
10000	0.286	1.281	9.03	1.3		
12000	0.290	1.281	9.09	2.0		
14000	0.294	1.281	9.14	4.3		
16000	0.307	1.282	9.30	4.8		
18000	0.313	1.282	9.37	2.5		
20000	0.317	1.282	9.41	3.8		
22500	0.330	1.283	9.56	3.8		
25000	0.336	1.283	9.63	3.2		
27500	0.346	1.283	9.74	5.6		
30000	0.364	1.283	9.92	5.7	7.4	8.35
31000	0.366	1.283	9.94	1.3	6.8	8.42

33000	0.368	1.283	9.96	1.5	6.0	8.51
35020	0.372	1.283	10.00	3.1		
40050	0.390	1.283	10.17	3.6		
45050	0.408	1.283	10.34	2.9		
50050	0.419	1.283	10.43	3.8		
55050	0.446	1.283	10.65	3.9		
60050	0.458	1.283	10.74	3.1	18.3	7.98
65050	0.477	1.285	10.89	4.2		
70050	0.500	1.285	11.04	5.3		
80060	0.556	1.285	11.39	3.1		
90050	0.562	1.288	11.43	2.4		
100050	0.603	1.295	11.65	4.4		
110050	0.649	1.333	11.96	4.4	18.4	8.87
111002	0.651	1.334	11.97	6.2	17.2	9.01
115050	0.680	1.337	12.10	7.2		
120000	0.716	1.342	12.25	6.1		
130000	0.771	1.364	12.50	4.9		
145100	0.840	1.403	12.82	5.4		
160000	0.932	1.442	13.16	6.2		
160100	0.933	1.442	13.16	5.2		
175100	1.010	1.494	13.49	4.9		
190100	1.079	1.533	13.75	5.5		
205100	1.176	1.610	14.17	6.4	29.9	9.03
214950	1.237	1.629	14.32	7.4		
229900	1.360	1.730	14.83	9.3		
244900	1.516	1.858	15.46	12.0		
259900	1.720	1.988	16.10	15.1		
274900	1.969	2.203	17.08	20.0		
289900	2.321	2.374	17.88	28.5		
305005	2.827	2.910				

Filename: B7L–DK.WK3

– Light shaded regions represent estimated values based on a linear interpolation between adjacent measured values.

▨ – Dark shaded regions represent estimated values, as measured values indicated a reduction in crack length.

Using the secant method for determining da/dN.

Data title: Right side corner crack. Data filename: b7−right.dat

Specimen ID Number: B7 Number of Points: 68

Width: 7.965 mm Thickness: 7.998 mm P_{min}: −1593 N P_{max}: 15926 N

R: −0.10 S_{min}: −25 MPa S_{max}: 250 MPa N_{EoT} = 305,155 cycles

Cycles	a_R (mm)	C_R (mm)	delta K MPa(m)$^{1/2}$	da/dN mm/cycle x 10^{-6}	Pop/Pmax (%)	delta K_{eff} MPa(m)$^{1/2}$
0	0.078	0.820				
2	0.088	0.820	5.22	555.6		
18	0.088	0.820	5.22	0.0	−1.8	4.83
28	0.088	0.820	5.22	0.0	1.0	4.70
35	0.088	0.820	5.22	0.0	−0.5	4.77
52	0.088	0.820	5.22	0.0	1.8	4.66
100	0.088	0.820	5.22	0.0	6.5	4.44
125	0.088	0.820	5.22	0.0	0.6	4.72
150	0.088	0.820	5.22	0.0	8.8	4.33
200	0.088	0.820	5.22	0.0	5.2	4.50
250	0.088	0.820	5.22	0.0	7.4	4.40
330	0.088	0.820	5.22	0.0	8.4	4.35
500	0.088	0.820	5.22	0.0	6.9	4.42
756	0.088	0.820	5.22	20.0	5.3	4.50
1000	0.098	0.820	5.49	18.8	7.5	4.62
1500	0.102	0.820	5.59	3.2	9.4	4.61
2250	0.102	0.820	5.59	2.9	8.5	4.65
3244	0.107	0.820	5.72	2.1	4.9	4.94
4658	0.107	0.820	5.72	0.0	3.2	5.03
4674	0.107	0.820	5.72	0.0	−5.0	5.46
5000	0.107	0.820	5.72	4.8	−1.8	5.29
5500	0.111	0.820	5.81	4.0	−2.5	5.42
6000	0.111	0.820	5.81	0.0	−1.0	5.34
6500	0.111	0.820	5.81	0.0	1.7	5.20
7000	0.111	0.820	5.81	0.0	0.6	5.25
7500	0.111	0.820	5.81	0.0	−0.5	5.31
8000	0.111	0.820	5.81	0.0	−0.2	5.30
9000	0.111	0.820	5.81	1.5	−1.0	5.34
10000	0.114	0.820	5.89	1.0	3.2	5.18
12000	0.114	0.820	5.89	0.0	7.8	4.93
14000	0.114	0.820	5.89	0.0	10.7	4.78
16000	0.114	0.820	5.89	0.0	8.7	4.88
18000	0.114	0.820	5.89	0.0	11.3	4.75
20002	0.114	0.820	5.89	0.0	7.0	4.98
22500	0.114	0.820	5.89	1.2	14.3	4.59
25000	0.120	0.820	6.02	3.4	13.0	4.76
27500	0.131	0.820	6.26	3.4	13.6	4.92
30000	0.137	0.820	6.39	1.7	15.9	4.88
31060	0.137	0.820	6.39	0.7	16.8	4.83
33060	0.139	0.820	6.43	1.5	21.8	4.57
35000	0.143	0.820	6.51	2.6	20.6	4.70
40000	0.157	0.820	6.77	1.6	19.8	4.94
45000	0.159	0.820	6.81	0.5	19.1	5.01

50000	0.162	0.820	6.86	0.7	20.3	4.97
55000	0.166	0.821	6.94	0.6	21.4	4.96
60000	0.168	0.821	6.97	0.5	20.7	5.02
61435	0.169	0.821	6.99	0.6	17.4	5.25
65000	0.171	0.821	7.02	0.9	15.1	5.42
70000	0.177	0.821	7.12	0.4	16.8	5.39
80000	0.177	0.821	7.12	1.2	23.1	4.98
111624	0.226	0.821	7.84	2.1	27.8	5.14
115000	0.250	0.821	8.13	5.2	9.6	6.68
120100	0.270	0.821	8.35	3.4	13.0	6.60
129523	0.300	0.821	8.64	3.6		
130100	0.306	0.821	8.69	4.1		
145000	0.364	0.821	9.13	3.0		
160000	0.395	0.821	9.32	1.0		
175003	0.395	0.827	9.34	0.5		
190000	0.409	0.832	9.43	0.8		
205000	0.419	0.842	9.51	1.2	37.0	5.45
210000	0.432	0.844	9.59	2.0		
214950	0.439	0.845	9.62	1.9		
230000	0.469	0.850	9.77	2.3		
245000	0.508	0.872	10.00	3.3		
260000	0.567	0.889	10.25	2.7		
275000	0.588	0.922	10.44	1.9		
289900	0.625	0.929	10.56	1.9		
304905	0.645	0.983				

Filename: B7R–DK.WK3

– Light shaded regions represent estimated values based on a linear interpolation between adjacent measured values.

▨ – Dark shaded regions represent estimated values, as measured values indicated a reduction in crack length.

Using the secant method for determining da/dN.

Data title: Left side corner crack. Data filename: b8-left.dat

Specimen ID Number: B8 Number of Points: 37

Width: 7.960 mm Thickness: 8.052 mm P_{min}: −1602 N P_{max}: 16023 N

R: −0.10 S_{min}: −25 MPa S_{max}: 250 MPa N_{EoT} = 141,540 cycles

Cycles	a_L (mm)	C_L (mm)	delta K MPa(m)$^{1/2}$	da/dN mm/cycle x 10^{-6}	Pop/Pmax (%)	delta K_{eff} MPa(m)$^{1/2}$
600	0.078	2.004				
800	0.078	2.004	5.00	2.5	11.3	4.03
1000	0.079	2.005	5.03	20.0	12.0	4.02
1250	0.087	2.005	5.28	22.0	10.7	4.28
1500	0.090	2.006	5.36	2.4	11.9	4.30
2500	0.090	2.008	5.36	0.0	10.5	4.37
3000	0.090	2.008	5.37	0.0	13.5	4.22
3500	0.090	2.009	5.37	0.0	15.6	4.12
4000	0.090	2.010	5.37	2.0	13.9	4.20
4500	0.092	2.011	5.42	5.0	14.5	4.22
5003	0.095	2.012	5.51	2.7	14.4	4.29
6000	0.096	2.014	5.54	1.3	13.0	4.38
8000	0.099	2.018	5.62	1.0	15.8	4.30
10005	0.100	2.021	5.65	0.4	14.9	4.37
12500	0.101	2.026	5.68	0.2	4.6	4.92
15000	0.101	2.030	5.68	0.2	7.1	4.80
17500	0.102	2.035	5.71	0.2	7.9	4.78
20000	0.102	2.039	5.71	0.0	8.7	4.74
25000	0.102	2.049	5.71	0.5	12.9	4.52
30000	0.107	2.058	5.84	0.5	10.6	4.75
35000	0.107	2.067	5.84	0.0	7.4	4.92
40000	0.107	2.076	5.84	0.0	13.1	4.62
45000	0.107	2.085	5.84	0.0	12.4	4.65
50000	0.107	2.094	5.84	0.0	11.6	4.70
55000	0.107	2.103	5.84	1.0	9.7	4.80
60000	0.117	2.112	6.11	1.9		
65000	0.126	2.121	6.33	2.7		
70006	0.144	2.131	6.76	2.1		
75000	0.147	2.140	6.83	4.2		
80000	0.186	2.149	7.65	5.6		
85000	0.203	2.158	7.97	4.3		
90000	0.229	2.167	8.44	6.0		
100000	0.293	2.185	9.47	6.5		
110000	0.359	2.204	10.39	7.9		
120000	0.451	2.222	11.48	10.9		
130000	0.576	2.240	12.70	14.0		
140000	0.731	2.258				

Filename: B8L-DK.WK3

- Light shaded regions represent estimated values based on a linear interpolation between adjacent measured values.

▨ – Dark shaded regions represent estimated values, as measured values indicated a reduction in crack length.

Using the secant method for determining da/dN.

Data title: Right side corner crack. Data filename: b8−right.dat

Specimen ID Number: B8 Number of Points: 35

Width: 7.960 mm Thickness: 8.052 mm P_{min}: −1602 N P_{max}: 16023 N
R: −0.10 S_{min}: −25 MPa S_{max}: 250 MPa N_{EoT} = 141,540 cycles

Cycles	a_R (mm)	C_R (mm)	delta K MPa(m)$^{1/2}$	da/dN mm/cycle x 10^{-8}	Pop/Pmax (%)	delta K_{eff} MPa(m)$^{1/2}$
0	0.377	2.404				
2	0.383	2.404	10.75	1000.0		
6	0.383	2.404	10.75	0.0		
8	0.383	2.404	10.75	0.0	0.9	9.69
16	0.383	2.404	10.75	0.0	−1	9.87
22	0.383	2.404	10.75	0.0	0.6	9.71
32	0.383	2.404	10.75	181.8	−2.8	10.05
44	0.387	2.404	10.80	125.0	−3.5	10.16
64	0.387	2.404	10.80	0.0	−2.9	10.10
88	0.387	2.404	10.80	0.0	−5.6	10.37
124	0.387	2.404	10.80	0.0	−6.4	10.45
200	0.387	2.404	10.80	0.0	−6.6	10.47
250	0.387	2.404	10.80	0.0	−3.3	10.14
300	0.387	2.404	10.80	0.0	−5.5	10.36
400	0.387	2.404	10.80	0.0	−5.6	10.37
600	0.387	2.405	10.80	0.0	−5.4	10.35
800	0.387	2.405	10.80	0.0	−7.1	10.52
1000	0.387	2.405	10.80	0.0	−7	10.51
1250	0.387	2.405	10.80	0.0	−3.6	10.17
1500	0.387	2.405	10.80	1.3	−5.1	10.32
2000	0.388	2.406	10.81	2.0		
2500	0.389	2.406	10.83	2.0		
3000	0.390	2.407	10.84	2.0		
3500	0.391	2.407	10.85	2.0		
4000	0.392	2.408	10.86	2.0		
4500	0.393	2.408	10.88	2.0		
5003	0.394	2.408	10.89	1.3		
6000	0.395	2.409	10.90	10.7		
8000	0.426	2.411	11.27	9.7		
10005	0.434	2.413	11.37	2.0		
12500	0.435	2.413	11.38	3.2		
15000	0.450	2.413	11.55	5.6		
17500	0.463	2.413	11.69	8.0		
20000	0.490	2.413	11.98	7.7		
25000	0.521	2.413	12.29	6.4		
30000	0.554	2.413	12.61	7.6		
35000	0.597	2.413	12.99	7.2		
40000	0.626	2.413	13.24	8.6		
45000	0.683	2.413	13.69	9.8		
50000	0.724	2.413	14.00	10.1		
55000	0.784	2.438	14.43	10.9		
60000	0.833	2.440	14.74	11.1		
65000	0.895	2.450	15.12	10.9		

70006	0.942	2.475	15.40	11.1
75000	1.006	2.496	15.75	13.9
80000	1.081	2.520	16.13	16.9
85000	1.175	2.553	16.57	16.7
90000	1.248	2.585	16.90	16.4
100000	1.421	2.676	17.64	19.4
110000	1.635	2.798	18.48	21.4
120000	1.849	2.974	19.38	30.7
130000	2.248	3.207		

Filename: B8R–DK.WK3

– Light shaded regions represent estimated values based on a linear interpolation between adjacent measured values.

▒ – Dark shaded regions represent estimated values, as measured values indicated a reduction in crack length.

Using the secant method for determining da/dN.

Appendix B

Computer code for collection and analysis of strain gauge data.

```
/*                           GILMORE.C                                   */

/* Program for acquisition and manipulation of data from the Gilmore     */
/* servo hydraulic testing machine, Rm 1-10 Mechanical Engineering       */
/* University of Alberta.                                                */

/* By David Craig, 3 April 1993 with lots of help from Ian Buttar.       */

/* This program is written for the 8088 computer which has been provided */
/* as a dedicated unit for this testing machine.  It is in some sort of  */
/* a turbo mode (8MHz), hence the system clock is somewhat faster than   */
/* the DAS-8 card assumes.  This is compensated for in how the counters  */
/* are set up.  The computer has 640kb of memory, a 10Mb hard disk and   */
/* a math coprocessor.                                                   */

/* This program has been written and compiled using Microsoft QuickC     */
/* 2.5, using the large memory model.                                    */

/* As presently set up this will allow for a maximum of 7 data           */
/* conversions
per event.  One should be aware that the data as                         */
/* recorded is not coincident (ie. the values are not recorded           */
/* simultaneously).  This presently is using the new Mode 21 call to     */
/* the DAS-8 card which does "N" Conversions in "X" Channel Bursts.      */

/* To increase the duration over which the conversions are made (ie. to  */
/* slow the conversion trigger clock beyond 133 Hz) it would be          */
/* necessary to cascade a couple of the counters together.               */

#include <stdio.h>
/* #include <stdlib.h>                                                   */
#include <string.h>     /*  For strcat()                                 */
#include <graph.h>

#include "gilmtool.h"
#include "gilmgraf.h"

#define CHANNEL_LO 0    /*  DAS-8 channels to monitor.                   */
#define CHANNEL_HI 5

/* The NUMBER_OF_EVENTS recorded should be sufficient to give a good     */
/* description of a full cycle.  To record the one loop worth of data    */
/* with a given number of events counter #2 must be loaded with a        */
/* suitable value which is a function of the NUMBER_OF_EVENTS and the    */
/* GILMORE_LOADING_FREQUENCY.  The actual number of data sets recorded   */
/* will be approximately 5% higher than this to insure a full loop is    */
/* recorded if the loading frequency is a little below 2 Hz.             */
#define COMPUTER_SPEED 3996600

#define FREQ 0.23F

/* There may be two command line parameters additional to the program    */
/* executable file.  The first is an input data file name, the second    */
/* is an output data file name.  If no output data file name is used     */
/* then no output file will be generated.                                */

void main( int argc, char *argv[] )
{
    int number_of_conversions_per_event, npoints, number_of_events,
        output=0 ;

    double counter_load_value ;

    float load_freq;

    char file_name[FILENAME_MAX], out_file[FILENAME_MAX] ;

/*  Description of variables
    argc = the number of command line arguments
    argv = a pointer to the command line arguments
    number_of_conversions_per_event = the number of data conversions
                                      desired per event. (ie. 4)
    npoints = number of events or sets of data (the number of
              points on the loop).
              counter_load_value = value loaded into counter #2.
    load_freq = the loading frequency when the data was collected
    file_name = the name of the input data file
    out_file = the name of the output data file.
    output = a switch indicating whether an output file should be generated
              or not.  0 means do not generate, anything else to make an
              output file.
                                                                           */
   _clearscreen( _GCLEARSCREEN ) ;
    number_of_conversions_per_event = CHANNEL_HI - CHANNEL_LO + 1;

    if (argc < 2)
    {
     printf("\tRead the data from the DAS-8 card or an existing file?\n ");
     printf("\t(enter file name or das-8): ") ;
     scanf("%s", file_name) ;
    }
    else {  strcpy(file_name, argv[1]) ;  }

/*  If argc ==3 then an output file name must have come in on the          */
/*  command line too.                                                      */
    if (argc == 3) {  strcpy(out_file, argv[2]), output=1 ;   }

    if (strcmp(file_name, "das-8")==0)
    {         /*   Query the board                                         */

/*  Since the frequency of the data collection cycle is usually 0.23 I     */
/* will hard program that so I don't have to keep entering it each time.  */

/*  Prompt for the Gilmore load frequency                                  */
/*  printf("\n\tPlease enter the loading frequency: ") ;                   */
/*  scanf("%f", &load_freq ) ;                                           */
    load_freq = FREQ ;

    if ((load_freq == 0.23F)||(load_freq == 2.0F))
     number_of_events = (load_freq == 0.23F) ? 800 : 250 ;
      else    { printf("\n\tPlease enter the number of events: ") ;
     scanf("%d", number_of_events ) ;                                    }

/*  Calculate the appropriate value to load into the counter.              */
/*  This involves rounding the value off a bit.                            */
    counter_load_value = COMPUTER_SPEED / number_of_events ;
   counter_load_value = counter_load_value / load_freq ;
   counter_load_value = ((int)(counter_load_value + 500) / 1000 ) * 1000 ;

/* Initialize the DAS-8 board and set up  counter #2                    */
   initialize_das8_card((int)counter_load_value);

/* Set the multiplexer describing which channels of the DAS-8 to scan    */
   set_das8_multiplexer( CHANNEL_LO, CHANNEL_HI ) ;

   collect_data(  number_of_conversions_per_event,  number_of_events,
                load_freq, file_name ) ;
   }

/* Read the data from the data file.                                     */
/* Presently set up to only read 6 values from each line of the          */
/* data file.                                                            */

/* Now display a graph of the data.                                      */
   plot_the_data( file_name, out_file, output );

}  /*        End of the main program                                     */
```

```
/*              GILMGRAF.C                                                  */

/*  The plotting subroutines for the Gilmore data acquisition program.     */
/*  David Craig, Mechanical Engineering, University of Alberta.            */

#include <stdio.h>
#include <stdlib.h>
#include <string.h>
#include <dos.h>
#include <math.h>
#include "nrutil.h"
#include "gilmtool.h"
#include "gilmcurv.h"
#include "gilmgraf.h"
#include "geograf.h"

#define LOAD_MULT  10.8207   /*  10 * 2215 / 2047 or 5*2215/2047          */
#define PLOT 0               /*  0 means use screen display else printer  */

/* ================================================================== */
/*  Subroutine to plot the data.                                       */
/* ------------------------------------------------------------------ */
/*  For now I will assume that this deals with only one loop which may    */
/*  or may not overlap a bit.  The fitting aspects really only apply to   */
/*  the partial loading loops.                                            */

void plot_the_data(char* data_in, char* data_out, int output )
{
/*  Variables for data manipulation routines                              */
    int i, j, k, npoints, columns, **data_array, *p_lin, *p_curv,
      loop_points, x_divisions, x_subdivs=5, y_divisions, y_subdivs=5,
      length, order, gain ;

    short ierr ;

    long int cycle_no ;

    float load_freq ;

    double *x, *temp_x, *temp_y, *x_array, *y_array, *load, *strain, ymin,
      y_start, ymax, pmin, pmax, e_min, e_max, x_ave, y_ave, e_shift,
      intercept1, slope1, intercept2, slope2, chi2, *fitted_linex,
      *fitted_liney, strain_ave, p_open, p_close, x1, plot_x_min,
      plot_x_max, plot_x_scale, plot_y_min, plot_y_max,
      plot_y_scale, xaxis_start=0, xaxis_length=8, yaxis_start=0,
      yaxis_length=5, *half_loop_strain, *half_loop_load, e_slope ;

    char xform[4] = "*I", temp[4], text[25], sample_no[8] ;

    FILE *outfile ;

/*     These are the points of interest if we assume a series of straight
      line fits.
      p_lin[0] = index of original data array corresponding to minimum load
      p_lin[1] = index a little bit up from the bottom on the loading side
      p_lin[2] = index of the top point on the lower loading branch
      p_lin[3] = index of the bottom point on the upper loading branch
      p_lin[4] = index of the top point on the upper loading branch
      p_lin[5] = index of ymax
      p_lin[6] = index of the top point on the upper unloading branch
      p_lin[7] = index of the bottom point on the upper unloading branch
      p_lin[8] = index of the top point on the lower unloading branch
      p_lin[9] = index of the bottom point on the lower unloading branch   */

/*    These are the points of interest if we assume a non-linear fit
      p_curv[0] = index of ymax
      p_curv[1] = most of the variables are not actually used.
      p_curv[2] =
      p_curv[3] =
      p_curv[4] =
      p_curv[5] =
      p_curv[6] =
      p_curv[7] =
      p_curv[8] =
      p_curv[9] =                                                          */

/*  Variables for fitting lines to the data                                */
/*  Variables for plotting routines                                        */

    look_at_data_file(data_in, &npoints, &columns, sample_no, &cycle_no,
      &load_freq, &gain) ;

/*  Set aside sufficient memory space for the data                         */
    data_array = imatrix(0, npoints - 1, 0, columns - 1 ) ;

    get_the_data( data_in, npoints, data_array ) ;

/*  Identify how many points are required to cover the entire loop         */
    loop_points = points_on_loop(data_array, npoints) ;

    temp_x = dvector(0, loop_points-1) ;   /*  x working arrays            */
    temp_y = dvector(0, loop_points-1) ;   /*  y working arrays            */
    p_lin = ivector(0, 9) ;  /* Integer array of the indices of points of */
     p_curv = ivector(0, 9) ;/* interest around the loop.                  */

    for(i=0; i<loop_points; i++)
    {
     x_ave = 0.0, y_ave = 0.0 ;
     for(k=0;k<columns;k+=2)
     {  x_ave += data_array[i][k+1], y_ave += data_array[i][k] ; }
     temp_x[i] = x_ave*2/columns, temp_y[i] = y_ave*2/columns ;
    }

/*  If you are only going to pull strain values of data_array[][] once     */
/*  you could now free up the memory set aside for that data if you only   */
/*  plotted one data set.                                                  */
    free_imatrix(data_array, 0, npoints - 1, 0, columns - 1);

/*  Identify the location and value of the global load min and max         */
    for(i=0; i<loop_points; i++)
    {
     if(i==0) ymin = temp_y[i], ymax = temp_y[i] ;
     if (temp_y[i]<=ymin) ymin = temp_y[i], p_lin[0] = i ;
     ymax = (temp_y[i] > ymax) ? temp_y[i] : ymax ;
    }
```

```
/* Set aside memory for manipulating the data.                              */
   x_array = dvector(0, loop_points-1) ;  /*  x  working arrays             */
   y_array = dvector(0, loop_points-1) ;  /*  y  working arrays             */

/* Load the working arrays, first element to correspond to minimum load   */
/* Shift the working arrays                                                 */
   for(i=0; i<loop_points; i++)
   {
    j = (i + p_lin[0]) % loop_points ;
    y_array[i] = temp_y[j], x_array[i] = temp_x[j] ;
   }

/* Free up the memory used for the temporary data arrays                    */
   free_dvector(temp_x, 0, loop_points - 1 ) ;
   free_dvector(temp_y, 0, loop_points - 1 ) ;

/* Identify key points of interest on the loop:
              p_lin[1] through p_lin[9] based load.                         */

   points_of_interest_linear( loop_points, p_lin, y_array, ymax ) ;
   p_curv[0] = p_lin[5] ;
   points_of_interest_curve( loop_points, p_curv, y_array, ymin, ymax ) ;

/* Set aside memory for final values of strain and load.  Add two extra   */
/* positions to the array for the plot parameters.                          */
   strain = dvector(0, loop_points-1+2) ; /* x values converted to strain*/
   load = dvector(0, loop_points-1+2) ; /* y values converted to Newtons  */

/* Load the data result arrays for plotting the actual data                 */
   for (i=0; i<loop_points; i++)
   {
    load[i] = y_array[i] * LOAD_MULT ;
    strain[i] = calculate_strain(x_array[i], gain) ;
   }

   free_dvector(x_array, 0, loop_points-1) ;
   free_dvector(y_array, 0, loop_points-1) ;

   for(i=0; i<loop_points; i++)
   {
    if(i==0) e_min = strain[i], e_max = strain[i] ;
    e_min = (strain[i] < e_min) ? strain[i] : e_min ;
    e_max = (strain[i] > e_max) ? strain[i] : e_max ;
   }

   for (i=0; i<loop_points; i++) strain[i] = strain[i] - e_min ;
   e_max -= e_min ;

   pmin = (double)ymin * LOAD_MULT, pmax = (double)ymax * LOAD_MULT ;

/* Write the load-strain data to an output data file for additional        */
/* processing.  The name of that file will be the same as the .dat file   */
/* but the suffix will be .out .                                            */
   printf("\n\tProcessing data file: %s\n", data_in) ;
   printf("\tThe relative loop strain is d'= %.2e.\n", e_max/(pmax-pmin) );

/* Write appropriate data to the out_file, if need be create the file.    */
   if(output !=0)
   {
   /*        First check if the data file already exists.                  */
     strcat(data_out, ".dat") ;
     if((outfile = fopen(data_out, "r")) == NULL)
   /*  Ok, the file does not exist, create it, and write in a header.     */
     {
      outfile = fopen (data_out, "w") ;
      fprintf(outfile,
      "File Name\tCycle No.\tPmax\t Pmin\tLoad Ratio\td'(*10E-3)\t\
        Fitted Const. and Results of Pass #1 (m,K',n',Po,Pa,PaR%%)\t\
        Fitted Const. and Results of Pass #2 (m,K',n',Po,Pa,PaR%%)\t\
        Linear Intersection Results\n" ) ;
      fclose (outfile) ;
     }
     else fclose (outfile) ;
   }

   e_shift = calculate_top_slope( load, strain, p_curv, pmin, &e_slope ) ;

   if (output == 0)
   write_output_file( load, strain, p_curv, pmin, data_in,
               loop_points, e_shift ) ;

   if(output !=0)
   {
      outfile = fopen (data_out, "a") ;
     fprintf(outfile, " %s  \t %ld\t\t%.0f\t%.0f\t  %5.3f\t  %4.2f\t\t",
        data_in, cycle_no, pmax, pmin, pmin/pmax, e_max*1000/(pmax-pmin) );
     fclose (outfile ) ;
   }
/* Calculation of curvilinear fits                                         */
/* Compare the fitted curve to the best fits to sections of the data       */
/* Only do the where on curve test if you are going to feed the info       */
/* to a data file.  The purpose of this is to speed up the processing      */
/* of that 8088 computer I'm using to do my data aquisition.               */

/* Trying to get a modified version of the program running to process     */
/* the ADJ files, so I'll remark out this curvelinear fit section.         */
/* if(output != 0)
   p_open = where_on_curve ( p_curv, load, strain, pmin, e_shift, e_slope,
    data_out, output) ;                                                    */
/* ===================================================================    */
/* Getting ready to plot this up.                                          */
/* -------------------------------------------------------------------    */

/* Only plot the data if you are cranking through one data set.            */
   if(output == 0)
   {
     dscale(strain, xaxis_length, loop_points, 1, 0);
     dscale(load, yaxis_length, loop_points, 1, 0);

/* Round off the plot parameters for the horizontal axis.                  */
     plot_x_min = (double)((int)(strain[loop_points] - 0.5)) / 1 ;
     order = order_of(1/(float)e_max) + 1 ;
     plot_x_max = (double)(int)(e_max * pow(10,order) + 1.0 ) /
              pow(10,order) ;
     plot_x_scale = (plot_x_max - plot_x_min) / xaxis_length ;
     strain[loop_points] = plot_x_min, strain[loop_points+1] = plot_x_scale;
    x_divisions = (int)((plot_x_max - plot_x_min)*(pow(10,order))) ;

    prepare_graphics_screen(PLOT) ;

/*  Plot the lower horizontal axis.                                       */
   order = 1 - order ;  /*  Simply to obtain the correct number of        */
   itoa(order, temp, 10);  /*  significant figures on the horiz axis.     */
   strcat(xform, temp) ;

   naxis(0.,0.,"Differential Strain",-19, xaxis_length, 0.0,
       plot_x_min, plot_x_scale, x_divisions, x_subdivs, xform) ;

/*  Plot the upper horizontal axis.                                       */
    AxisLine(xaxis_start, yaxis_length, xaxis_length, 0.0, -x_divisions,
       x_subdivs, 0) ;

/*  Round off the plot parameters for the vertical axis.                  */

    plot_y_min = (((int)load[loop_points] - 500) / 1000 ) * 1000 ;
    plot_y_max = (double)((int)(pmax/1000+1) * 1000) ;
    plot_y_scale = (plot_y_max - plot_y_min)/yaxis_length ;
    load[loop_points] = plot_y_min, load[loop_points+1] = plot_y_scale ;
    y_divisions = (int)((plot_y_max - plot_y_min) / 1000) ;

/*  Plot the left hand vertical axis.                                     */
   naxis(0., 0., "Load, (N)", 9, yaxis_length, 90, plot_y_min,
            plot_y_scale, y_divisions, y_subdivs, "-I2" ) ;

/*  Plot the right hand vertical axis.                                    */
   AxisLine(xaxis_length, yaxis_start, yaxis_length, 90., y_divisions,
       y_subdivs, 0) ;

/* Add text to the graph                                                  */
   add_text1(sample_no, cycle_no, data_in, load_freq, pmin, pmax,
     loop_points, gain ) ;

   SetMarkerHeight(0.02);  /*  Sets the size of the point markers         */
/*
PLOT THE DATA SET                                                         */
/* ---------------------------------------------------------------------- */
/*  Separate the loading and unloading branches                           */

    half_loop_strain = dvector(0, (int)(0.7*loop_points) ) ;
     half_loop_load = dvector(0, (int)(0.7*loop_points) ) ;

    split_loop(0, p_lin[5], loop_points, strain, load, half_loop_strain,
               half_loop_load, plot_x_min, plot_x_scale, plot_y_min,
             plot_y_scale) ;

    NewPen(11) ;  /*  Light Blue                                          */
    dline(half_loop_strain,half_loop_load,p_lin[5],1,0,0,0) ;
     legend_text(8.2F, 2.9F, "Loading", "2", "1");
    split_loop(p_lin[5], loop_points-p_lin[5], loop_points, strain, load,
     half_loop_strain, half_loop_load, plot_x_min, plot_x_scale,
     plot_y_min, plot_y_scale) ;

    NewPen(13) ;  /*  Purple                                              */
    dline(half_loop_strain,half_loop_load,loop_points-p_lin[5],1,0,0,0) ;
```

```
     free_dvector(half_loop_strain, 0, (int)(0.7*loop_points) ) ;
     free_dvector(half_loop_load, 0, (int)(0.7*loop_points) ) ;

     legend_text(8.2F, 1.9F, "Unload", "2", "1");
     NewPen(14) ;  /*  Yellow                                                */
      dline(strain, load, loop_points,-1,0,0,0) ;

      NewPen(15) ;  /*  White                                                */
     SetLineType(2) ;

/*  Perform the linear regression successive parts of the loop               */

/*  Plotting arrays for the fitted lines.                                    */
     fitted_linex = dvector(0,3), fitted_liney = dvector(0,3) ;

     fitted_linex[2] = plot_x_min, fitted_linex[3] = plot_x_scale ;
      fitted_liney[2] = plot_y_min, fitted_liney[3] = plot_y_scale ;

/*  p_lin[1] to p_lin[2]                                                     */
     fit(load, strain, p_lin[1], p_lin[2], &intercept1, &slope1, &chi2) ;
/*  p_lin[3] to p_lin[4]                                                     */
      fit(strain, load, p_lin[3], p_lin[4], &intercept2, &slope2, &chi2) ;
      if(fabs(slope1) < pow(10,-10))
     {
      strain_ave = average(strain, p_lin[1], p_lin[2]) ;
      fitted_liney[0] = load[0] ;
      fitted_linex[0] = strain_ave ;
      fitted_liney[1] = load[p_lin[3]] ;
      fitted_linex[1] = strain_ave ;
      p_open = (strain_ave*slope2+intercept2) ;
     }
     else
     {
      slope1 = 1 / slope1 ;
      intercept1 = (-slope1*intercept1) ; /* Simply the intercept at p=0 */
      load_fitted_line(fitted_linex, fitted_liney, slope1, intercept1,
              load[0], load[p_lin[3]], plot_x_max ) ;
      p_open = (intercept1*slope2 - intercept2*slope1)/(slope2-slope1) ;
     }
      dline(fitted_linex, fitted_liney, 2, 1, 0, 0, 0) ;

/*  p_lin[3] to p_lin[4]                                                     */

      load_fitted_line(fitted_linex, fitted_liney, slope2, intercept2,
              load[p_lin[2]], load[p_lin[5]], plot_x_max ) ;
      dline(fitted_linex, fitted_liney, 2, 1, 0, 0, 0) ;

/*  p_lin[6] to p_lin[7]                                                     */
     fit(strain, load, p_lin[6], p_lin[7], &intercept1, &slope1, &chi2) ;
     fit(load, strain, p_lin[8], p_lin[9], &intercept2, &slope2, &chi2) ;
     load_fitted_line(fitted_linex, fitted_liney, slope1, intercept1,
              load[p_lin[5]], load[p_lin[8]], plot_x_max ) ;
      dline(fitted_linex, fitted_liney, 2, 1, 0, 0, 0) ;

/*  p_lin[8] to p_lin[9]                                                     */

      if(fabs(slope2) < pow(10,-10))
      {
```

```
      strain_ave = average(strain, p_lin[8], p_lin[9]) ;
      fitted_liney[0] = load[p_lin[7]] ;
      fitted_linex[0] = strain_ave ;
      fitted_liney[1] = load[0] ;
      fitted_linex[1] = strain_ave ;
      p_close = (strain_ave*slope1+intercept1) ;
     }
     else
     {
      slope2 = 1 / slope2 ;
      intercept2 = (-slope2*intercept2) ; /* Simply the intercept at p=0  */
      load_fitted_line(fitted_linex, fitted_liney, slope2, intercept2,
              load[p_lin[7]], load[0], plot_x_max ) ;
      p_close = (intercept1*slope2 - intercept2*slope1)/(slope2-slope1) ;
     }
      dline(fitted_linex, fitted_liney, 2, 1, 0, 0, 0) ;
     free_dvector(fitted_linex, 0, 3) ;
     free_dvector(fitted_liney, 0, 3) ;

     p_open = p_op_lin2 ( p_lin, load, strain, p_open ) ;

     add_text2(p_open, p_close, e_max/1000000) ;

     ierr = EndPlot(-2) ;
     ierr = ResetPlot() ;
    }
   else
    {
      if((outfile = fopen(data_out, "a"))!= NULL )
     {  /*    Then write data to the file                                  */
        p_open = p_open_linear( strain, load, p_lin);

/* For now simply rem out this close condition of getting p_open for       */
/* the linear plots.                                                     */
/*    p_open = p_op_lin2 ( p_lin, load, strain, p_open ) ;                 */


      printf( "\n\tP_open(act) = %.0f PaR = %.1f%%\n",
               p_open, p_open/(PMAX/100) ) ;
      fprintf(outfile, "\t%.0f %.1f\n", p_open, p_open/(PMAX/100) ) ;
      /*      159.25 is Specimen #B7 test pmax/100.                        */
      /* For specimen #B8 use 160.23.                                      */

         fclose(outfile) ;
     }
     else printf("\n\tCan't open that file.\n") ;
    }

    free_ivector(p_lin, 0, 9) ;
    free_ivector(p_curv, 0, 9) ;
    free_dvector(strain, 0, loop_points-1+2) ;
    free_dvector(load, 0, loop_points-1+2) ;
}    /*  End of subroutine GILMGRAF.C                                      */
```

```
/*                                    GILMCURV.C                          */
/*                                                                        */
/* Additional subroutines for the Gilmore program.  These ones are        */
/* intended for use on the curve fitting.                                 */
#include <stdio.h>
#include <stdlib.h>
#include <string.h>
#include <dos.h>
#include <conio.h>
#include <math.h>
#include "nrutil.h"
#include "mytools.h"
#include "gilmtool.h"
#include "gilmgraf.h"
#include "geograf.h"
#include "gilmcurv.h"

#define FITPOINTS 11  /*  The number of points to include in the          */
              /*  polynomial piecewise fit.                               */
/* #define PMAX 15926 */  /*  Specific to Specimen #B7                    */
/* #define PMIN -1593 */

/* #define PMAX 16023 */  /*  Specific to Specimen #B8                    */
/* #define PMIN -1602 */

/* =====================================================================  */
/* Subroutine for calculating the points of interest around the loop.     */
/* for the curvilinear fit.
/* ---------------------------------------------------------------------  */

void points_of_interest_curve( int npoints, int *p, double *y_array,
     double ymin, double ymax )
{
   int i=0, temp_i ;

   while(y_array[i]<((ymax+ymin)/2))  /* To obtain the mid_point          */
   {  temp_i = i, i++ ; }  /*  loading branch.                            */
   p[1]=temp_i-(int)(0.01*npoints), p[2]=temp_i+(int)(0.01*npoints) ;

   while(y_array[i]>=((ymax+ymin)/2))  /*  To obtain the mid_point        */
   {  temp_i = i, i++ ; }  /*  loading branch.                            */
   p[3]=temp_i-(int)(0.01*npoints), p[4]=temp_i+(int)(0.01*npoints) ;

/* This should identify about the top 1/4 of the unloading branch         */
/* to be used in calculating that top slope.                              */
   p[5] = p[0] + (int)(0.01*npoints) ;
   p[6] = p[0] + (int)(0.12*npoints) ;
}

/* =====================================================================  */
/* Subroutine for calculating that top slope of the unloading branch.     */
/* ---------------------------------------------------------------------  */
double calculate_top_slope( double *load, double *strain, int *p_curv,
     double pmin, double *e_slope )
{
   int i, j, k ;
   double slope1, intercept1, slope2, intercept2, chi2,
     e1, e2, e3, p2, p3 ;
/* Obtain the coordinates of the key descriptor points of the curve and  */
/* calculate the hypothetical origin assuming the curve to be            */
/* symmetrical.                                                         */

   p3=load[p_curv[0]], e3=strain[p_curv[0]] ;
   fit(strain, load, p_curv[1], p_curv[2], &intercept1, &slope1, &chi2) ;
   fit(strain, load, p_curv[3], p_curv[4], &intercept2, &slope2, &chi2) ;
   p2=(p3+pmin)/2 ;
   e2=((p2-intercept1)/slope1 + (p2-intercept2)/slope2)/2 ;
   slope1=(p3-p2)/(e3-e2);
   intercept1=(p2-slope1*e2) ;
   e1 = (pmin-intercept1)/slope1 ;

   *e_slope=(load[p_curv[5]]-load[p_curv[6]]) /
       (strain[p_curv[5]]-strain[p_curv[6]]) ;
/* Return the value of the zero shift in units of the DAS-8 card.        */
   return(e1) ;
}


/* ====================================================================  */
/* Subroutine for generating the output file.                            */
/* --------------------------------------------------------------------  */
void write_output_file( double *load, double *strain, int *p_curv,
   double pmin, char *file_name, int loop_points, double e1 )
{
   int i, j, k ;

   char data_out[FILENAME_MAX] ;
/* A subsequent data file of compliance data in engineering units.       */
   FILE *outfile ;

   strcpy(data_out, file_name) ;

/* Write the data to the output file.                                    */
/* Only write the output file if you are not cranking through a batch    */
/* processing of a whole bunch of files.                                 */

   outfile = fopen(strcat(data_out,".out"), "w");
   k = p_curv[1]-(int)(0.08*loop_points) ;
   i = p_curv[0]-(int)(0.01*loop_points)-k ;

   for(j=0; j<i; j++)
   {
      fprintf(outfile, "%9.8f\t%f\t%9.8f\t%f\n",
            strain[j]-e1, load[j]-pmin, strain[j+k]-e1, load[j+k]-pmin );
   }
   for(j=i; j<loop_points; j++)
     fprintf(outfile, "%9.8f\t%f\n", strain[j]-e1, load[j]-pmin);

   fclose(outfile) ;
   printf("\n\tOutput file %s has been written to the disk.\n", file_name);
}


/* ====================================================================  */
/* Subroutine for determining if the experimental compliance curve is    */
/* close to the best fit of the Ramberg-Osgood type relationship.        */
/* ------------------------------------------------------------------------   */

double where_on_curve ( int *p, double *load, double *strain,
     double pmin, double e_shift, double e_slope, char* data_out,
     int output )
{

   int num, i, j, consecutive_points = 0, ndata, ma, mfit, *lista,
      i_count=0, count = 1 ;

   double *loads, *delta, *coefs, p_open, temp_strain1, temp_strain2,
      k, n, *y_load, *x_disp, *sig, *a, **covariance, **curvature,
      chisq, alamda = -1, chi2, error;

   void (*funcs)(double, double *, double *, double *, int);

   FILE *outfile ;

   num = FITPOINTS - 1 ;
   loads = dvector(0,num), delta = dvector(0,num), coefs = dvector(0,2);

   printf("\n\tThe slope on the top part of the unloading branch is:
      %.1f\n", e_slope) ;

/* Determine the constants for the top part of the loading branch.        */
   ndata = p[0]-p[1] ;
   y_load = dvector(0, ndata-1), x_disp = dvector(0, ndata-1) ;
   ma = 4, mfit = 4 ;
   sig = dvector(0, ndata-1), a = dvector(0, ma-1),
      lista = ivector(0, mfit-1) ;
   covariance = dmatrix (0, ma-1, 0, ma-1),
      curvature = dmatrix (0, ma-1, 0, ma-1 ) ;

   for(j=0; j<ndata; j++)
   {
    y_load[j] =  (load[j+p[1]]-pmin) ;
    x_disp[j] =  (strain[j+p[1]]-e_shift) ;
    sig[j] = 1.0 ;
   }

   a[0] = 0.0 ;
   a[1] = e_slope ;
   a[2] = 10000 ;
   a[3] = 0.3 ;
   funcs=ramberg_osgood ;

   while(count!=3)
   {
    if(count==1)  /*  Hold the first 2 constants at their present value. */
     {
      alamda = -1 ;
      lista[0] = 2 ;
      lista[1] = 3 ;
      mfit = 2 ;
     }
    if(count==2)  /*  Allow the first constant to be fitted.             */
    {
      alamda = -1 ;
```

```
/*    lista[0] = 0 ;*/  /*Letting all four constants fit.                 */
/*    lista[1] = 1 ;
      lista[2] = 2 ;
      lista[3] = 3 ;
      mfit = 4 ;    */

      lista[0] = 1 ;  /*  Leave the first constant, the error term,        */
      lista[1] = 2 ;  /*  as zero.                                         */
      lista[2] = 3 ;
         mfit = 3 ;
      }

/* Call the function to begin solving for the ‘best fit’ constants.        */
     printf("\n\tAll just part of the thinking process: " ) ;
     marquardt_min(y_load, x_disp,  sig, ndata, a, ma-1, lista, mfit-1,
        covariance, curvature, &chisq, funcs, &alamda);

     while ((chisq>0.001)&&(i_count<50))
     {
      i_count++;
      for (i=0;i<ma;i++)
        marquardt_min(y_load, x_disp,  sig, ndata, a, ma-1, lista, mfit-1,
               covariance, curvature, &chisq, funcs, &alamda);
      printf("%2d\b\b", i_count ) ;
     }
     /* Call Marquardt_min once more with alamda = 0 to repack
      the covariance and curvature matrices.                                */

     printf("\n\t There were %d iterations.\n",i_count);
     printf("\t Chi-squared was reduced to: %f\n", chisq);

     if(output == 0) j=getch();

     for (i=0;i<ma;i++) printf("\t\t\ta[%d] = %f\n",i, a[i]);
     alamda = (REAL)0.0;
     marquardt_min(y_load, x_disp,  sig, ndata, a, ma-1, lista, mfit-1,
               covariance, curvature, &chisq, funcs, &alamda);
     mfit = 3 ;
     printf("\n\t The covariance matrix is:\n");
     for (i=0;i<ma;i++)
     {
      for (j=0;j<ma;j++) printf("\t\t%8.2f",covariance[i][j]);
      printf("\n");
     }

     printf("\n\t The curvature matrix is:\n");
     for (i=0;i<ma;i++)
     {
      for (j=0;j<ma;j++) printf("\t\t%5.2e",curvature[i][j]);
      printf("\n");
     }
     k = a[2] ;
     n = a[3] ;
     e_slope = a[1] ;
     error = a[0] ;

   for(j=p[1]/10;j<=p[1];j++)
   {
     p_open = load[j] - pmin ;
       for(i=0; i<=num; i++)
     {
       loads[i] = load[j-num/2+i] - pmin ;
       delta[i] = strain[j-num/2+i] - e_shift ;
     }
    polynomial_fit( delta, loads, num+1,  coefs) ;

    temp_strain1=coefs[2]*pow((p_open),2)+coefs[1]*p_open+coefs[0] ;

    temp_strain2 = pow((p_open/k),(1/n)) ;
    temp_strain2 = error + p_open/e_slope + temp_strain2 ;

/*  Make sure that three consecutive points are close.                  */

/*    fprintf(outfile, "%9.8f\t%f\n", temp_strain1, (p_open) );         */

     if(temp_strain1<(temp_strain2*1.03))
     {
      consecutive_points++ ;
      if(consecutive_points>2)  p_open = load[j-2] - pmin,  j=j+p[1] ;
     }
     else consecutive_points = 0 ;
    }

/*printf("\n\tOutput file %s. has been written to the disk.\n",file_name);*/

    free_dvector(loads,0,num), free_dvector(delta,0,num),
      free_dvector(coefs,0,2);
    printf("\tThe relative opening load is: %5.0f\n", p_open ) ;
    printf("\tThe actual opening load is: %5.0f\n", p_open + PMIN ) ;
    printf("\tThe opening load ratio is: %3.1f %%\n", (p_open +
        PMIN)*100/PMAX ) ;
    printf("\n\tThis exited at pass number %d, the limit was %d . \n",
        j-p[1]-2, p[1] ) ;
    printf("\tThe fitted constants were slope = %.1f, K'=%.1f, n'=%.3f,
        err=%.3f\n", e_slope, k, n, error ) ;

    if(output == 0)
    {
     printf("\tHit any key to continue." ) ;
     j=getch();
    }

/*  Now write appropriate data to the output file, if appropriate.      */
    if(output != 0)
    {
      if((outfile = fopen(data_out, "a"))!= NULL )
     {  /*    Then write data to the file                                */
      fprintf(outfile, "\t%.1f %.1f %.3f %.3f ", e_slope, k, n, error ) ;
      fprintf(outfile, "\t%.0f %.0f %.1f%\t\t\t", p_open, p_open+PMIN,
             (p_open + PMIN)*100/PMAX ) ;
         fclose(outfile) ;
     }
     else printf("\n\tCan't open that file.\n") ;
    }
    count++;
    i_count = 0 ;
    }
    free_dvector(y_load, 0, ndata-1), free_dvector(x_disp, 0, ndata-1) ;
    free_dvector(sig, 0, ndata-1), free_dvector(a, 0, ma-1) ;
    free_ivector(lista, 0, mfit-1) ;
    free_dmatrix( covariance, 0, ma-1, 0, ma-1) ;
    free_dmatrix( curvature, 0, ma-1, 0, ma-1 ) ;

    return(p_open) ;
}

/*  ====================================================================   */
/*  Subroutine for calculation of p_open using the close condition of      */
/*  the curvilinear fit.  Determines when the fitted line and the data     */
/*  are "close" together.                                                  */
/*  --------------------------------------------------------------------   */

double p_op_lin2 ( int *p_lin, double *load, double *strain,
     double p_start )
{
    int num, i, j, consecutive_points = 0, ndata,
       i_count=0, count = 1 ;

   double *loads, *delta, *coefs, temp_strain1, temp_strain2,
        intercept2,  slope2, chi2 ;

/*  num = FITPOINTS - 1 ;                                                  */
    num = 11 - 1 ;
    loads = dvector(0,num), delta = dvector(0,num), coefs = dvector(0,2);

    fit(strain, load, p_lin[3], p_lin[4], &intercept2, &slope2, &chi2) ;

    for(j=p_lin[2];j<=p_lin[4];j++)
    {
/*   if(load[j]>p_start*0.8)                                               */
     {
       p_start = load[j] ;

          for(i=0; i<=num; i++)
       {
        loads[i] = load[j-num/2+i] ;
        delta[i] = strain[j-num/2+i] ;
       }
          polynomial_fit( delta, loads, num+1,  coefs) ;

          temp_strain1=coefs[2]*pow((p_start),2)+coefs[1]*p_start+coefs[0] ;

       temp_strain2 =  (p_start - intercept2) / slope2 ;

    /*  Make sure that three consecutive points are close.                 */

    /*   fprintf(outfile, "%9.8f\t%f\n", temp_strain1, (p_start) );        */

       if((temp_strain1>temp_strain2*0.99)&&
              (temp_strain1<temp_strain2*1.01))
       {
        consecutive_points++ ;
        if(consecutive_points>2)  p_start = load[j-2],  j=j+p_lin[4] ;
       }
```

```
      else consecutive_points = 0 ;
     }
    }
    free_dvector(loads,0,num), free_dvector(delta,0,num),
        free_dvector(coefs,0,2);

    return(p_start) ;
}   /*  End of GILMCURV.C subroutine file.                               */
```

```
/*               GILMTOOL.C                                                  */

/* Software tools - functions, declarations, definitions, subroutines     */
/*  for program GILMORE.C                                                    */

#include <stdio.h>
#include <stdlib.h>
#include <string.h>
#include <dos.h>
#include <math.h>
#include "nrutil.h"
#include "geograf.h"   /*  A library of graphing subroutines.                */
#include "gilmtool.h"
#include "gilmgraf.h"

#define DATA_MAX 2047   /*  Maximum value from the DAS-8 card.               */

/*  ==================================================================== */
/*  This is the main function call to the DAS-8 A/D board                  */
/*  The items passed to the card must be cast as near pointers because I   */
/*  have chosen to use the large memory model which defaults to far        */
/*  pointers.  The actual subroutines of DAS8() are written in assembler   */
/*  (MicroSoft Macro Assembler) originally for QuickBasic.  These have     */
/*  been modified for use with C and the program file renamed              */
/*  DAS8NEW.OBJ.  To use them with this program you must link the C       */
/*  object file with the DAS8NEW.OBJ file (simply include it in the .MAK */
/*  file and it works great!                                               */
/*  --------------------------------------------------------------------   */

 extern void DAS8(int near *, int near *, int near *) ;

/*  The base address of this card is 300 hex ( 768 decimal )               */
/*  The interrupt jumper on the DAS-8 board is set for IRQ 3               */
#define BASE_ADDRESS 768
#define INTERRUPT_NO 3

/*  The counters are set up on the DAS-8 board based on system             */
/*  information and prompting the user for the loading frequency.  The     */
/* board will attempt to acquire data at intervals of 250 Hz and the       */
/*  bursts are as fast as the board will go (~55usec per channel of        */
/*  conversion).                                                           */

/*  ==================================================================== */
/*  Subroutine to initialize the DAS-8 card;                              */
/*  set base address, prepare counter #2                                   */
/*  --------------------------------------------------------------------   */
void initialize_das8_card ( int counter_load_value )
{
   int error_flag ;

   /*  Description of variables
    error_flag = error return flag from the DAS-8 card               */

/*  Set the base address of the DAS-8 card                                 */
   set_base_address( BASE_ADDRESS ) ;

/*  Initialize Counter #2, square wave                                     */
/*  Counter #2 is loaded to run at The value passed in counter_load_value*/
/* Counter #2 is internally connected on the DAS-8 card to a system       */
/*  derived signal of 3996600 Hz. Example  3996600 / 16000 = 249.79       */
/*  The actual value is calculated in GILMORE.C and passed to this        */
/*  function.                                                             */
   prepare_counter(2, 3,counter_load_value);
}

/* ==================================================================== */
/*  Set the base address                                                 of
the DAS-8 card, MODE 0                                                    */
/* -------------------------------------------------------------------- */
void set_base_address(int address )
{
    int flag, mode ;

    /*  Description of variables
      address = base address of the DAS-8 board
      flag = error return flag from the DAS-8 board
       mode = describes the type of subroutine call to the DAS-8 board   */

    mode = 0 ;
    DAS8 (&flag, &address, &mode ) ;
    if (flag != 0) da_error1("Error on mode 0, setting the base address");
}

/* ==================================================================== */
/* Set the multiplexer describing which channels of the DAS-8 to scan,  */
/*  MODE 1                                                               */
/* -------------------------------------------------------------------- */
/*  This function assumes that all channels between lo and hi, including  */
/*  lo and hi are to be scanned                                           */
void set_das8_multiplexer(int lo, int hi )
{
    int flag, d[2], mode ;

    /*  Description of variables
      lo = first channel to convert
      hi = last channel to convert
      flag = error return flag from the DAS-8 board
      d[] = a small integer array for passing items to the DAS-8 board
      mode = describes the type of subroutine call to the DAS-8 board   */

    mode = 1, d[0] = lo, d[1] = hi ;
    DAS8(&flag, &d[0], &mode);
    if (flag != 0) da_error1("Error on mode 1, setting the multiplexer");
}

/* ==================================================================== */
/*  Initialize and load a counter on the DAS-8 board, MODE 10 & 11       */
/* -------------------------------------------------------------------- */
void prepare_counter(int counter_number, int configuration,

int counter_load_value )
{
    int flag, d[2], mode ;

    /*  Description of variables
      flag = error return flag from the DAS-8 board
      d[] = a small integer array for passing items to the DAS-8 board
      mode = describes the type of subroutine call to the DAS-8 board   */

/*  Initialize Counter                                                   */
    mode = 10, d[0] = counter_number, d[1] = configuration ;
    DAS8(&flag, &d[0], &mode);
    if (flag != 0) da_error1("Error on mode 10, initializing counter");

/*  Counter will be loaded with the counter load value                   */
    mode = 11, d[0] = counter_number, d[1] = counter_load_value ;
    DAS8(&flag, &d[0], &mode);
    if (flag != 0) da_error1("Error on mode 11, loading counter");
}


/*  =================================================================== */
/*  Subroutine for collecting the data from the DAS-8 card. MODE 21      */
/*  ------------------------------------------------------------------- */
void collect_data( int number_of_conversions_per_event, int
     number_of_events, float load_freq, char *file_name )
{
   int flag, d[6], mode=21, segment, npoints, *data_buffer, **data_array,
      i, j, k, number_of_conversions ;

   char data_out[FILENAME_MAX] ;

/*  Add on a few extra points to get at least a full loop.               */
   npoints =  (int)((number_of_events * 10.4) / 10) ;
   number_of_conversions = number_of_conversions_per_event * npoints ;

/*  Set aside memory for the data                                        */
   data_buffer = ivector(0, number_of_conversions - 1);
   data_array = imatrix(0, npoints - 1,
     0, number_of_conversions_per_event  - 1 ) ;

/*  Obtain the name of the output data file, append a .dat suffix        */
     printf("\n\tPlease enter the name of the output data file: ") ;
     scanf("%s", data_out) ;
     strcpy(file_name, data_out) ;
     strcat(data_out, ".dat") ;

/* Collect data from the DAS-8 board                                     */
/*  Perform conversions based on the interrupt                           */
/*  First specify which channel to begin conversion on, then start       */
/*  conversion of the analog signal.                                     */

   segment = FP_SEG(data_buffer) ;

   d[0] = 0, d[1] = -1, d[2] = number_of_conversions, d[3] = INTERRUPT_NO;
   d[4] = FP_OFF(data_buffer), d[5] = segment ;
   DAS8(&flag, &d[0], &mode);
   if (flag != 0) da_error2("Error on mode 21, data conversion", flag);

   d[0] = 1, d[1] = 0, d[2] = 1 ,d[3] = 100, d[4] = 100, d[5]= 0;
   DAS8(&flag, &d[0], &mode);
     if (flag != 0) da_error2("Error on mode 21, data conversion", flag);

   while (number_of_conversions != d[3])
```

```
    {
     d[0] = 2, d[1] = 0, d[2] = 0 ;
     DAS8(&flag, &d[0], &mode);
        if (flag != 0) da_error2("Error on mode 21, data conversion", flag);
    }

/*  Transfer values from the data_buffer to final storage in data_array  */
/*  and run some checks on the data                                      */

     for(j=0; j < number_of_conversions ; j++)
       {
        i = j / number_of_conversions_per_event ;
        k = j % number_of_conversions_per_event ;
        data_array[i][k] = data_buffer[j] ;
        if((data_array[i][k]>=DATA_MAX)¦¦(data_array[i][k]<=DATA_MAX*(-1)))
              da_error2("Data out of range for the card", 2047) ;
       }

     printf("\n\tAll data has been collected and transferred\n") ;

/*  Write the data to a file                                             */
    write_data_to_file(data_out, npoints, number_of_conversions_per_event,
                  data_array, load_freq );
    printf("Data written to the file\n");

/*  Now that all the data has been collected, free up the memory buffer   */
/*  used to store data from the DAS-8 card.                              */

    free_ivector(data_buffer, 0, number_of_conversions - 1 ) ;
    free_imatrix(data_array, 0, npoints - 1,
       0, number_of_conversions_per_event  - 1 ) ;
}

/* ==================================================================== */
/*  Error handling subroutines for the Gilmore program.                  */
/* -------------------------------------------------------------------- */
/* Gilmore data acquisition program standard error handler. Type 1 error  */
void da_error1(char error_text[])
{
    fprintf(stderr, "\nGilmore program run-time error...\n");
    fprintf(stderr,"%s\n",error_text);
    fprintf(stderr,"...now exiting to system...\n");
    exit(-1);
}

/* Gilmore data acquisition program standard error handler. Type 2 error*/
void da_error2(char error_text[], int error)
{
    fprintf(stderr, "\nGilmore program run-time error...\n");
    fprintf(stderr,"%s, error #%d\n",error_text, error);
    fprintf(stderr,"Not exiting to system. Program operation will
       continue.\n");
}
```

```
/* ==================================================================== */
/* The subroutine for reading pertinent information from the data file.  */
/* -------------------------------------------------------------------- */
void look_at_data_file(char *file_name, int *npoints,
    int *number_of_conversions, char *sample_no, long int *cycle_no,
    float *load_freq, int *gain)
{
    int number_of_data_lines = 0, i=0, j=0, k ;
    char *buffer, data_in[FILENAME_MAX] ;
    FILE *infile ;

/* Description of variables
     buffer = a small memory for reading data in from the data file
      number_of_data_lines = the number of lines in the data file
      infile = a pointer to the input file
      data_in = a pointer to the variable containing the name of the
               input file
     npoints = a pointer to main program variable "npoints"
     sample_no = a pointer to main program variable "sample_no"
     load_freq = a pointer to main program variable "load_freq"
     gain = a pointer to main program variable "gain"                  */

/* Open the data file for reading                                        */
    strcpy(data_in, file_name) ;
    strcat(data_in, ".dat") ;
    if((infile = fopen(data_in, "r")) != NULL)
      {

/* Set aside a small memory buffer for reading data from the data file.  */
        buffer = (char *)malloc(BUFSIZ);

/* Count the number of lines in the data file                            */
      *number_of_conversions = 0 ;
      while (fgets(buffer, BUFSIZ, infile) != NULL)
      {
        if(number_of_data_lines==1)
        {  while(buffer[j++] != '\0')
              {  k=0 ;
               while(buffer[j++] == ' ')
               {  if(k++==0) (*number_of_conversions)++ ;   }  }  }
              number_of_data_lines ++ ;
         }
      fclose(infile);

/* Less one because of the header line.                                  */
      *npoints = number_of_data_lines - 1 ;

/* Read that first line of information.                                  */
      infile = fopen(data_in, "r") ;
      fgets(buffer, BUFSIZ, infile) ;
      sscanf(buffer, "%*[^ ]%s%*[^0-9]%ld%*[^0-9]%f%*[^0-9]%d",
               sample_no, cycle_no, load_freq, gain ) ;
      fclose(infile) ;
      free( buffer ) ;
     }
     else da_error1("Unable to open that data file");
}
```

```
/* =============================================================   */
/* The subroutine for reading the actual data from the data file.    */
/* ------------------------------------------------------------- */
void get_the_data( char *file_name, int npoints, int **data_array )
{
    int i ;
    char *buffer, data_in[FILENAME_MAX] ;
    FILE *infile ;

/*  Set aside a small memory buffer for reading data from the data file.  */
        buffer = (char *)malloc(BUFSIZ);

/*  Open the data file for reading                                     */
    strcpy(data_in, file_name) ;
    strcat(data_in, ".dat") ;
    infile = fopen(data_in, "r") ;

/*  Read that first line of information.                               */
       fgets(buffer, BUFSIZ, infile) ;
       for(i=0;i<npoints;i++)
       {
/*  For now simply read in 6 integer values                            */
             fgets(buffer, BUFSIZ, infile) ;
             sscanf(buffer, "%d%*[^-0-9]%d%*[^-0-9]%d%*[^-0-9]%d%*[^-0-9]\
               %d%*[^-0-9]%d", &data_array[i][0], &data_array[i][1],
               &data_array[i][2], &data_array[i][3], &data_array[i][4],
               &data_array[i][5] ) ;
       }
       fclose(infile) ;
       free( buffer ) ;
}

/* ============================================================== */
/* The subroutine for writing data to a data file                     */
/* -------------------------------------------------------------- */
void write_data_to_file(char *data_out, int rows, int columns,

int **data_array, float load_freq )
{
    int j, k, gain ;
    long int cycle_no ;
    char sample_no[8] ;

    FILE *outfile ;

/*  Description of variables
      cycle_no  = the number of cycles on the specimen
      sample_no = the sample number
      outfile = a pointer to the input file
      load_freq = the Gilmore loading frequency
      gain = gain of the strain gauges
      data_out = the variable containing the name of the output file      */

/*  Prompt for the sample number and cycle number                       */
    printf("\n\tPlease enter the sample number: ") ;
    scanf("%s", sample_no ) ;

    printf("\n\tPlease enter the cycle number: ") ;
```

```
   scanf("%ld", &cycle_no ) ;

   printf("\n\tPlease enter the gain of the strain gauges: ") ;
   scanf("%d", &gain ) ;

   outfile = fopen(data_out, "w");
   fprintf(outfile, "Sample: %s\tCycle: %ld\tFreq: %f\tGain: %d\n",
               sample_no, cycle_no, load_freq, gain )                      ;
   for(j=0; j<rows; j++)
   {
     for(k=0; k<columns; k++)
     {
        fprintf(outfile, "%d   ", data_array[j][k]);
     }
     fprintf(outfile, "\n");
   }
   fclose(outfile) ;
}

/* ===================================================================== */
/* Subroutine to set up the graphics screen.  You must ensure that the
   correct drivers are accessible.                                         */
/* --------------------------------------------------------------------- */
void initialize_screen( int output )
{
   short idev, ierr ;
   if(output==0) idev = LoadDriver("SCREEN.DRV") ;
   if(output!=0) idev = LoadDriver("PRINTER.DRV") ;
   if(idev < 0) printf("\nUnable to load the screen driver.
        Error %d",idev);
   if(output==0) ierr = InitPlot("CON", 1) ;
   if(output!=0) ierr = InitPlot("LPT1", 0) ;
   switch (ierr)
   {
     case -1 : printf("Graphics driver not loaded or device already"
                " in graphics mode\n" ) ;
               break ;
     case -2 : printf("Write error\n") ;
               break ;
     case -3 : printf("Inconsistent device or device not found\n") ;
               break ;
     case -4 : printf("Out of memory (printer)\n") ;
               break ;
     case -6 : printf("Inconsistent parameters\n") ;
     default :
               break ;
   }
}

/* =====================================================================   */
/* From a given integer value from the DAS-8 return the corresponding     */
/* value for the strain.                                                   */
/* ---------------------------------------------------------------------   */
double calculate_strain(double x, int gain)
{
/* Strain gauge constants                                                  */
   double Kg = 2.09F, u = 0.292F, Vex = 5.0F, volts, strain ;
   if(x == 0) { strain = 0.0F ; }
   else        /*  The strain gauge formula                              */
   {
     volts = x * 0.0024425989 ;  /*  5/2047                              */
     strain = 2/(Kg*Vex*gain/volts-Kg*Vex*gain*(1-u)/2/volts-Kg*(1-u));
   }
/* Multiply return value by 1,000,000 to render values in micro strain.  */
   return(strain*1000000) ;
}

/* ====================================================================  */
/* Subroutine for calculating the points of interest around the loop.    */
/* for the linear fit.                                                   */
/* --------------------------------------------------------------------  */
void points_of_interest_linear( int npoints, int *p, double *y_array,
     double ymax )
{
   int i ;

   p[1] = (int)(0.03 * (float)npoints) ;

   i=p[1] ;
   while(y_array[i]<=0)   /*  To obtain the top point of the lower       */
   {  p[2] = i, i++ ; }   /*  loading branch.                            */

   while(y_array[i]<350)  /* To obtain the lower point of the upper      */
   {  p[3] = i, i++ ; } /*  loading branch.                              */

  while(y_array[i]<ymax)   /*  To obtain the index of ymax.              */
   {  i++, p[5] = i ; }

/* The top end of the upper loading branch                               */
   p[4] = p[5] - (int)(0.25 * (float)npoints) ;
   p[4] = p[5] - (int)(0.05 * (float)npoints) ;

/* The top end of the upper unloading                                    */
   p[6] = p[5] + (int)(0.05 * (float)npoints) ;

   i = p[6] ;
   while(y_array[i]>=250)  /*  The bottom end of the upper unloading     */
   {  p[7] = i, i++ ; }

   while(y_array[i]>0)  /*  The top end of the lower unloading branch    */
   {  p[8] = i, i++ ; }

/* The bottom end of the lower unloading                                 */
   p[9] = (int)(0.97 * (float)npoints) ;
}


/* ====================================================================  */
/* A small subroutine for writing text to the graph                      */
/* --------------------------------------------------------------------  */
void add_text1(char *sample_no, long int cycle_no, char *file_name,
   float load_freq, double pmin, double pmax, int npoints, int gain )
{
   int length ;
   char text[30] ;
```

```
    strcpy(text, "Crack Closure Investigation: ") ;
    length = strlen(text) ;
    symbol(1.5, 7.0, 0.25, text, 0.0, length) ;

    strcpy(text, "Sample No: ") ;
    strcat(text, sample_no ) ;
    length = strlen(text) ;
    symbol(0.0, 6.3, 0.15, text, 0.0, length) ;

    strcpy(text, "Cycle No: ") ;
    length = strlen(text) ;
    symbol(0.0, 5.8, 0.15, text, 0.0, length) ;
    nnumber(1.1, 5.8, 0.15, cycle_no, 0.0, "+I3") ;

    strcpy(text, "File Name: ") ;
    strcat(text, file_name) ;
    length = strlen(text) ;
    symbol(2.4, 6.3, 0.15, text, 0.0, length) ;

    strcpy(text, "Number of Points: ") ;
    length = strlen(text) ;
    symbol(5.2, 6.3, 0.15, text, 0.0, length) ;
    nnumber(7.1, 6.3, 0.15, npoints, 0.0, "+I5") ;

    strcpy(text, "Load Freq: ");
    length = strlen(text) ;
    symbol(2.3, 5.8, 0.15, text, 0.0, length) ;
    nnumber(3.5, 5.8, 0.15, load_freq, 0.0, "+F2.1") ;

    strcpy(text, "Gauge Gain: ") ;
    length = strlen(text) ;
    symbol(4.5, 5.8, 0.15, text, 0.0, length) ;
    nnumber(5.9, 5.8, 0.15, gain, 0.0, "+I1") ;

    strcpy(text, "R: ");
    length = strlen(text) ;
    symbol(6.7, 5.8, 0.15, text, 0.0, length) ;
    nnumber(7.0, 5.8, 0.15, pmin/pmax, 0.0, "+F5.3") ;

    strcpy(text, "Pmin: ") ;
    length = strlen(text) ;
    symbol(0.0, 5.3, 0.15, text, 0.0, length) ;
    nnumber(0.7, 5.3, 0.15, pmin, 0.0, "+I1") ;

    strcpy(text, "Pmax: ") ;
    length = strlen(text) ;
    symbol(1.85, 5.3, 0.15, text, 0.0, length) ;
    nnumber(2.65, 5.3, 0.15, pmax, 0.0, "+I1") ;

}

/* ==================================================================   */
/*  Write the p_open, p_closed and e_max values to the graph.           */
/*  As determined by the intersection of the two straight lines.        */
/* ------------------------------------------------------------------   */
void add_text2(double p_open, double p_close, double e_max )
{
    int length, ierr ;
    char text[25] ;

    SetLineType(1) ;
    strcpy(text, "P open: ") ;
    length = strlen(text) ;
    symbol(3.6, 5.3, 0.15, text, 0.0, length) ;
    nnumber(4.5, 5.3, 0.15, p_open, 0.0, "+I1") ;

    strcpy(text, "P close: ") ;
    length = strlen(text) ;
    symbol(5.4, 5.3, 0.15, text, 0.0, length) ;
    nnumber(6.3, 5.3, 0.15, p_close, 0.0, "+I1") ;

    ierr = LoadFont("SG.FNT");
    if(ierr<0)  printf("Error loading font %d", ierr) ;

    strcpy(text, "e") ;
    length = strlen(text);
    symbol(7.1, 5.3, 0.25, text, 0.0, length ) ;

    strcpy(text, "l") ;
    length = strlen(text);
    symbol(8.35, 5.3, 0.15, text, 0.0, length ) ;


    ierr = LoadFont("SR.FNT");

    strcpy(text, "max: ") ;
    length = strlen(text) ;
    symbol(7.3, 5.3, 0.15, text, 0.0, length) ;
    nnumber(7.9, 5.3, 0.15, e_max*1000000, 0.0, "+I3") ;

}

/* ==================================================================   */
/* A subroutine to separate the loading and unloading branches for plot */
/* ------------------------------------------------------------------   */
void split_loop(int start, int stop, int total, double *strain,
        double *load, double *half_loop_strain, double *half_loop_load,
        double plot_x_min, double plot_x_scale, double plot_y_min,
        double plot_y_scale)
{
    int i, j ;

    for(i=0; i<stop; i++)
    {
     j = (i + start) % total ;
      half_loop_strain[i] = strain[j] ;
     half_loop_load[i] = load[j] ;
    }
    half_loop_strain[i]=plot_x_min, half_loop_strain[i+1]=plot_x_scale ;
    half_loop_load[i]=plot_y_min, half_loop_load[i+1]=plot_y_scale ;
}
```

```
/* ==================================================================== */
/* Initialize the Graphics Screen and prepare it for generation of      */
/* the graph.                                                           */
/* -------------------------------------------------------------------- */
void prepare_graphics_screen(int output)
{
   short ierr ;
   initialize_screen( output );

   if((ierr = StartPlot(0)) < 0 )   {
    printf("Error %d: Geograf  StartPlot\n", ierr ) ;
    exit(15) ;  }

   SetViewport(0, 0.0, 0.0, 1.0, 1.0) ;
   if(output==0) SetWindow(0, 0.0, 0.0, 10.0, 8.0); /* For Screen display*/
   if(output!=0) SetWindow(0, 0.0, 0.0, 12.5, 10.0);/*For Printer output  */

   SetAxisParam(1,0.20);  /* Sets the title heights to 0.20 window units  */
   SetAxisParam(2,0.14);  /* Sets the scale heights to 0.14 window units  */
   SetAxisParam(3,0.10);  /* Sets the height of division tick marks       */
   SetAxisParam(4,0.05);  /* Sets the height of subdivision ticks         */

   ierr = LoadFont("SR.FNT");
   if(ierr<0) printf("Error loading font %d", ierr) ;
   NewPen(15) ;  /*  White                                                */
   if(output==0) plot(1.0,0.75,-3) ;  /*  Sets up the position to start
                              plotting  */
   if(output!=0) plot(2.0,1.5,-3) ;  /*  Sets up the position to start
                             plotting                                     */
}


/* ==================================================================== */
/* Subroutine for adding legend text to the graph                       */
/* -------------------------------------------------------------------- */
void legend_text(float x, float y, char *title, char *first, char *second)
{
   int length ;
   float increment ;
   short ierr ;
   char text[10] ;

   strcpy(text, title) ;
   length = strlen(text) ;
   symbol(x, y, 0.15, text, 0.0, length ) ;
   x-=0.0, y-=0.35 ;

   ierr = LoadFont("SG.FNT");
   if(ierr<0) printf("Error loading font %d", ierr) ;

   strcpy(text, "e") ;
   length = strlen(text);
   symbol(x, y, 0.25, text, 0.0, length ) ;

   strcpy(text, first) ;
   length = strlen(text);
   x+=0.2, y-=0.05 ;
   symbol(x, y, 0.10, text, 0.0, length ) ;
```

```
    strcpy(text, "-") ;
    length = strlen(text);
    x+=0.10, y+=0.07 ;
    symbol(x, y, 0.15, text, 0.0, length ) ;

    strcpy(text, "e") ;
    length = strlen(text);
    x+=0.2, y-=0.02 ;
    symbol(x, y, 0.25, text, 0.0, length ) ;

    strcpy(text, second) ;
    length = strlen(text);
    x+=0.2, y-=0.05 ;
    symbol(x, y, 0.10, text, 0.0, length ) ;

    ierr = LoadFont("SR.FNT");
}

/* ======================================================================   */
/* Load up the points for plotting the straight lines                       */
/* ----------------------------------------------------------------------   */
void load_fitted_line(double *fitted_linex, double *fitted_liney,
     double slope, double intercept, double load1, double load2,
     double x_max)
{
   fitted_linex[0] = (load1-intercept)/slope ;
    if(fitted_linex[0] < 0.0)
         fitted_linex[0] = 0.0, fitted_liney[0] = intercept ;
   else if(fitted_linex[0] > x_max)
         fitted_linex[0] = x_max, fitted_liney[0] = slope*x_max+intercept;
   else fitted_liney[0] = load1 ;

   fitted_linex[1] = (load2 - intercept)/slope ;
    if(fitted_linex[1] < 0.0)
         fitted_linex[1] = 0.0, fitted_liney[1] = intercept ;
   else if(fitted_linex[1] > x_max)
         fitted_linex[1] = x_max, fitted_liney[1] = slope*x_max+intercept;
   else fitted_liney[1] = load2 ;
}

/* ======================================================================   */
/* Identify how many points are required to cover the entire loop           */
/* ----------------------------------------------------------------------   */
int points_on_loop(int **data_array, int npoints)
{
    int y_start, i=2, j=0, loop_points=0 ;

    y_start = data_array[0][0] ;

   if((data_array[i][0] <= y_start)&&(j==0))
    {  while(data_array[i++][0] < y_start) loop_points = i ;
     i+=2;
     while((data_array[i][0] >= y_start)&&(i++<npoints)) loop_points = i ;
     j=1; }

    if((data_array[i][0] > y_start)&&(j==0))
    {  while(data_array[i++][0] > y_start) loop_points = i ;
     i+=2;
     while((data_array[i][0] <= y_start)&&(i++<npoints)) loop_points = i ;
     j=1; }

    return(loop_points) ;
}

/* ======================================================================   */
/* Averaging function                                                       */
/* ----------------------------------------------------------------------   */
double average(double *x, int start, int stop)
{
    int i ;
    double total=0, ave ;

    for(i=start; i<stop; i++) total += x[i] ;
    ave = total/(stop-start) ;
    return (ave) ;
}

/* ======================================================================   */
int order_of( float number )
/* ----------------------------------------------------------------------   */
{
    int i = 0 ;
    if(fabs(number)>=1.0)
    {
     while(number != 0)
         number = number / 10, number = (int)number, i++ ;
    }
    else
    {
     while(number != 0)
    {
      number = number * 10;
      if(fabs(number)>1) number = 0 ;
      i-- ;
    }
   }
   return(i) ;
}

/* ======================================================================   */
/* Perform the linear regression                                            */
/* ----------------------------------------------------------------------   */
void fit(double *x, double *y, int start, int stop, double *intercept,
     double *slope, double *chi2)
{
    int i ;

    double sx=0, sy=0, ss, sxoss, t, st2=0 ;

    for(i=start; i<stop; i++)
    sx += x[i], sy += y[i] ;

    ss = stop - start ;
    sxoss = sx/ss ;

    *slope = 0 ;
   for(i=start; i<stop; i++)
   {
      t = x[i] - sxoss ;
     st2 += t*t ;
     *slope += t*y[i] ;
   }
   *slope /= st2 ;
   *intercept = (sy - sx*(*slope))/ss ;

   *chi2 = 0 ;
   for(i=start; i<stop; i++)
   {
      *chi2 += (y[i]-(*intercept)-(*slope)*x[i])*
              (y[i]-(*intercept)-(*slope)*x[i]) ;
   }
}

/* ====================================================================   */
/* Second order polynomial fit to num points.                             */
/* Choosing the coefficients as best fit in the least squares sense.      */
/* --------------------------------------------------------------------   */
void polynomial_fit(double *aa, double *nn, int num, double *bb)
{
   int j;
   double x, yy, sx=0,sx2=0,sx3=0,sx4=0,sy=0,syx=0,syx2=0, determ,
      t2, t3, t4, yb ;

      for (j=0;j<num;j++)
      {
       x = nn[j], yy = aa[j];
       sx += x, sx2 += pow(x,2), sx3 += pow(x,3);
       sx4 += pow(x,4), sy += yy, syx += x*yy;
       syx2 += yy * pow(x,2);
      }
      determ = num*(sx2*sx4-pow(sx3,2))+
              sx*(sx2*sx3-sx*sx4)+sx2*(sx*sx3-pow(sx2,2));
      t2 = sy*(sx2*sx4-pow(sx3,2))+
              syx*(sx2*sx3-sx*sx4)+syx2*(sx*sx3-pow(sx2,2));
      bb[0] = t2/determ;
      t3 = num*(syx*sx4-syx2*sx3)-
              sx*(sy*sx4-syx2*sx2)+sx2*(sy*sx3-syx*sx2);
      bb[1] = t3/determ;
      t4 = num*(sx2*syx2-sx3*syx)-sx*(sx*syx2-sx3*sy)+sx2*(sx*syx-sx2*sy);
      bb[2] = t4/determ;
}

/* ====================================================================   */
/* Subroutine for calculation of p_open using the intersection of two     */
/* straight lines.                                                        */
/* --------------------------------------------------------------------   */
double p_open_linear( double *strain, double *load, int *p_lin)
{
   double intercept1, intercept2, slope1, slope2,
        chi2, strain_ave, p_open ;

   fit(load, strain, p_lin[1], p_lin[2], &intercept1, &slope1, &chi2) ;
   fit(strain, load, p_lin[3], p_lin[4], &intercept2, &slope2, &chi2) ;
   if(fabs(slope1) < pow(10,-10))
```

```
    {
       strain_ave = average(strain, p_lin[1], p_lin[2]) ;
    p_open = (strain_ave*slope2+intercept2) ;
    }
    else
    {
      slope1 = 1 / slope1 ;
      intercept1 = (-slope1*intercept1) ;  /*  Simply the intercept at p=0 */
    p_open = (intercept1*slope2 - intercept2*slope1)/(slope2-slope1) ;
    }
    return(p_open) ;
}
```

Appendix C

Opening load data for specimens B7 and B8.

Specimen #: B7 Using data from active strain gauge on top of the c−face crack.
R=−0.10 P_{max}: 15926 N N_{EoT}=305,155 cycles

Left side crack. $e_1 - e_2$

File #	Cycle #	Differential Compliance (μ/N*10^{-3})	P_{open}/P_{max}[1] (%)	P_{open}/P_{max}[2] (%)	
1b	1	13.27	31	7.3	R[3]
3	4	9.55	6.8	10.4	
5	12	9.53	6.9	2.0	
7	20	9.19	7.0	1.4	
9	30	9.29	7.0	1.3	
11	40	9.31	8.4	2.6	
13	60	9.34	10.8	4.4	
15	74	9.34	8.4	3.3	
17	90	9.45	9.8	2.9	
19	120	9.61	11.8	6.4	
21	145	9.61	11.6	2.7	
23	195	9.60	16.5	4.8	
25	245	9.68	13.0	3.6	
27	325	9.83	13.6	5.3	
29	495	9.93	14.1	4.0	
31	750	10.06	12.6	0.3	
33	995	10.17	15.1	3.5	
35	1494	10.51	12.5	−1.3	
37	2245	10.80	14.6	1.7	
40	3250	11.14	12.8	1.4	
42	4660	18.00	9.4	0.4	
44	4674	17.92	9.8	−1.3	
45	4780	17.81	11.1	0.9	
46	4994	18.08	11.4	−1.7	
48	5490	18.21	12.3	−2.1	
50	5994	18.49	11.4	−2.3	
52	6494	18.77	11.7	−1.5	
54	6990	18.98	12.7	1.9	
56	7494	19.23	11.3	0.2	
58	7990	19.43	12.5	1.8	
60	8994	23.03	21.0	25.2	R
83	30004	27.99	8.8	7.4	
84	30010	28.02	8.6	7.2	
85	30025	28.11	8.7	7.1	
86	30100	27.98	8.3	5.6	
87	30260	27.44	11.1	10.8	
88	31000	28.30	8.7	6.8	
90	33000	28.88	8.5	6.0	
104	60053	39.67	10.3	18.3	
106	60070	39.81	10.3	17.2	
107	60100	39.94	10.3	17.5	
108	60200	40.05	10.1	16.9	
109	60500	40.01	9.0	17.7	R
110	60550	40.44	10.0	16.3	
112	61010	40.95	9.9	16.2	
113	61020	40.96	9.9	15.8	
128	110052	57.68	9.2	18.4	
129	110060	57.80	9.2	18.9	
131	110100	58.12	8.8	18.1	

Right side crack. $e_3 - e_4$

File #	Cycle #	Differential Compliance (μ/N*10^{-3})	P_{open}/P_{max}[1] (%)	P_{open}/P_{max}[2] (%)	
2b	2	3.22	13	4.8	R
4	6	3.03	4.2	12.5	
6	18	2.67	3.4	−1.8	
8	28	2.61	7.5	1.0	
10	35	2.67	7.0	−0.5	
12	52	2.58	9.3	1.8	
14	69	2.70	8.1	1.7	
16	80	2.67	9.7	3.4	
18	100	2.55	8.6	6.5	
20	125	2.73	8.8	0.6	
22	150	2.98	12.7	8.8	
24	200	3.14	10.3	5.2	
26	250	3.19	13.8	7.4	
28	330	3.13	11.4	8.4	
30	500	3.16	10.2	6.9	
32	756	3.26	12.1	5.3	
34	1000	3.26	12.1	7.5	
36	1500	3.54	12.2	9.4	
38	2250	3.52	16.0	8.5	
39	3244	3.46	11.4	4.9	
41	4658	3.53	11.4	3.2	
43	4662	5.45	8.7	−5.0	
47	5000	5.39	10.0	−1.8	
49	5500	5.41	11.1	−2.5	
51	6000	5.50	9.4	−1.0	
53	6500	5.56	11.4	1.7	
55	7000	5.52	11.5	0.6	
57	7500	5.64	9.6	−0.5	
59	8000	5.67	12.3	−0.2	
61	9000	5.85	10.4	−1.0	
64	10000	5.88	12.2	3.2	
65	11000	5.94	12.9	4.0	
66	12000	6.05	12.2	7.8	
68	14000	6.07	12.0	10.7	
70	16000	6.23	11.3	8.7	
72	18000	6.37	14.3	11.3	
74	20000	6.50	10.9	7.0	
76	20030	6.79	11.2	11.5	
78	22500	6.99	12.0	14.3	
79	25000	7.14	13.0	13.0	
81	27500	7.19	12.4	13.6	
82	30000	7.39	13.1	15.9	
89	31060	7.15	12.7	16.8	
91	33060	7.27	12.5	21.8	
92	35000	7.44	12.3	20.6	
94	40000	7.88	11.5	19.8	
96	45000	8.11	12.0	19.1	
98	50000	8.55	13.4	20.3	
100	55000	8.86	12.8	21.4	

132	110500	58.43	8.2	17.6
134	111002	59.56	8.3	17.2
166	205142	145.00	17.4	29.9
167	205145	145.12	17.2	29.9
168	205155	145.60	17.3	29.8
174	205180	153.85	15.9	27.5

This combines data files: B7-RIGHT.DAT & B7-LEFT.DAT
This is stored in directory /B7 in filename B7-POPEN.WK3

B7-LEFT.DAT is generated from .BAT file B7LFILES.
B7-RIGHT.DAT is generated from .BAT file B7RFILES

102	60000	9.17	12.2	20.7
115	61435	9.42	11.7	17.4
116	65000	9.96	11.0	15.1
118	70000	10.43	10.6	16.8
120	80000	11.08	12.9	23.1
122	90000	11.84	15.5	27.7
124	100000	12.44	15.2	28.2
126	110000	14.01	18.9	31.3
130	110065	13.71	20.4	33.8
135	111627	12.65	16.6	27.8
136	111650	12.72	16.3	26.8
137	111678	12.73	16.2	26.3
138	112000	12.81	15.7	25.2
139	115000	16.35	14.0	9.6
142	120100	16.82	11.4	13.0
160	205116	18.11	20.6	37.2
162	205130	18.16	20.6	37.0
170	205164	18.22	20.6	37.0
172	205170	18.22	20.3	36.7
177	205210	18.24	20.5	36.7
179	205300	18.26	20.3	36.7
181	205350	18.29	20.6	36.9
183	205400	17.79	23.4	37.4
185	205500	18.08	22.2	37.4
187	205700	18.13	22.2	37.2
189	206000	18.18	22.4	37.2
192	206500	18.21	22	37.1
195	207000	18.27	22	36.9
197	208000	18.39	23	36.9
199	209000	18.51	23	36.5
201	210000	18.63	23	36.2
203	212500	18.97	22	36.3

---

[1] Intersection of linear best fit lines to upper and lower parts of the loading branch of the compliance curve.

[2] Ramberg-Osgood type curve fitted to the upper part of the loading branch of the compliance curve, and subsequently compared to the data based on your 'close' criterion.

[3] An **R** on the right side of the data indicates that data point can be rejected.

Specimen #: B7 Using data from active strain gauge adjacent to the a-face crack.
R = −0.10 P_{max}: 15926 N N_{EoT} = 305,155 cycles

Left side crack. $e_6 - e_8$					Right side crack $e_7 - e_8$				
File #	Cycle #	Differential Compliance (μ/N*10^{-3})	P_{open}/P_{max}[1] (%)	P_{open}/P_{max}[2] (%)	File #	Cycle #	Differential Compliance (μ/N*10^{-3})	P_{open}/P_{max}[1] (%)	P_{open}/P_{max}[2] (%)
63	9057	0.13	166	42.8	143	129526	0.98	8.1	12.8
67	12073	0.15			144	129535	0.98	12.7	11.9
69	15960	0.18	104	40.9	147	130100	1.00	4.3	18
71	17960	0.21	−14	5.2	148	145000	0.73	14.4	12.5
73	19960	0.26	9.3	31.4	150	160000	0.59	61	22.3
75	20006	0.39	3.9	−0.2	152	175003	0.45	240	25.1
77	22450	0.29	5.8	0.5	154	190000	0.37	60.5	13.9
80	27450	0.25	0.4	−0.2	156	204998	0.31	35.6	39.7
93	35020	0.38	8.1	8.6	161	205119	0.35	−9.8	13.5
95	40051	0.56	21	20.5	171	205167	0.37	−15	17.2
97	45050	0.64	17.1	16.2	178	205214	0.40	4.8	21.7
99	50050	0.59	15.8	10.8	180	205302	0.38	−10	5.7
101	55050	0.84	9.1	1.2	184	205402	0.32	42.9	57.1
103	60050	0.31	6.7	29.5	186	205502	0.30	13.5	41.9
114	61420	0.61	−8.1	22.0	188	205702	0.30	49.4	38
117	65050	0.52	0.4	1.3	191	206004	0.30	41	29.2
119	70050	0.54	−14	21.9	193	206502	0.32	51.2	40.9
121	80060	0.56	−346	25.6	194	206992	0.30	−1.6	32
123	90000	0.74	63.6	24.6	196	207990	0.31	36.3	39.2
125	100050	0.50	35	20.2	198	208990	0.29	22.2	40.8
127	110050	0.29	29	30.4	200	209990	0.29	30.8	37.7
140	115050	0.72	24.1	23.3	202	212490	0.30	9.8	38.9
141	120000	0.90	24.8	24.6	204	214950	0.30	45.3	39.3
145	129544	1.37	23.1	26.9	207	230000	0.48	21.5	29.2
146	130000	1.44	21.9	25.5	209	245000	0.81	24.9	26.5
149	145100	1.99	18.8	25.4	211	260000	1.37	23.2	25.4
151	160100	2.95	16	25.5	213	275000	2.13	19.2	24.6
153	175100	3.87	15.6	25.5	214	289900	3.50	16.3	19.5
155	190100	4.86	20.5	28.3	216	304900	6.25		
157	205100	5.16	28	47.2	218	305105	6.16		
163	205133	5.67	26.1	30.1					
169	205158	5.69	26.4	30.2					
175	205185	5.69	27.4	29.7					
206	229897	8.96	21.3	25.3					
208	244900	10.89	17.5	25.2					
210	259900	13.04	15.3	23.3					
212	274900	15.13	10.2	17.4					
215	289950	16.24	15.7	19.6					

This combines data from files: B7-LEFT3.DAT & B7-RITE3.DAT

This is generated with .BAT file B7LFILE3 & B7RFILE3.

This is stored in directory /B7 in filename B7-POP-A.WK3

[1] Intersection of linear best fit lines to upper and lower parts of the loading branch of the compliance curve. The top point of the unloading branch is 0.25*npoints.

[2] Linear best fit to the upper portion of the loading branch and comparing the data curve to the fitted line. Using an accept band of 0.96 – 1.08 .

Specimen #: B8 Using data from active strain gauge on top of the c−face crack.
R=−0.10 P_{max}: 16023 N N_{EoT}=141,540 cycles

Left side crack. e_3-e_4

File #	Cycle #	Differential Compliance (μ/N*10^{-3})	P_{open}/P_{max}[1] (%)	P_{open}/P_{max}[2] (%)
2	6	13.82	13.3	14.9
6	18	13.88	12.9	15.9
8	28	14.13	12.6	12.9
11	42	14.44	11.1	8.5
17	88	14.62	14.0	10.5
23	210	15.04	18.4	11.9
24	230	15.09	19.6	11.5
25	250	15.13	19.4	11.1
28	310	15.14	19.4	14.1
29	350	15.24	20.8	12.7
32	420	15.28	20.3	12.8
33	490	15.39	22.0	12.9
36	620	15.67	21.1	11.8
37	700	15.80	22.1	9.6
40	835	15.88	23.4	11.9
41	900	15.94	22.2	12.0
44	1115	16.18	21.5	12.1
45	1250	16.26	21.1	10.7
48	1600	16.43	23.9	12.4
49	1800	16.59	23.1	13.1
52	1825	16.61	23.2	12.7
53	1990	16.71	23.1	12.0
54	2500	17.60	21.8	10.5
55	2600	17.18	22.7	12.9
56	2900	17.33	22.2	11.5
57	2990	17.37	21.5	13.5
58	3500	17.60	22.8	15.6
59	3600	17.58	22.7	14.0
60	3990	17.81	21.6	13.9
61	4500	18.01	22.9	14.5
62	4600	18.00	21.4	14.2
63	4997	18.19	21.8	14.4
64	5520	18.45	21.8	11.7
65	5990	18.65	21.1	13.0
66	7010	18.97	21.0	15.0
67	7990	19.34	21.0	15.8
68	9150	19.75	20.3	16.9
69	10000	20.15	19.5	14.9
71	10020	19.69	16.5	5.5
72	10205	19.79	18.6	2.7
73	10500	19.83	17.9	3.2
74	11505	20.07	18.4	4.9
75	12490	20.44	18.0	4.6
76	14995	21.15	17.8	7.1
77	17498	21.84	16.6	7.9
78	17500	23.93	16.8	6.7
79	17550	22.05	17.3	10.2
80	17575	24.12	16.4	5.3
81	19600	24.75	15.8	6.8

Right side crack e_1-e_2

File #	Cycle #	Differential Compliance (μ/N*10^{-3})	P_{open}/P_{max}[1] (%)	P_{open}/P_{max}[2] (%)
1	2	55.82	9.9	9.7
3	8	54.48	7.5	0.9
4	10	54.86	7.2	8.5
5	16	55.14	7.8	−1.0
7	22	55.16	8.5	0.6
10	32	55.84	10.4	−2.8
12	44	56.04	10.0	−3.5
13	54	68.51	11.4	−4.0
15	66	68.41	11.3	−2.7
16	86	68.99	16.7	−5.9
18	96	68.87	12.5	−4.3
19	124	69.45	19.0	−6.4
20	154	57.20	11.6	−3.9
21	180	57.66	17.7	−6.2
22	200	57.88	18.8	−6.6
26	262	57.64	13.9	−2.5
27	300	58.09	16.2	−5.5
30	355	58.24	15.4	−4.4
31	400	58.60	16.2	−5.6
34	515	58.93	15.8	−4.9
35	600	59.40	17.8	−5.4
38	705	59.82	15.0	−6.0
39	800	60.27	17.2	−7.1
42	905	60.38	15.1	−5.5
43	1000	60.86	17.0	−7.0
46	1275	61.34	14.9	−3.3
47	1500	62.58	16.5	−5.1
50	1804	71.14	19.3	4.4 R

e_1 failed at ~ 1820 cycles.

14−Feb

This combines data files: B8−LEFT1.DAT & B8−LEFT.DAT.
is stored in directory /B8/DFC−FILE in filename:
B8−POP−C.WK3

B8−LEFT1.DAT is generated from .BAT file B8LFI
B8−RIGHT.DAT is generated from .BAT file B8RFI

[1] Intersection of linear best fit lines to upper and lower parts of the loading branch of the complian
curve.

82	19720	22.40	14.1	-1.3	R
83	19725	24.67	17.4	9.8	
84	20000	24.77	17.5	8.7	
85	20100	24.88	17.6	9.6	
86	22500	25.46	18.3	14.1	
87	24900	25.99	18.1	14.6	
88	24990	26.15	17.5	12.4	
89	30000	28.25	15.2	10.6	
90	30150	28.83	14.2	5.6	
91	32500	29.41	13.4	4.3	
92	34925	30.84	16.9	17.1	
93	35000	30.81	13.4	7.4	
94	35100	31.13	11.7	1.6	
95	37500	31.78	14.1	13.4	
96	39950	32.43	15.3	14.8	
97	40000	32.60	13.7	13.1	
98	40100	31.94	15.0	12.9	
99	42500	33.24	14.3	11.8	
100	44950	34.26	14.4	12.4	
101	45000	34.32	14.4	12.4	
102	45100	34.33	14.5	12.6	
103	49992	36.98	13.6	11.6	
104	55000	40.66	12.2	9.7	
105	55005	40.48	12.4	9.5	
106	55100	40.59	12.2	9.2	
107	55500	41.02	12.5	9.9	
109	55810	42.25	13.9	11.5	

e_3 failed at ~55810 – 55970 cycles.

[2] Ramberg–Osgood type curve fitted to the uppe part of the loading branch of the compliance curv and subsequently compared to the data based on your 'close' criterion.

Specimen #: B8 Using data from active strain gauge adjacent to the a−face crack.
R=−0.10 P_{max}: 16023 N N_{EoT}=141,540 cycles

Left side crack.	$e_7 - e_8$				Right side crack.	e[illegible] − e[illegible]			
File #	Cycle #	Differential Compliance (μ/N*10^{-3})	P_{open}/P_{max}[1] (%)	P_{open}/P_{max}[2] (%)	File #	Cycle #	Differential Compliance (μ/N*10^{-3})	P_{open}/P_{max}[1] (%)	P_{open}/P_{max}[2] (%)
3	52	1.44	−22	24.8	1	20	0.25	−14	57.7
5	94	4.76	−11	9.5	2	50	0.42	6.4	58.1
7	260	1.38	−17	23.9	4	92	3.18	−2.2	−0.2
9	510	1.58	−9.4	14.3	6	255	0.61	5.6	48.6
10	825	1.64	−10	21.7	8	500	0.5	48.3	36.7
13	1530	1.60	−15	18.0	11	830	0.44	24.4	57.4
23	4080	1.67	−6.9	25.7	12	1525	0.51	39.4	58.4
26	5000	1.78	−27	27.4	14	2000	0.63	65.9	57.1
31	6075	1.49	−3.3	21.0	15	2275	1.21	−592	24.3
39	10036	1.41	3.7	0.0	16	2325	0.59	−12	17.1
46	12500	1.56	206	21.8	17	2375	0.93	29.7	28
47	14997	1.41	1.4	0.3	18	2490	0.9	−23	29.8
51	17494	1.28	−29	4.4	19	3000	0.95	−11	1.6
53	19990	1.39	24.2	21.9	20	3050	1.33	−16	24.2
55	24995	1.46	−70	0.7	21	3450	1.22	−287	28.3
61	29995	1.03	71	26.4	22	4000	1.07	471	29.8
62	34990	1.01	35.8	19.9	24	4100	0.99	−51	25.6
64	39990	0.97	−60	27.2	25	4490	1.23	−29	24.8
66	44990	1.36	3.7	14.4	27	5003	1.11	−22	28.4
68	49995	1.37	9.6	9.6	28	5105	1.23	−9.4	20.9
74	54997	1.39	12.2	6.5	29	5500	1.19	−7.2	27.7
77	59995	1.23	72.1	3.2	30	6000	1.18	−17	26.4
84	65000	1.05	5.8	6.7	32	6100	1.32	−8.3	24.4
92	70006	0.86	−6.7	21.4	33	7000	1.24	−9.1	24.2
97	75000	0.69	11	2.3	34	8000	1.22	−8	27.7
103	79990	0.60	6.9	7.7	35	8125	1.21	−4.1	0.6
112	84990	0.51	6.8	18.1	36	9125	1.22	−3.9	26.5
120	89992	1.09	−26	19.9	37	10005	1.2	−15	27.7
126	99980	1.02	63.3	28.7	38	10034	3.31	−5.8	−0.1
133	109990	0.51	21.5	22.3	40	10050	3.34	−6.2	−0.2
138	119985	1.29	15.8	13.6	41	10100	3.48	65.8	7.6
139	120000	1.28	18.4	19.4	42	10200	3.53	39.5	10.4
140	120003	0.97	27.8	26.6	43	10505	3.5	−243	6
141	120010	1.07	31.2	22.3	44	11500	3.51	33.1	0.4
142	120050	1.16	34.4	19.0	45	12495	3.36	46.6	−0.2
143	120500	1.36	30.3	18.2	48	15000	2.34	19.7	2.5
144	122505	1.79	19.5	22.3	49	15050	2.09	−134	0
145	122510	1.76	22.8	16.2	50	17490	2.62	10.7	3.3
146	125005	2.22	14.2	14.4	52	19650	2.16	5.4	−0.2
147	129925	3.36	8.5	9.6	54	19995	2.23	9.0	0.1
150	130000	3.38	7.5	9.5	56	25000	2.3	8.3	3.5
151	130002	2.51	18.0	25.2	57	25100	2.07	18.4	16.8
152	130015	2.64	18.3	26.1	58	27500	2.42	19.0	17.0
153	130100	2.81	17.2	24.6	59	29900	2.57	22.3	10.1
154	130110	2.85	13.8	22.0	60	29990	2.53	18.5	11.5
155	130500	3.05	13.4	20.5	63	34995	2.9	11.7	12.2
156	131500	3.44	11.5	16.0	65	39995	3.87	12.4	17.3
157	135005	5.05	7.3	11.3	67	44995	4.86	16.2	15.6
158	136400	5.78	5.4	9.6	69	50000	6.16	14.6	17.4
159	139050	7.57	2.9	4.4	70	50150	5.75	18.5	21.8
160	139950	8.40	1.8	1.3	71	50500	6	18.3	21.0

72	54925	7.25	15.8	18.3
73	54990	7.29	15.3	17.2
75	56000	6.81	20.1	22.5
76	59925	8.21	17.4	21.0
78	60000	8.32	16.3	19.3
79	60002	7.4	24.3	25.3
80	60010	7.66	22.4	24.1
81	60050	7.89	21.9	23.6
82	60500	8.33	20.2	23.2
83	64990	10.46	15.3	17.0
85	65005	8.74	22.6	24.8
86	65050	9.2	21.4	23.1
87	65150	9.47	20.8	22.3
88	65350	9.72	19.9	21.9
89	65750	9.99	19.7	20.8
90	66502	10.47	18.6	20.7
91	69990	12.11	16.6	19.3
93	70010	10.18	23.0	25.9
94	70500	11.44	19.5	24.0
95	71500	12.03	18.8	23.6
96	74990	13.74	16.9	21.5
98	75002	11.73	23.2	25.8
99	75005	12.56	20.2	24.3
100	75008	12.75	19.3	24.0
101	75025	12.87	19.1	23.6
102	79925	15.51	17.3	21.5
104	80000	15.61	16.5	21.6
105	80004	12.3	24.9	25.9
107	80050	13.83	22.2	24.1
108	80200	14.55	20.0	23.9
109	80750	15.44	18.8	22.3
110	82000	16.23	18.3	22.0
111	84950	17.94	16.7	20.6
113	85000	18.22	15.2	19.9
114	85002	15.42	23.1	25.7
115	85010	16.23	21.5	25.1
116	85100	16.98	20.0	24.4
117	85500	17.84	18.5	23.3
118	86500	18.5	17.9	22.5
119	89925	20.51	16.9	21.3
121	90003	20.57	16.0	19.2
122	90105	21.23	14.1	18.3
123	91000	22.03	13.8	17.2
124	95000	23.99	13.5	16.5
125	99950	26.48	12.8	16.4
127	100000	26.65	12.3	16.1
129	100500	26.69	13.6	16.8
130	105000	28.97	11.5	15.4
131	109925	30.96	11.7	16.1
134	110000	30.97	11.6	16.2
135	110010	30.55	12.9	17.0
136	115000	32.6	13.2	15.1
137	119950	34.04	12.4	13.3
148	129950	36.15	6.9	6.9
162	139995	35.25		
163	140000	8.55	2.0	2.4
164	140002	6.73	14.5	24.0
165	140015	7.19	13.4	24.2
166	140100	7.55	13.0	22.0
167	140500	8.09	12.3	20.7
168	141500	9.54	10.0	16.6
169	141510	9.53	8.3	15.8
170	141520	9.55	8.1	14.6

This data generated from .BAT files:
B8LFILE4 & B8RFILE4

This is stored in directory /B8/ADJ−FILE in filename B8−POP−A.WK3

[1] Intersection of linear best fit lines to upper and lower parts of the loading branch of the compliance curve.

[2] Linear best fit to the upper portion of the loading branch and comparing the data curve to the fitted line.